Cryospheric Teleconnections: The Response of Northern Hemisphere Snow to the Atmospheric and Arctic Sea Ice Variations

by

DEBJANI GHATAK

A dissertation submitted to the Graduate Faculty in Earth and Environmental Sciences in partial fulfillment of the requirements for the degree of Doctor of Philosophy,

The City University of New York

2011

This manuscript has been read and accepted for the
Graduate Faculty in Earth and Environmental Sciences in satisfaction of the
dissertation requirement for the degree of Doctor of Philosophy.

Dr. Allan Frei
_____

_____ _____
Date Chair of Examining Committee

Dr. Yehuda Klein
_____

_____ _____
Date Executive Officer

Dr. Stanley David Gedzelman
_____

Dr. Haydee Salmun
_____

Dr. David A. Robinson
_____
Supervisory Committee

THE CITY UNIVERSITY OF NEW YORK

Abstract

Cryospheric Teleconnections: The Response of Northern Hemisphere Snow to the Atmospheric and Arctic Sea Ice Variations

by

Debjani Ghatak

Adviser: Professor Allan Frei

The primary focus of this dissertation is the land-surface snow cover, which plays a significant role in modulating the earth's surface energy balance. It is an indicator of climatic variations as well as a part of the earth's system of feedback mechanisms that control the climate. The main goal of the thesis is to contribute to our understanding of the factors causing variations in snow. In order to fulfill this goal, specific objectives are formulated with a particular focus on an under-utilized snow pack metric, i.e. the snow depth. These objectives include the spatially robust explanation of climate-driven North American snow depth variability as well as the investigation of any evidence of a climate change signal and/or Arctic sea ice loss signal in the Northern Hemisphere snow cover record.

This thesis identifies major winter climate teleconnection modes i.e. the North Atlantic Oscillation (NAO) and the Pacific-North American pattern (PNA) as the two main drivers of the snow depth variations over North America. Furthermore, the distinct mechanistic pathways linking circulation patterns to snow variations are also determined. These involve regional winter circulation patterns and hydrologic fluxes. Next, analyses of observational datasets show increased snow over Siberia during fall and early winter, which may be related to the loss of summer Arctic sea ice. Historic and future simulations of Community Climate System Model version3 (CCSM3) indicate the emergence of a similar signal during the last half of the 21st century. Finally, a suite of Community Atmosphere Model Version 3 (CAM3) experiments is analyzed, which suggests a key role played by the high-latitude surface forcings due to the SST and sea ice in generating the snow signal over the Eurasian landmasses as emerges in observations.

This thesis contributes to the state of the knowledge of snow – climate interactions by focusing on the snow depth – climate interaction. Furthermore, the identification of a snow response to the recent climatic changes including the loss of Arctic sea ice is another original contribution. Thus, this work may enhance the prediction capabilities of the future hydro-climatic changes over the high latitude regions.

Acknowledgements

Here, I offer my gratitude to few people without whom my journey as a doctoral student would not have been possible. At first, I want to thank my thesis adviser, Dr. Allan Frei; though, it is impossible to detail all his contributions in this section. I got the opportunity over these years to see him as an academic adviser, as well as a teacher. He not only taught me many fundamental aspects of research, for e.g. questioning the quality of the data, application of various statistical techniques in research, understanding the physical processes; but also inspired me to be an honest scientist. His scientific questions have always been very intriguing, which made me think deeper about the subject. He always promptly responded to my questions/emails with a smiling face. As a teacher, he is very respectful to the students as well as a great educator in the classroom. He will be a role model to me in my teaching career. Besides supervising my thesis, he tried to expose me to the ongoing cutting-edge research in the field of Earth-science by encouraging me to attend the academic conferences. He set up a weather station at Hunter College and encouraged me to take sky observations and to maintain the weather station. This gave me an opportunity to achieve hands-on-training. Moreover, I am grateful to his enormous and continuous efforts in receiving the external funding for our research, which helped me to survive in this city. He also provided his moral support in difficult times of my life. He made me enrolled in many organization/forum/list-servers (e.g. PYRN, CSG, CRYOLIST), which I found later very useful in getting job information and to stay tuned with the research community. I am very fortunate to work with Allan and to know such wonderful person.

Dr. Gavin Gong is another person whose contribution in my training as a scientist and a researcher is extraordinary. I have worked very closely with him as he was one of the principal investigators in our project. In my research, his role was not just limited to a role of PI; he advised me like his own graduate student. He participated in numerous discussions and countless revisions of the manuscripts. His office was always open to me in spite of the enormous workload at his end and he was never tired of answering my endless emails with questions. He possesses great understanding in science and he could convey his knowledge in a very lucid way. He has been immensely motivating to me as a scientist. I got the opportunity to have him as a teacher in a course in Columbia, which enhanced my scientific knowledge too. Furthermore, I learnt from him how to write scientific manuscripts in a concise and organized form. I feel myself extremely fortunate to work with Gavin who is a wonderful human being too.

I am thankful to my dissertation committee members Drs. Stanley Gedzelman, Haydee Salmun and David Robinson. Professor Gedzelman's profound knowledge in the field of atmospheric science inspired me while I was taking classes with him in City College. Haydee always encouraged me to complete the thesis in time. Dr. Robinson's advice in my project and his deep knowledge especially in the field of cryospheric science have been extremely beneficial to me. I also greatly appreciate Dr. Julienne Stroeve for providing me the opportunity to work with her and for her valuable scientific feedback in our project.

Dr. Yehuda Klein, executive officer of the EES program took the office at the same time when I joined the program as a student. I appreciate his endeavor to help me financially during my Ph.D. studies. He encouraged my research by attending my presentation in conference and always guided me to satisfy all the degree requirements in time. I also want to thank Ms. Lina McClain who is the assistant program officer in the program. Lina has helped me through all the official formalities since the day one of my doctoral career. Moreover, her presence in the EES office makes the office feel like home. I appreciate Mr. Douglas Ewing (Director of the Office of International Students) who helped me many times to maintain my foreign student status in this country and I found him always willing to help students.

Department of Geography at Hunter College has been my second home as I spent most of my time during last few years. The group of faculties, students and staffs of the department has been very friendly and supportive. I appreciate the folks at Hunter College, especially Nguyen, Ylli, Shihyan, Wenze, Henry, Nidhi, Enrique, Mike and Andreea whose company made the days at Hunter enjoyable. I would like to appreciate Ms. Dana Reimer's effort to provide me teaching assignments which helped me financially. Martha has always been very supportive in my graduate life. I also appreciate Dr. William Solecki for providing me the office space and Dr. Traci Warkentin for helping me with the job search. Tom, Nguyen and Amy always provided me the technical help needed for research.

I would like to mention a special friend of mine, Anuradha Swatantran whose friendship is a treasure to me. Our brainstorming discussions included variety of topics ranging from science to philosophy, and kept us focused in research. Her support in my personal life has been extremely valuable. Dr. Yan Ge's help in research has been very useful. I am thankful for getting valuable and good friends like Yan Ge, Fernanda Santos and Nelun Fernando in my doctoral career. I have lots of happy and fun-filled memories with them.

The person who is the main inspiration of my scientific career since my college days is my husband Somdeb Mitra. His scientific excellence as well as his unfathomable knowledge in many different fields always motivated me to pursue my scientific goals. Moreover, I could successfully finish my thesis work because of his tremendous faith in my scientific ability. His contributions in many different ways to support me cannot be described in words.

My father, Mr. Asok Kumar Ghatak who passed away few months ago always dreamt of seeing me to accomplish this degree. I've learnt that time can only heal my grief of this loss. I am grateful to my father as well as to my mother, Mrs. Malabika Ghatak for their extraordinary efforts and sacrifice to make me eligible to achieve this in my life. They are always in my heart. A special thank goes to my brothers (Barda and Chorda), sisters-in-law (Bara-boudi and Choto-boudi) and sisters for their love, continuous encouragements and also for their unconditional support to my parents when I am far away from home. I can't thank enough to Lakshmi-di who always looked after

me. I also want to thank Mr. Chandan Bagchi for his unconditional help during my admission to the program and Mr. Kanakendu Mitra and Mrs. Kshama Mitra for their encouragement.

I truly appreciate NASA Cryospheric Sciences Division (#NNX08AQ70G) for sponsoring my research.

TABLE OF CONTENTS

LIST OF TABLES

Chapter 3

Chapter 5

LIST OF FIGURES

Chapter 1

Chapter 3

Chapter 4

Chapter 5

Chapter 1

Introduction

1.1 Land-surface snow over Northern Hemisphere:

The cryosphere encompasses those regions of the Earth which are perennially or seasonally covered by snow, sea ice, lake ice, glacier or permafrost (IPCC, Technical summary). Snow is one of the main components of the cryosphere, and forms an integral part of the climate system (the role of snow in climate system will be discussed in section 1.1.1). The body of research on snow has grown dramatically since the advent of the satellite era, when continuous record of reliable satellite observations became available (Kukla and Robinson, 1981; Robinson 1993, 1999; Ge and Gong, 2008). Snow cover is a spatially extensive cryospheric feature and an important land-surface characteristic of the Northern Hemisphere landmasses, fluctuating between a mean peak of over 46×10^6 km^2 in winter (January and February) and a minimum of under 4×10^6 km^2 in summer (August) (Robinson and Frei, 2000).

Furthermore, snow has significant impact on human civilization, for e.g. water budgets, soil microclimate, agricultural productivity, tourism industry, forestry, hydro-electric generations, ecological variations, and the lives of both indigenous and non-indigenous people (Bell and Bliss, 1979; Brooks et al., 1996; Bürki et al., 2003; Hassol, 2004; Armstrong and Brun, 2008; Williamson et al., 2008). One of the most important among them is its role as water reservoir; snowmelt runoff determines streamflow and ground water recharge, specifically important for central Asia and western North America (NA) (Armstrong and Brun, 2008). Jones and Pomeroy (1999) showed the

major role of snow in cold region habitats through their study in Wolf Creek, Yukon, and investigated the interaction between snow and micro-organisms, animal, plants.

Considering the significance of snow, many researchers examined the spatial and temporal pattern of projected changes in snow during 21st century, as simulated by the General Circulation Models (GCMs) (Frei and Gong, 2005; Barry et al., 2007; Räisänen, 2008). Evaluation of NA snow cover extent (i.e. the surface area covered by snow) as simulated by coupled Atmosphere-Ocean GCMs (AOGCMs) participating in the Fourth Assessment Report of the Intergovernmental Panel on Climate Change (IPCC-AR4) showed that the most of the models underestimate the 20th century observed snow cover extent over NA, although individual ensemble members do capture the magnitude of decadal-scale variability (Frei and Gong, 2005). In addition, this study indicates that the future loss of snow extent in response to the greenhouse gases warming is expected to be dramatic (Frei and Gong, 2005). Barry et al. (2007) reported that ECHAM5 model simulations for 21st century climate show a decrease of 60% to 80% in monthly maximum SWE over most of the mid-latitudinal region of the Northern Hemisphere between 1981–2000 and 2080–2100, but an increase over the Canadian Arctic and Siberia.

All the above-mentioned predicted changes in snow can affect the future climate system too. Alexander et al. (2010) investigated the effects of prescribed future loss of snow through the specific experiments conducted by National Center for Atmospheric Research (NCAR) Community Atmosphere Model (CAM3) coupled to the Community Land Model (CLM3). These modelling experiments predict large increases in the (i) absorption of the solar radiation by the surface, (ii) upward longwave radiation and (iii)

latent and sensible heat flux due to the loss of snow in 21st century compared to the 20th century. Loss of snow also generates circulation responses including local low-level trough, remote Rossby wavetrains and increase in geopotential height (Alexander et al., 2010). A recent study shows that the lengthening of the snow free season in the Alaska has triggered the summer warming in such a magnitude which is similar to the regional warming due to doubling of CO_2 over several decades (Chapin III F.S. et al., 2005). In summary, snow over the land-surface always attracted the attention of the scientists because of its huge impact on the Earth-climate system and on human civilization, and it still draws attention considering its potential future changes and possible effects on society.

There are several snow metrics that are used to analyze snow by researchers. They are (a) snow extent (SNE), (b) snow depth (SND), (c) snow density and (d) snow water equivalent (SWE). SNE describes the presence or absence of snow or the spatial extent; whereas SND indicates the thickness of the snow pack (Armstrong and Brun, 2008). SWE indicates the depth of water obtained from melting the snow pack (Armstrong and Brun, 2008) and is expressed in kg m^{-2} or in mm; whereas, snow density is generally expressed in kg m^{-3}.

1.1.1 Snow in the climate system: Snow Extent vs. Snow Depth:

Role of snow in the climate system is complex in nature because of the complicated feedback mechanisms between snow and atmosphere; this is evident in the numerous scientific literatures as discussed below. Many studies reported the importance of snow in influencing air temperature (Dewey, 1977; Walsh et al., 1982, 1985; Foster et al., 1983; Namias, 1985; Ceveny and Balling, 1992; Leathers and Robinson, 1993;

Groisman et al., 1994). The response of snow to the atmospheric circulation, and to the North Atlantic Oscillations (NAO), Arctic Oscillation (AO), and the Pacific-North American teleconnection pattern (PNA) is also widely known (Gutzler and Rosen, 1992; McCabe and Legates, 1995; Derksen et al., 1997; Clark et al., 1999). On the other hand, both empirical and modelling studies showed how snow can affect the atmospheric circulation pattern at hemispheric-scale too (Clark and Serreze, 2000; Cohen and Entekhabi, 2001; Gong et al., 2003; Saunders et al., 2003). Furthermore, few studies examined the relationship between snow and monsoon system (Hahn and Shukla, 1976; Dey and Kumar, 1983; Barnett et al., 1989; Yasunari et al., 1991; Kripalani et al., 1996; Sankar-Rao et al., 1996; Gutzler and Preston, 1997; Bamzai and Shukla, 1999; Bamzai and Marx, 2000; Gutzler, 2000; Fiona and Clark, 2002; Hawkins et al., 2002; Robok et al., 2003; Matsui et al., 2005; Zhu et al., 2005). Many of these above-mentioned studies used 'snow extent' as their snow metric (Foster et al., 1983; Gutzler and Rosen, 1992; Leathers and Robinson, 1993; Groisman et al., 1994; Clark et al., 1999; Clark and Serreze, 2000; Cohen and Entekhabi, 2001; Gong et al., 2003; Saunders et al., 2003).

Continental-scale reconstructions of snow extent data, based on satellite and station observations gave us an opportunity to examine the changes in snow cover during the 20^{th} century prior to the satellite era (Frei et al., 1999; Brown, 2000). These reconstructed datasets showed the increase in fall and winter snow extent over the mid-latitudinal areas of NA (Frei et al., 1999; Brown, 2000), whereas rapid reduction of April snow extent occurred both over NA and Eurasia (Brown, 2000). Spatial and temporal pattern of variations in SNE are not always consistent with the variations in SND (Ge and Gong, 2008). Ge and Gong (2008) showed that the SNE and SND are correlated over the

regions close to the snow line, strongest during fall and spring; whereas, their variabilities are inconsistent over the high latitude regions, north of the snow line during the winter season. High latitude region remains 100% snow cover during winter, but snow depth varies over both space and time (Ge and Gong, 2008).

Snow affects the local and regional climate through the modulation of surface energy balance (Wagner, 1973; Kierkus and Colborne, 1989; Cohen and Rind, 1991; Ellis and Leathers, 1999; Kumar and Yang, 2003; Marshall et al., 2003; Gong et al., 2004), as well as affects the ground thermal regime (Zhang, 2005). The radiative property of snow such as reflectance partially depends on the depth of the snow pack too. A deep enough snow-layer with low impurities acts as a good diffuser and allows individual photon at visible wavelength to travel long distance within snow pack (Armstrong and Brun, 2008). In the course of its travel, the chances of photon to be reflected and refracted without being absorbed are enhanced; thus, it increases the probability of photon to be ejected (Armstrong and Brun, 2008). Furthermore, ≥10 cm snow pack lowers the average maximum and minimum air temperature up to 8.4^{o}C than any snow free days during winter (Baker et al., 1992).

As SND plays significant role in affecting the surface energy balance, it is important to include SND information rather than exclusively snow extent when studying snow & climate interaction (Ge and Gong, 2008, 2009). A new, gridded snow depth datasets (Dyer and Mote, 2006, will be discussed in detail in chapter 3) gave the opportunity to study i) the SND at continental-scale, (ii) its response to the large-scale atmospheric circulation (Ge and Gong, 2008, 2009; Ge et al., 2009), and (iii) its influence on affecting atmospheric temperature (Mote, 2008). Furthermore, Ge and Gong (2009)

showed through the empirical analysis that snow depth variations can affect the regional climate greatly, which is distinctly different from the role of snow extent in climate variability. They reported the strong correlations between snow depth and the Pacific – Decadal Oscillation (PDO) and the Pacific – North America (PNA) pattern over NA during snow season; whereas, the weak correlation exists between snow extent and PNA /& PDO in late spring, which is the residual of snow depth-climate relationship.

1.1.2 Limitations of Snow Depth/SWE Data:

There is lack of reliable snow depth data for Eurasian continent; thus, it is difficult to examine the recent changes in the snowpack. SWE is a close proxy to SND and is an important snow metric by its own right too, which is available from 'Global Monthly EASE-Grid Snow Water Equivalent' datasets derived from Scanning Multichannel Microwave Radiometer (SMMR) and selected Special Sensor Microwave/Imagers (SSM/I). But it contains some problems, as is reported by Yang et al. (2007). They found some inconsistencies over Lena river basin in Siberia and indicated the limitations of the use of this SWE data. Moreover, they suggested that the inconsistency is due to the SWE retrieval algorithm in the areas with different physical characteristics. Generation of reliable SWE data at regional-scale is under investigation (Derksen et al., 2005, 2009; Tedesco and Miller, 2007). SWE data over central NA has been made highly reliable (Derksen et al., 2004). But considering its spatial constraint, this is not helpful in hemispheric-scale study.

1.2 Rapid loss of Arctic sea ice – a component of recent pan-Arctic changes

The Arctic region has been changing considerably in recent decades (Hassol, 2004), ranging from thawing of permafrost (Anisimov and Nelson, 1996; Nelson et al., 2001; Payette et al., 2004; Zhang et al., 2005), to arctic-wide warming (Serreze et al., 2009) to the rapid increase in the Arctic river discharge (Peterson et al., 2002; Wu et al., 2005; McClelland et al., 2004, 2006; Rawlins et al., 2009). One of these major changes is the rapid decline of Arctic sea ice, and is discussed as follows.

The Arctic sea ice cover is another spatially extensive and seasonally varying cryospheric feature of the Northern Hemisphere like snow cover. Fig 1 shows the Arctic Ocean and its contiguous marginal seas. Its areal extent spans around the North Pole with an average maximum coverage of ~16x10^{6} km^{2} in March during the satellite era (Parkinson et al., 1999; Serreze et al., 2007).

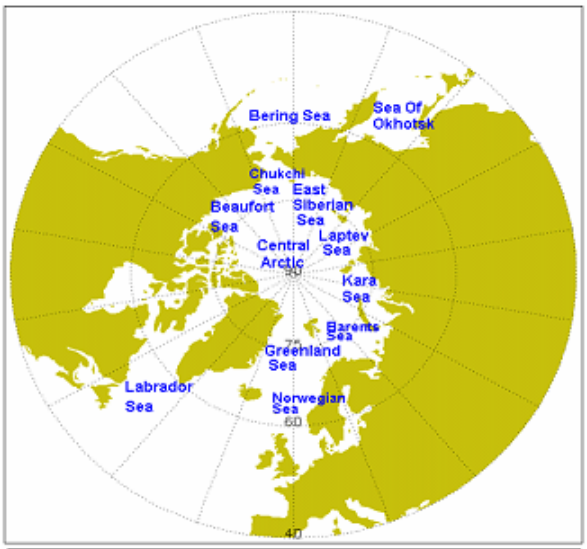

The Arctic Ocean and its contiguous marginal seas

Fig.1

1.2.1 Variability in Arctic Sea Ice:

Arctic sea ice extent (defined as the area of the ocean with at least 15% ice concentration) has been decreasing steadily, though the rate of change varies between summer and winter (Meier et al., 2005; Stroeve et al., 2005; Comiso, 2006; Serreze et al., 2007). The most rapidly decreasing sea ice extent has been noticed in September (Serreze et al., 2007; Comiso et al., 2008). Moreover, the lowest September sea ice cover in the last 50 years of record has been recorded in 2007 and the remarkable negative trend of the perennial ice extent and area are -10.2% and -11.4% per decade respectively for the period of 1979-2007 (Comiso et al., 2008). On the contrary, trend in March sea ice extent is very small, but still shows significant negative trend of -2.9%/decade for the period of 1979-2006 (Stroeve et al., 2007). Furthermore, recent analysis shows that the trend in September Arctic sea ice extent (from 1953–2006) is even larger than any of the IPCC AR4 simulations (Stroeve et al., 2007).

Availability of reliable sea ice concentration data on a regular basis has become possible since the advent of passive microwave satellite era. Visible band satellite, data from ships and aircrafts, sonar record, and submarine-acquired data provided information to the researchers of the earlier period of time (Rothrock et al., 1999, 2003; Serreze et al., 2007). In the passive microwave record, minima were also observed in 1990, 1993, 1995, 1998, 2002, 2003, 2004, 2005 (Serreze and Barry, 2005; Serreze et al, 2007). The Hadley Centre sea ice and sea surface temperature (SST) dataset (HadISST1) is the longest time series available, which dates back to 1871 (Rayner et al., 2003). It is extremely useful for long term analysis of sea ice and to identify the trends; though, it has to be used with caution due to sparse data set during the earlier period of records (Stroeve et al., 2005). This reconstructed dataset is based on passive microwave records, other types of satellite

data, aircraft reconnaissance and ship reports. This monthly global dataset has a spatial resolution of 1degree latitude x 1degree longitude (for the details about this dataset see Rayner et al., 2003).

Projected changes in Arctic sea ice during 21st century as simulated by the models participating in the IPCC AR4 suggest the rapid loss of Arctic sea ice through the 21st century in response to the greenhouse gases (Zhang and Walsh, 2006). Multi-model ensemble mean indicates a loss of 31.1%, 33.4%, and 21.6% in the last 20 yr of the 21st century compared to 1979–99 in Special Report on Emission Scenarios (SRES) A1B, A2 and in B1 scenarios respectively (Zhang and Walsh, 2006). Uncertainty lies in the timing of the ice-free summer in future, though most of the studies predict the ice-free condition by the mid of the 21st century (Holland et al., 2006; Wang and Overland, 2009).

Accelerated rate of decreasing Arctic sea ice is of great concern. The physical mechanism of declining sea ice is complicated as it involves both dynamic and thermodynamic processes. The current state of knowledge of decreasing Arctic sea ice will be discussed in the next few paragraphs.

1.2.2 Causes of retreating sea ice:

Dynamic Processes:

Inter-annual variations in winter-time climate of the Northern Hemisphere are characterized by the dynamic processes involving changes in wind and ocean currents due to anomaly in sea level pressure (SLP) associated with Arctic Oscillation (AO)/ North Atlantic oscillation (NAO). AO refers to a pattern of variability in large scale atmospheric winter-time circulation over Northern Hemisphere and its index is defined as the leading principal component (PC) of Northern Hemisphere monthly mean sea level

pressure (SLP) anomaly field over the domain poleward of 20°N (Thompson and Wallace, 1998). During high index phase of AO there is higher than normal pressure over the North Atlantic and North Pacific when there is lower than normal pressure over the Arctic. Since 1989, AO index shifts to strongly positive phase than the earlier period of record. But in recent years (since late 1990s) AO has been shifted to more-neutral phase. AO is hemispheric scale form of more regional 'North Atlantic oscillation' (NAO) (Thompson and Wallace, 1998) (more discussion of NAO will be in the 3rd chapter). NAO is also a source of inter-annual and decadal variability in the atmospheric circulation of Northern Hemisphere, which has been calculated as the difference of normalized pressures between Lisbon, Portugal, and Stykkisholmur, Iceland (Hurrell, 1995).

Rigor et al. (2002) explained the huge ice loss in the light of AO/NAO. During positive phase of AO, altered surface wind causes cyclonic sea ice motion in the Arctic and thus strengthens the transpolar drift stream (sea ice motion that runs across the pole from the coast of Siberia to the North Atlantic via the Fram Strait). Moreover, the advection of sea ice away from the coast of Siberia and Alaska has also been observed. All these led to the divergence of sea ice and thus created openings, though the openings refroze during winter. As a result, the thin ice is formed and it is prone to rapid melting during the following summer. Thus, it further causes more absorption of solar radiation by ocean.

Continued ice loss in recent years when AO shifted to more neutral state is also explained by Rigor and Wallace (2004). It is shown that the surface wind associated with anomalous AO removed the thick, multiyear ice and most of the Arctic Ocean thus

became covered with 'young' ice. Therefore, the conditions leading to the recent minima in summer sea ice were preset during the years of extreme high index phase of AO (in 1989-1990) (Rigor and Wallace, 2004).

Thermodynamic Processes:

The trend in sea ice is also consistent with the observed increase in surface air temperature (SAT) over the pan-arctic region. Several studies reported the warming over the Arctic. Serreze et al. (2000) showed the increased SAT over the central Arctic Ocean and also over western North America and Eurasia during winter and spring. Observations and analysis based on International Arctic Buoy Programme/Polar Exchange at the Sea Surface (IABP/POLES) dataset, Rigor et al. (2000) also supported arctic wide warming during spring. Comiso (2003) observed increasing SAT over the pan-arctic region based on clear-sky satellite thermal infrared data. Positive seasonal temperature trend has been found in spring, summer and autumn. Comiso (2003) also suggested that the recent warming is related to the phase of Arctic oscillation which is in turn linked to the elevated greenhouse gas concentrations in the atmosphere. Irrespective of the attributing causes of increasing SAT, trends in SAT are important because they determine the rate of melting and freezing.

The magnitude of warming in the Arctic is amplified with respect to the global average because of the feedback effects, such as the positive ice-albedo feedback (Holland and Bitz, 2003). Moreover, the amplification of SAT over the Arctic Ocean is already visible as a consequence of sea ice loss, as is suggested by Serreze et al. (2009).

Declining sea ice in recent years when AO is in more neutral phase is also explained by the increased downward long-wave flux. Increased cloud amount, liquid-

water-containing-cloud and water vapor over the Arctic associated with recent warming enhance the downward long-wave flux and cause further melting (Francis and Hunter, 2006). Therefore, the surface energy balance plays key role in ice reduction rather than dynamic effect of wind in very recent years.

Oceanic Influences:

Recent changes in the oceanic circulation also explain the ice loss in the Arctic. Oceanographic surveys indicate intrusion of anomalously warm water into the Arctic Ocean from the Atlantic (Polyakov et al., 2005). As a result, the Atlantic water layer thickness is increased, consequently leading to the enhancement in water column heat content in East Eurasian basin and in the Fram strait. This inflow will eventually enter into the Arctic Ocean and will increase the temperature of Arctic basin. As a result, this will give impetus to the further ice loss and also will hinder ice growth.

The deleterious effect of warm Atlantic water is also found from the study of cold halocline layer (Steele et al., 1998). Cold halocline layer marks the transition between cold fresh water and salty, heavier (Atlantic) water. This layer is important for the formation of sea ice in the Arctic and has an insulating effect on sea ice from the underlying warm Atlantic water too. Recent retreat of the cold halocline layer from the Eurasian basin northward causes the increased heat flux from the deep Atlantic water to the surface and thus affects the surface energy balance and mass balance of sea ice.

In summary, the causes of retreating sea ice include many physical processes, and they are both natural and anthropogenic in origin. Modeling studies support the view of rising SAT as one of the major factors of decreasing sea ice (Rothrock and Zhang, 2005; Lindsay and Zhang, 2005). In addition, based on their results from the coupled ice-ocean

model, Rothrock and Zhang (2005) argued that even without the forcing of AO/NAO the trend in sea ice would still be negative. The trend, however, would be smaller than the observed.

1.2.3 Consequences of Sea ice loss:

In recent decades, extreme loss of sea ice attracted the attention of the scientists. Consequently, they investigated the impact of sea ice loss; though they vary in terms of their research methodologies and approach (e.g. Magnusdottir et al., 2004; Alexandar et al., 2004; Kvamsto et al., 2004; Gerdes, 2006; Singarayer et al., 2006; Francis et al., 2009; Deser et al., 2010). Few of these studies are based on modeling experiments (e.g. Magnusdottir et al., 2004; Alexandar et al., 2004; Kvamsto et al., 2004; Gerdes, 2006; Singarayer et al., 2006; Deser et al., 2010); whereas some of them are based on observational analyses (Deser et al., 2000; Francis et al., 2009). Modeling experiments also vary with respect to the forcing fields; some of them use the historic sea ice loss as their boundary condition (e.g. Magnusdottir et al., 2004; Alexandar et al., 2004); whereas, some of them use predicted future loss of sea ice as the boundary condition (e.g. Singarayer et al., 2006; Seierstad and Bader, 2008).

Modelling experiments based on Community Climate model (CCM3) from NCAR with prescribed SST and sea ice concentrations over the Atlantic generated winter time circulation response as negative NAO (Deser et al., 2004; Magnusdottir et al., 2004). Negative NAO/AO-like circulation response to the ice anomalies over Atlantic also appears in other modeling experiments (Alexandar et al., 2004; Kvamsto et al., 2004; Seierstad and Bader, 2008); whereas, the circulation response over the Pacific generates a wavetrains over NA (Alexandar et al., 2004). Deser et al. (2010) reported significant

circulation response during winter; though they identified different response between early winter (November-December) vs. mid-winter (January-March). Early winter circulation response is dominated by the baroclinic structure over the Arctic with the low pressure anomalies near the surface; whereas, the negative NAO-like response appears during February (Deser et al., 2010). Circulation response also includes the shifts/changes in mid-latitudinal storm tracks (Kvamsto et al., 2004; Singarayer et al., 2006; Deser et al., 2007). Deser et al. (2010) also suggested that the dynamic response to the loss of sea ice varies more between different modeling studies than the thermodynamic responses.

Arctic-wide warming as a result of observed sea ice loss, mainly during autumn is already apparent (Serreze et al., 2009; already mentioned in Section 1.2.2 and will be discussed in detail in chapter 4). Modelling experiments performed by Hadley Centre Atmospheric Model (HadAM3) show significant warming (upto $22^{\circ}C$ of positive anomaly) over the ocean and also over the high latitude, when they are forced with the observed sea ice concentration from 1980 to 2000, and also from the projected sea ice loss till 2100 (one under moderate CO_2 scenario and another under CO_2 severe scenario) (Singarayer et al., 2006). Another Community Climate Model (CCM3.6) also generates near-surface warming, enhanced precipitation in response to the historic loss of sea ice (Alexandar et al., 2004). Deser et al. (2010) reported maximum warming and precipitation increase over Siberia and northern Canada. Moreover, they specifically examined the projected future changes in snow over the Northern Hemisphere as a result of retreating Arctic sea ice using the Community Atmosphere Model version 3 (CAM3). They identified an increase in snow depth (SND) over Siberia in response to the prescribed future loss of sea ice concentration and thickness. In addition, the role of sea

ice loss has been found in the changing precipitation over the high-latitude regions based on observations (Francis et al., 2009). Strong connection between sea ice loss and precipitation over southwestern and northwestern NA has also been established, and this linkage doesn't depend on the model, resolution or on experimental design (Sewall, 2005).

1.3 References

Alexander, M. A., U. S. Bhatt, J. E. Walsh, M. S. Timlin, J. S. Miller and J. D. Scott, 2004: The atmospheric response to realistic Arctic sea ice anomalies in an AGCM during Winter. J. Climate , 17, 890-905.

Alexander, M. A., R. Tomas, C. Deser, and D. L. Lawrence, 2010: The Atmospheric Response to Projected Terrestrial Snow Changes in the Late 21st Century. J. Climate, accepted.

Anisimov, O. A., and Nelson, F. E., 1996: Permafrost Distribution in the Northern Hemisphere under Scenarios of Climatic Change. Global Planetary Change, 14, 59–72.

Armstrong, R. L., and E. Brun, 2008: Snow and Climate: Physical Processes, Surface Energy Exchange and Modeling. Cambridge University Press, 256 pp.

Baker, D.G., D.L. Ruschy, R.H. Skaggs and D.B. Wall, 1992: Air temperature and radiation depressions associated with snow cover. J. Appl. Meteor., 31, 247–254.

Bamzai, A. S., and J. Shukla, 1999: Relation between Eurasian snow cover, snow depth, and the Indian summer monsoon: an observational study. Journal of Climate, 12(10), 3117-3132.

Bamzai, A. S., and L. Marx, 2000: COLA AGCM simulation of the effect of anomalous spring snow over Eurasia on the Indian summer monsoon. Q.J.R. Meteorol. Soc., 126, 2575-2584.

Barnett, T.P., L. Dumenil, U. Schlese, E. Roeckner, and M. Latif, 1989: The effect of Eurasian snow cover on regional and global climate variations. J. Atmos. Sci., 46, 661–685.

Barry, R. G., R. Armstrong, T. Callaghan, J. Cherry, S. Gearhead, A. Nolin, D. Russell, and C. Zockler, 2007: Snow, in Global Outlook for Ice and Snow. UNEP (Ed.), Nairobi, Kenya, pp. 39-62.

Bell, K.L., and Bliss, L.C., 1979: Autoecology of Kobresia bellardii: why winter snow accumulation limits local distribution. Ecological Monographs, 49, 377-402.

Brooks, P.D., M. W. Williams, and S.K.Schmidt, 1996: Microbial activity under alpine snowpacks, Niwot Ridge, Colorado. Biogeochemistry, 32, 93-113.

Brown, R.D., 2000: Northern hemisphere snow cover variability and change, 1915-1997. J. Climate, 13(13), 2339-2355.

Bürki R., H. Elsasser, B. Abegg, 2003: Climate Change -Impacts on the Tourism Industry in Mountain Areas. 1st International Conference on Climate Change and Tourism, Djerba.

Cerveny, R. S., and R. C. Balling Jr., 1992: The impact of snow cover on diurnal temperature range. Geophys. Res. Lett., 19(8), 797–800, doi:10.1029/92GL00573.

Chapin, F.S. III, M. Sturm, M.C. Serreze, J. P. McFadden, J. R. Key, A. H. Lloyd, A. D. McGuire,T. S. Rupp, A. H. Lynch, J. P. Schimel, J. Beringer, W. L. Chapman, H. E. Epstein, E. S. Euskirchen, L. D. Hinzman,G. Jia, C.-L. Ping, K. D. Tape, C. D. C. Thompson, D. A. Walker, J. M. Welker, 2005: Role of Land-Surface Changes in Arctic Summer Warming. Science, 310, 657, DOI: 10.1126/science.1117368.

Clark, M. P., and M. C. Serreze, 2000: Effects of Variations in East Asian Snow Cover on Modulating Atmospheric Circulation over the North Pacific Ocean. Journal of Climate, 13, 3700-3710.

Clark, M.P., Serreze, M.C., and Robinson, D.A., 1999: Atmospheric control on Eurasian snow extent. Int. J. Climatol. 19, 27–40.

Cohen, J., and D. Rind, 1991: The effect of snow cover on climate. J. Climate, 4,689–706.

Cohen, J., and D. Entekhabi, 2001: The influence of snow cover on Northern Hemisphere climate variability. Atmos.-Ocean, 39, 35-53.

Comiso, J., 2003: Warming trends in the Arctic from clear-sky satellite observations. Journal of Climate, 16, 3498-3510.

Comiso, J.C., 2006: Abrupt decline in the Arctic winter sea ice cover. Geophys. Res. Letts., 33(L18504), 5 pp.

Comiso, J. C., C. L. Parkinson, R. Gersten, and L. Stock, 2008: Accelerated decline in the Arctic sea ice cover. Geophys. Res. Lett., 35, L01703, doi:10.1029/2007GL031972.

Derksen, C., K. Misurak, E. LeDrew, J. Piwowar, and B. Goodison, 1997: Relationship between snow cover and atmospheric circulation, central North America, winter 1988. Ann. Glaciol., 25, 347– 352.

Derksen, C., R. Brown, and A. E. Walker, 2004: Merging conventional (1915-92) and passive microwave (1978-2002) estimates of snow extent and water equivalent over central North America. Journal of Hydrometeorology, 5, 850-861.

Derksen, C., A. E. Walker, B. E. Goodison, and J. W. Strapp, 2005: Integrating in situ and multiscale passive microwave data for estimation of subrid scale snow water

equivalent distribution and variability. IEEE Transactions on Geoscience and Remote Sensing, 43(5), 960-972.

Derksen, C., M. Sturm, G. E. Liston, J. Holmgren, H. Huntington, A. Silis, and D. Solie, 2009: Northwest Territories and Nunavut snow characteristics from a subarctic traverse: implications for Passive Microwave remote sensing. Journal of Hydrometeorology, 10, 448-463, doi: 10.1175/2008JHM1074.1.

Deser, C., J.E. Walsh, and M.S. Timlin, 2000: Arctic sea ice variability in the context of recent atmospheric circulation trends. J. Climate, 13, 617-633.

Deser, C., G. Magnusdottir, R. Saravanan, and A. Phillips, 2004: The effects of North Atlantic SST and sea ice anomalies on the winter circulation in CCM3. Part II: Direct and indirect components of the response. J. Clim., 17, 877– 889.

Deser, C., R. A. Thomas, and S. Peng, 2007: The transient atmospheric circulation response to North Atlantic SST and sea ice anomalies. J. Clim., 20, 4751– 4767.

Deser, C., R. Tomas, M. Alexander, and D. Lawrence, 2010: The Seasonal Atmospheric Response to Projected Arctic Sea Ice Loss in the Late Twenty-First Century. J. Climate, 23, 333–351.

Dewey, Kenneth F., 1977: Daily Maximum and Minimum Temperature Forecasts and the Influence of Snow Cover. Mon. Wea. Rev., 105, 1594–1597.

Dey, B. and O. S. R. U. Kumar, 1983: Himalayan winter snow cover area and summer monsoon rainfall over India. Journal of Geophysical Research, 88(C9): 5471-5474.

Dyer, J. L., and T. L. Mote, 2006: Spatial variability and trends in snow depth over North America. Geophysical Research Letters, 33(L16503): doi:10.1029/2006GL027258.

Ellis, A.W., and D.J. Leathers, 1999: Analysis of cold airmass temperature modification across the U.S. Great Plains as a consequence of snow depth and albedo. J. Appl. Meteor., 38(6), 696.

Fiona, Lo, and Martyn P. Clark, 2002: Relationships between Spring Snow Mass and Summer Precipitation in the Southwestern United States Associated with the North American Monsoon System. J. Climate, 15, 1378–1385.

Foster, J., M. Owe, A. Rango, 1983: Snow Cover and Temperature Relationships in North America and Eurasia. J. Climate Appl. Meteor., 22, 460–469.

Francis J.A., E. Hunter, 2006: New Insight Into the Disappearing Arctic Sea Ice. EOS Trans. Am. Geophys. Union, 87, 509.

Francis, J.A., W. Chan, D.J. Leathers, J.R. Miller, and D.E. Veron, 2009: Winter northern hemisphere weather patterns remember summer Arctic sea ice extent. Geophys.Res. Lett., 36, L07503, doi:10.1029/2009GL037274.

Frei, A. and G. Gong, 2005: Decadal to century scale trends in North American snow extent in coupled Atmosphere-Ocean General Circulation Models. Geophysical Research Letters, 32: L18502, doi:10.1029/2005GL023394.

Frei, A., D.A. Robinson, and M.G. Hughes, 1999: North American Snow Extent: 1900-1994. Int. J. Climatol., 19, 1517–1534.

Ge, Y., and G. Gong, 2008: Observed Inconsistencies between Snow Extent and Snow Depth Variability at Regional/Continental Scales. J. Climate, 21, 1066–1082.

Ge, Y., and G. Gong, 2009: North American Snow Depth and Climate Teleconnection Patterns. J. Climate, 22, 217–233.

Ge, Y., G. Gong, and A. Frei, 2009: Physical Mechanisms Linking the Winter Pacific–North American Teleconnection Pattern to Spring North American Snow Depth. J. Climate, 22, 5135–5148.

Gerdes, R., 2006: Atmospheric response to changes in Arctic sea ice thickness. Geophys.Res. Lett., 33(18), L18709.

Gong, G., D. Entekhabi, and J. Cohen, 2003: Modeled Northern Hemisphere winter climate response to realistic Siberian snow anomalies. J. Clim., 16, 3917– 3931.

Gong, G., D. Entekhabi, and J. Cohen, 2004: Orographic Constraints on a Modeled Siberian Snow – Arctic Oscillation Teleconnection Pathway. Journal of Climate, 17: 1176-1189.

Groisman, P. Y., T. R. Karl and R. W. Knight, 1994: Observed Impact of Snow Cover on the Heat Balance and the Rise of Continental Spring Temperatures. Science, 263: 199-200.

Gutzler, David S., Richard D. Rosen, 1992: Interannual Variability of Wintertime Snow Cover across the Northern Hemisphere. J. Climate, 5, 1441–1447.

Gutzler, David S., and P. Preston, 1997: Evidence for a relationship between spring snow cover in North America and summer rainfall in New Mexico. Geophys. Res. Lett., 24, 2207–2210.

Gutzler, David S., 2000: Covariability of Spring Snowpack and Summer Rainfall across theSouthwest United States. J. Climate, 13, 4018–4027.

Hahn, D. G. and J. Shukla, 1976: An apparent relationship between eurasian snow cover and indian monsoon rainfall. Journal of the Atmospheric Sciences, 33: 2461-2462.

Hassol, S. J., 2004: Impacts of a Warming Arctic: Arctic Climate Impact Assessment. 139 pp., Cambridge Univ. Press, Cambridge, U.K.

Hawkins, T. W., A. W. Ellis, J. A. Skindlov and D. Reigle, 2002: Intra-annual Analysis of the North American snow cover - monsoon teleconnection: seasonal forecasting utility. Journal of Climate, 15, 1743-1753. DOI: 10.1175/1520-0442(2002)015<1743:IAAOTN>2.0.CO;2.

Holland, M.M., C.M. Bitz, 2003: Polar amplification of climate change in coupled models. Clim Dyn., 21, 221-232, doi:10.1007/s00382-003-0332-6.

Holland, M. M., C. M. Bitz, and B. Tremblay, 2006: Future abrupt reductions in the summer Arctic sea ice. Geophys. Res. Lett., 33, L23503, doi:10.1029/2006GL028024.

Hurrell,J.W., 1995: Decadal trends in the North Atlantic Oscillation: Regional temperatures and precipitation. Science,269,676-679.

IPCC, Third Assessment Report ,Climate change, 2001.Cambridge University Press.

Jones, H. G. and J. Pomeroy, W., 1999: The ecology of snow and snow-covered systems: summary and relevance to Wolf Creek, Yukon Wolf Creek Research Basin: hydrology, ecology, environment, Proc. Workshop (Whitehorse, Yukon, Mar. 1998) ed J W Pomeroy and R J Granger, pp 1–14.

Kierkus, W. T. and W. G. Colborne, 1989: Diffuse solar radiation - daily and monthly values as affected by snow cover. Solar Energy, 42(2), 143-147.

Kripalani, R. H., S. V. Singh, A. D. Vernekar and V. Thapliyal, 1996: Empirical study on nimbus-7 snow mass and indian summer monsoon rainfall. International Journal of Climatology, 16: 23-34.

Kukla, G. & D.A. Robinson, 1981: Accuracy of operational snow and ice charts. 1981 IEEE International Geoscience and Remote Sensing Symposium Digest, 974-987.

Kumar, A. and F. Yang, 2003: Comparative influence of snow and SST variability on extratropical climate in northern winter. J. Climate, 16(13), 2248-2261.

Kvamstø, N. G., P. Skeie, and D. B. Stephenson, 2004: Impact of Labrador sea-ice extent on the North Atlantic Oscillation. Int. J. Climatol., 24, 603–612.

Leathers, D.J., and D.A. Robinson, 1993: The association between extremes in North American snow cover extent and United States temperature. J. Climate, 6, 1345–1355.

Lindsay R.W., J. Zhang, 2005: The Thinning of Arctic Sea Ice, 1988–2003: Have We Passed a Tipping Point? J. Clim., 18, 4879-4894.

Magnusdottir, G., C. Deser, and R. Saravanan, 2004: The effects of North Atlantic SST and sea-ice anomalies on the winter circulation in CCM3. Part I: Main features and storm-track characteristics of the response. J. Climate, 17, 857-876.

Marshall, S., R.J. Oglesby, and A.W. Nolin, 2003: The predictability of winter snow cover over the western United States. J. Climate, 16, 1062– 1073.

Matsui, T., V. Lakshmi, E. E. Small., 2005: The Effects of Satellite-Derived Vegetation Cover Variability on Simulated Land–Atmosphere Interactions in the NAMS. Journal of Climate, 18:1, 21-40.

McCabe, G. J., and D.R. Legates, 1995: Relationships between 700 hPa height anomalies and 1 April snowpack accumulations in the western USA. International Journal of Climatology, 15: 517–530. doi: 10.1002/joc.3370150504.

McClelland, J. W., R. M. Holmes, B. J. Peterson, and M. Stieglitz, 2004: Increasing river discharge in the Eurasian Arctic: Consideration of dams, permafrost thaw, and fires as potential agents of change. J. Geophys. Res., 109, D18102, doi:10.1029/2004JD004583.

McClelland, J. W., S. J. De´ry, B. J. Peterson, R. M. Holmes, and E. F. Wood, 2006: A pan-arctic evaluation of changes in river discharge during the latter half of the 20th century. Geophys. Res. Lett., 33, L06715, doi:10.1029/2006GL025753.

Meier, W., J. Stroeve, F. Fetterer, K. Knowles, 2005: Reductions in Arctic sea ice cover no longer limited to summer. Eos, Transactions of the American Geophysical Union 86(36): 326, doi:10.1029/2005EO360003.

Mote, Thomas L., 2008: On the Role of Snow Cover in Depressing Air Temperature. J. Appl. Meteor. Climatol., 47, 2008–2022. doi: 10.1175/2007JAMC1823.1.

Namias, J., 1985: Some empirical evidence for the influence of snow cover on temperature and precipitation. Monthly weather review, 113: 1542-1552.

Nelson Frederick E., O. A. Anisimov, N. I. Shiklomanov, 2001: Subsidence risk from thawing permafrost. Nature, 410, 889-890, doi:10.1038/35073746.

Parkinson, C. L., D. J. Cavalieri, P. Gloersen, H. J. Zwally, and J. C. Comiso, 1999: Arctic sea ice extents, areas, and trends, 1978-1996. Journal of Geophysical Research – Oceans, 104(C9): 20,837.

Payette, S., A. Delwaide, M. Caccianiga, and M. Beauchemin, 2004: Accelerated thawing of subarctic peatland permafrost over the last 50 years. Geophys. Res. Lett., 31, L18208, doi:10.1029/2004GL020358.

Peterson Bruce J., R. M. Holmes, J. W. McClelland, C. J. Vörösmarty, R. B. Lammers, A. I. Shiklomanov, I. A. Shiklomanov, and S. Rahmstorf, 2002: Increasing River Discharge to the Arctic Ocean. Science, 298 (5601), 2171, DOI: 10.1126/science.1077445.

Polyakov I.V., et al., 2005: One more step toward a warmer Arctic. Geophys. Res. Lett., 32, L17605.

Raisanen, J., 2008: Warmer climates: less or more snow? Climate Dynamics, 30, 307-319, doi: 10.1007/s00382-007-0289-y.

Rawlins M A, Serreze M C, Schroeder R, Zhang X, and McDonald K C, 2009: Diagnosis of the record discharge of Arctic-draining Eurasian Rivers in 2007. Environ. Res. Lett., 4 045011.

Rayner, N. A., D. E. Parker, E. B. Horton, C. K. Folland, L. V. Alexander, D. P. Rowell, E. C. Kent, and A. Kaplan, 2003: Global analysis of sea surface temperature, sea ice, and night marine air temperature since the late nineteenth century. Journal of Geophysical Research, 108(D14): 4407, doi 4410.1029/2002JD002670.

Rigor, I.G., and J.M. Wallace, 2004: Variations in the age of Arctic sea-ice and summer sea-ice extent. Geophysical Research Letters, 31: L09401, doi:10.1029/2004GL019492.

Rigor, I.G., R.L. Colony, and S. Martin, 2000: Variations in Surface Air Temperature in the Arctic from 1979-1997. J. Climate, 13, 5, 896 - 914.

Rigor, I. G., J. M. Wallace, and R. L. Colony, 2002: Response of sea ice to the Arctic Oscillation. J. Climate, 15, 2648–2663.

Robinson, D. A., 1993: Hemispheric snow cover from satellites. Annals of Glaciology, 17: 367-371.

Robinson, D.A., 1999: Northern Hemisphere snow extent during the satellite era. Preprints: Fifth Conference on Polar Meteorology and Oceanography, Dallas, TX. American Meteorological Society, 255-258.

Robinson, D.A., and A. Frei, 2000: Seasonal variability of northern hemisphere snow extent using visible satellite data. Professional Geographer , 51, 307-314.

Robok A., and M. Mu, 2003: Land surface conditions over Eurasia and Indian summer monsoon rainfall. J. Geophys. Res., 108(D4), 4131.

Rothrock D. A , J. Zhang, 2005: Arctic Ocean sea ice volume: What explains its recent depletion? J. Geophys. Res., 110, C01002.

Rothrock, D.A., Y. Yu, G.A. Maykut, 1999: Thinning of the arctic sea-ice cover, Geophys. Res. Lett., 26(23), 3469-72.

Rothrock, D. A., J. Zhang, and Y. Yu, 2003: The arctic ice thickness anomaly of the 1990s: A consistent view from observations and models. J. Geophys. Res., 108(C3), 3083, doi:10.1029/2001JC001208.

Sankar-Rao, M., K. M. Lau, and S. Yang, 1996: On the relationship between eurasian snow cover and the asian summer monsoon. International Journal of Climatology, 16: 605-616.

Saunders, M. A., Q. Qian, and B. Lloyd-Hughes, 2003: Summer snow extent heralding of the winter North Atlantic Oscillation. Geophysical Research Letters, 30: 1378, doi:1310.1029/2002GL016832.

Seierstad, I. A., and J. Bader, 2008: Impact of a projected future Arctic sea ice reduction on extratropical storminess and the NAO. Clim. Dyn., doi10.1007/s00382-008-0463-x, in press.

Serreze M., and Barry R.G., 2005: The Arctic Climate System. Cambridge University press.

Serreze, M. C., J. E. Walsh, F. S. Chapin III, T. Osterkamp, M. Dyurgerov, V. Romanovsky, W. C. Oechel, J. Morison, T. Zhang and R. G. Barry, 2000: Observational Evidence of Recent Change in the Northern High-Latitude Environment. Climatic Change, 46: 159-207.

Serreze M.C., M. M. Holland, J. Stroeve, 2007: Perspectives on the Arctic's Shrinking Sea-Ice Cover. Science, 315: 1533-1536, DOI:10.1126/science.1139426.

Serreze, M. C., A. P. Barrett, J. C. Stroeve, D. N. Kindig, and M. M. Holland, 2009: The emergence of surface-based Arctic amplification. The Cryosphere, 3, 11–19.

Sewall, J. O., 2005: Precipitation shifts over western North America as a result of declining Arctic sea ice cover: The coupled system response. Earth Interact., 9, 1–23.

Singarayer, J.S., J.L. Bamber, and P.J. Valdes, 2006: Twenty-first-Century climate impacts from a declining Arctic sea ice cover. J. Climate, 19, 1109-1125.

Steele M., T. J. Boyd, 1998: Retreat of the cold halocline layer in the Arctic Ocean. J. Geophys. Res., 103, 10419.

Stroeve, J. C., M. C. Serreze, F. Fetterer, T. Arbetter, W. Meier, J. Maslanik, and K. Knowles, 2005: Tracking the Arctic's shrinking ice cover: Another extreme September minimum in 2004. Geophysical Research Letters, 32, doi:10.1029/2004GL021810.

Stroeve J., M. M. Holland, W. Meier, T. Scambos, M. Serreze, 2007: Arctic sea ice decline: Faster than forecast. Geophys. Res. Lett., 34, L09501, doi:10.1029/2007GL029703.

Tedesco, M., and J. Miller, 2007: Northern Hemisphere snow-covered area mapping: optical versus active and passive microwave data. IEEE Geoscience and Remote Sensing Letters, 4(2): 221-225.

Thompson, D. W. J., and J. M. Wallace, 1998: The Arctic Oscillation signature in the wintertime geopotential height and temperature fields. Geophys. Res. Lett., 25, 1297– 1300.

Wagner, J.A., 1973: The influence of average snow depth on monthly mean temperature anomaly. Mon. Wea. Rev., 101(8), 624-626.

Walsh, J. E., D. R. Tucek, M. R. Peterson, 1982: Seasonal Snow Cover and Short-Term Climatic Fluctuations over the United States. Mon. Wea. Rev., 110, 1474–1486.

Walsh, John E., W. H. Jasperson, B. Ross, 1985: Influences of Snow Cover and Soil Moisture on Monthly Air Temperature. Mon. Wea. Rev., 113, 756–768.

Wang, M., and J. E. Overland, 2009: A sea ice free summer Arctic within 30 years? Geophys. Res. Lett., 36, L07502, doi:10.1029/2009GL037820.

Williamson, S., M. Ruth, K. Ross and D. Irani, 2008: Economic impacts of climate change on New Jersey. The Center for Integrative Environmental Research (CIER) at the University of Maryland,19pp .

Wu, P., R. Wood, and P. Stott, 2005: Human influence on increasing Arctic river discharges. Geophys. Res. Lett., 32, L02703, doi:10.1029/2004GL021570.

Yang, D., Y. Zhao, R. Armstrong, D. Robinson, and M.-J. Brodzik, 2007: Streamflow response to seasonal snow cover mass changes over large Siberian watersheds. J. Geophys. Res., 112, F02S22, doi:10.1029/2006JF000518.

Yasunari, T., A. Kitoh, and T. Tokioka, 1991: Local and remote responses to excessive snow mass of Eurasia appearing in the northern spring and summer climate: A study with the MRI GCM. J. Meteor. Soc. Jpn., 69, 473– 487.

Zhang, T., et al., 2005: Spatial and temporal variability in active layer thickness over the Russian Arctic drainage basin. J. Geophys. Res., 110, D16101, doi:10.1029/2004JD005642.

Zhang, X., and J. E. Walsh, 2006: Towards a seasonally ice-covered ArcticOcean: Scenarios from the IPCC AR4 simulations. J. Clim., 19, 1730–1747.

Zhu, C., Dennis P. Lettenmaier, Tereza Cavazos, 2005: Role of Antecedent Land Surface Conditions on North American Monsoon Rainfall Variability. Journal of Climate, 18:16, 3104-3121.

Chapter 2

Research Objectives and Approach

2.1 Overall Goals:

Since most earlier studies focused on SNE, the first objective is to study the land-surface SND response to variability in atmospheric circulation. Due to the lack of long-term and reliable SND data over Eurasia (as also discussed in section 1.1.2), we focus mainly on North America SND variability. This portion of the research will also shed light on the potential drivers of winter and spring snow pack variability. These particular seasons are immensely significant because the summer water supply depends on the winter-spring snow pack.

The second objective is focused on the identification of any climate change, and/or sea ice related signal in the observed land-surface snow cover record. Snow not only responds to the atmospheric circulation, but also it is vulnerable to the generalized warming &/ recent pan-arctic atmospheric changes induced by Arctic sea ice (as discussed in section 1.1 and 1.2.3 from chapter 1). The spatial domain of this section includes the extra-tropical regions of Northern Hemisphere. The novelty of this part of the thesis lies in the study of a cryospheric teleconnection. Here, the term 'teleconnection' refers to how the state of the atmosphere, ocean and land surfaces at remote locations affects the conditions at another place (Dery et al., 2005). It is reasonable to hypothesize that because the land, atmosphere, cryosphere, and ocean are all components of the climate system, that they are intertwined through complex

feedback mechanisms and feedback loops which have components operate within each of these components too (IPCC, 2001).

2.2 Specific Objectives:

2.2.1 Objective 1:

1st objective is focused on an under-utilized snow pack metric, snow depth, and its response to the major winter climate teleconnection modes over North America, specifically the NAO and the PNA. This research will identify the specific mechanistic pathways through which the NAO and the PNA drive snow depth variability. For this purpose, atmospheric parameters (e.g. air temperature and snowfall) and seasonal lags are evaluated to develop an understanding of the physical processes involved.

2.2.2 Objective 2:

Here, we focus on whether there is currently any observational evidence of an emerging climate change signal, and/or sea ice related signal in Northern Hemisphere snow cover changes. Land-surface snow cover is vulnerable to the recent Arctic-wide warming. Moreover, GCMs suggest a future loss of snow in response to the greenhouse gases warming, as discussed in chapter 1 (Frei and Gong, 2005; Barry et al., 2007; Räisänen, 2007). In addition, modeling experiments also describe the expected changes in snow due to declining sea ice in the future (also discussed in chapter 1) (Deser et al., 2010). To meet this objective, we investigate the observed covariance between early season snow and the preceding summer sea ice, and the modeled covariance between these two fields for both recent and future time periods. This analysis is based on measures of statistical correlation, and is therefore unable to establish causation.

2.2.3 Objective 3:

To establish potential cause-and-effect relationships, a suite of Community Atmospheric Model version 3 (CAM3) experiments, which are designed to isolate the effects of SST and sea ice from the generalized warming due to the increased greenhouse gases, is utilized. Therefore, if the analysis for the second objective identifies any statistical link between snow and sea ice, this modeling study can be used to establish cause-and-effect relationships. Details about the model and the experiments are discussed in chapter 5. In summary, objective 2 and 3 together examines the linkage between snow and sea ice and also investigates any climate change signal in the observed snow cover.

2.3 Dissertation Outline:

Chapter 3 Objective 1. Winter climate modes and North American snow depth variations.

Chapter 4: Objective 2. Identification of covariability between Arctic Sea Ice losses and Northern Hemisphere snow variations.

Chapter 5: Objective 3. Investigation of cause-effect relationships between Arctic Sea Ice losses and high latitude snow variations.

Chapter 6: This chapter will summarize the conclusions drawn from this thesis and the limitations of this research. In addition, the future prospect will also be discussed, which will help to continue further this line of research

2.4 References

Barry, R. G., R. Armstrong, T. Callaghan, J. Cherry, S. Gearhead, A. Nolin, D. Russell, and C. Zockler, 2007: Snow, in Global Outlook for Ice and Snow. pp. 39-62, UNEP (Ed.), Nairobi, Kenya.

Déry, S. J., J. Sheffield, and E. F. Wood, 2005: Connectivity between Eurasian snow cover extent and Canadian snow water equivalent and river discharge. J. Geophys. Res., 110, D23, D23106, doi: 10.1029/2005JD006173.

Deser, C., R. Tomas, M. Alexander, and D. Lawrence, 2010: The Seasonal Atmospheric Response to Projected Arctic Sea Ice Loss in the Late Twenty-First Century. J. Climate, 23, 333–351.

Frei, A., and G. Gong, 2005: Decadal to century scale trends in North American snow extent in coupled Atmosphere-Ocean General Circulation Models. Geophysical Research Letters, 32: L18502, doi:10.1029/2005GL023394.

IPCC, Third Assessment Report, Climate change, 2001.Cambridge University Press.

Raisanen, J., 2008: Warmer climates: less or more snow? Climate Dynamics, 30, 307-319, doi: 10.1007/s00382-007-0289-y.

Chapter 3

North American Temperature, Snowfall and Snow Depth Response to Winter Climate Modes

Debjani Ghatak[1*], Gavin Gong[2], Allan Frei[1,3]

[1] Program in Earth and Environmental Sciences, The Graduate Center, The City University of New York, New York, NY

[2] Department of Earth and Environmental Engineering, Columbia University, New York, NY

[3] Department of Geography, Hunter College, The City University of New York, New York, NY

Part of this chapter has been published in Journal of Climate as: Ghatak, Debjani, Gavin Gong, Allan Frei, 2010: North American Temperature, Snowfall, and Snow-Depth Response to Winter Climate Modes. J. Climate, 23, 2320–2332. doi: 10.1175/2009JCLI3050.1

3.1 Abstract:

The snowpack is an important seasonal surface water storage reservoir that affects the availability of water resources during the spring and summer seasons in mid to high latitudes. Not surprisingly, interannual variations in snow cover extent and snow water equivalent have been extensively studied in arid regions such as western North America. This study broadens the focus by examining snow depth as an alternative snowpack metric, and considers its variability over different parts of North America. We use singular value decomposition (SVD) in conjunction with linear and partial correlation to show that regional snow-depth variations can be largely explained by the winter North Atlantic Oscillation (NAO) and the Pacific-North American (PNA) modes of atmospheric variability, through distinct mechanistic pathways involving regional winter circulation patterns and hydrologic fluxes. The high index phase of the NAO generates positive winter air temperature anomalies over eastern parts of North America, causing thinning of the winter snowpack via snowmelt. Meanwhile, the high index phase of the PNA generates negative winter snowfall anomalies across mid-latitudinal areas of North America, which also serve to thin the snowpack. Positive PNA anomalies have also been shown to increase temperatures and decrease snow depths over western North America. The PNA influence extends across the continent; whereas the NAO influence is limited to eastern North America. The winter snow-depth variations associated with all of these pathways exhibit seasonal persistence, which ultimately yield regional-scale spring snow-depth anomalies throughout much of North America.

3.2 Introduction

Snow cover modulates many components of the energy balance over terrestrial surfaces (Namias, 1985; Ellis and Leathers, 1999; Grundstein, 2003; Zhang, 2005). The high solar reflectivity of snow covered vs. snow-free surfaces is traditionally considered to be the most influential factor. However, this reflectivity also partially depends on the diffusive properties and hence the mass (i.e., thickness) of the snowpack (Armstrong and Brun, 2008). Baker et al. (1991) showed that a discernible layer of snow is required for albedo to reach 0.7; this depth varies from 5cm for bare soil to 15cm for alfalfa cover. Other energy fluxes such as sensible-heat conduction between the ground, snowpack and surface air, and latent heat via snowmelt and sublimation, are also influenced by both the presence and mass of the snowpack (McFadden and Ragotzkie, 1967; Cohen, 1994).

The response of snow to climate drivers has been studied over the past several decades. Although snow extent (SNE) has been investigated most extensively, snowpack mass expressed as snow water equivalent (SWE) has also received considerable attention. These SWE studies have largely been motivated by the need to assess water resource availability for specific regions such as the mountainous western United States (e.g., Cayan, 1996; McCabe and Dettinger, 2002; Jin et al., 2006; Mote, 2006). Collectively they portray a modest and ambiguous SWE response to large scale teleconnections such as the Pacific North American (PNA) pattern, the El Nino-Southern Oscillation (ENSO), and the Pacific Decadal Oscillation (PDO), which suggests that our understanding of snow-climate linkages is incomplete. Studies using North American snow depth (SND, the total depth of old and new snow on the ground) are less common, although the

recently released Dyer and Mote (2006) (hereafter DM06) SND data provides the opportunity for research at continental scales. For example, DM06 reported significant negative trends in spring SND over vast areas of Canada along with a retreat of the deepest (>40 cm) SND. Ge and Gong (2009) reported a link between spring SND over much of North America and Pacific climate variability as expressed through the PNA and the PDO modes. Their results are consistent with the previous SWE based regional studies.

The PNA pattern is considered a dominant mode of winter atmospheric variability over North America (Wallace and Gutzler, 1981; Barnston and Livezey, 1987). It is tied strongly to the surface climate variability via associated regional temperature and precipitation anomalies (Leathers et al., 1991). The PNA pattern is often depicted through four concurrent geopotential height anomalies centered over Hawaii, the North Pacific, western Canada, and the southeast United States (US). The positive phase of this pattern corresponds to anomalously high ridges over Hawaii and western Canada, and anomalously deep troughs over the North Pacific and the southeastern United States, while the negative phase corresponds to lower ridges and shallower troughs over these same regions. The position of the mean stationary waves determines the spatial location of this teleconnection (Leathers et al., 1991). Recently, Ge et al. (2009; hereafter GGF09) identified two distinct physical mechanisms through which the winter PNA influences spring SND, involving the aforementioned regional temperature and precipitation variations. During the positive phase, the enhanced ridge over western Canada interrupts the cold Arctic air flow into this region, which leads to increased air temperature and melting of the snowpack. At the same time, the blockage of westerly flow from the

Pacific and southerly flow from the Gulf of Mexico (due to an enhanced southeast US trough) decreases oceanic moisture influx and thus reduces the precipitation across the mid-latitude US. These regional winter patterns result in a diminished winter SND over much of North America; these anomalies then persist into spring.

The North Atlantic Oscillation (NAO) is another major source of inter-annual and decadal-scale variability in the winter atmospheric circulation over North America (Walker and Bliss, 1932; Wallace and Gutzler, 1981; Barnston and Livezey, 1987; Hurrell, 1995, 1996; Wettstein and Mearns, 2002). Years with a positive NAO index are identified by an enhanced Icelandic low-pressure center and Azores high-pressure center. Anomalous southerly flow over the eastern US, and anomalous northerly flow over Western Greenland and the Canadian Arctic are typically observed during positive NAO years. Correspondingly, higher temperatures occur over the eastern US and lower temperatures occur over Quebec (Wettstein and Mearns, 2002). These anomalies can potentially affect the regional snowpack. Prior studies involving snowfall and SWE have reported only modest relationships with the NAO (Hartley and Keebles, 1998; Morin et al., 2007; Sobolowski and Frei, 2007), but the response of SND has yet to be explicitly considered.

The objective of this study is to develop a physically based understanding of the continental-scale SND response to the major winter climate teleconnection modes over North America, specifically the NAO and the PNA, as is already discussed in chapter 2 (Research Objectives and Approach). By considering all of North America, we broaden our focus beyond regional water management in the western US. This is reasonable since climate teleconnections may not be regionally constrained and can span continents. By

evaluating SND, we consider an underutilized snowpack metric, facilitated by a recently available gridded North American SND dataset (see Section 3.3). By considering Atlantic as well as Pacific teleconnections, we build upon recent work by GGF09 that has focused primarily on Pacific drivers, thereby providing a more spatially robust explanation of climate-driven North American SND variability. Here, we develop a mechanistic understanding of the physical processes involved by analyzing climatic fields and seasonal lags.

Figure 1 shows generalized physical pathways that are investigated, through which winter climate modes can potentially affect SND. A temperature pathway (denoted by black arrows) considers the effect of winter temperature anomalies on concurrent SND, while a snowfall pathway (denoted by grey arrows) considers the effect of winter snowfall variability on concurrent SND. Winter anomalies are hypothesized to persist into the spring season. Each step in Figure 1 is systematically investigated using empirical observations and spatio-temporal statistics including singular value decomposition analysis (SVD, see Section 3.4), to discern the responsible climate modes and their regions of influence. For all analyses, mean DJF (December, January and February) and MAM (March, April and May) quantities have been used to represent the winter and spring season, respectively. We discuss the datasets used in this project in section 3.3, and the analytical methodology in section 3.4. Results are presented in Section 3.5, and conclusions are provided in section 3.6, including a discussion of how the work presented here complements that of GGF09.

3.3 Datasets

Snow Depth (SND) and Snowfall (SNF):

We use gridded data described in DM06, which was generated from station observations throughout the United States and Canada. This was gridded following the Shepard (1968) interpolation procedure. These datasets offer a fine spatial (1^0 X 1^0) resolution over all of North America, and temporal (daily) resolution for the last 100 years. The most recent version of these datasets which are available from the Rutgers University global snow lab (http://climate.rutgers.edu/snowcover/) extends from 1900-2003. This study is limited to the period 1979–2003, however, since for much of the 20th century the available station data is sparse and unevenly distributed, resulting in erroneous interpolated gridcell values. This time domain also has the benefit of falling within the period of the satellite remote sensing snow cover record, which serves as an independent data source for validating the DM06 dataset (Ge and Gong, 2008). More detailed information on this dataset pertaining to quality control, validation, weaknesses and applicability to continental-scale studies, has been provided in DM06, Ge and Gong (2008) and GGF09, and will not be repeated here. Furthermore, Kluver (2007) explicitly examined the reliability of DM06 snowfall dataset. We present results from SVD analyses (Section 3.5), which show significant correlations over regions characterized by high station densities according to Kluver's analysis.

Figure 2 provides a visual representation of the magnitude and variability of SND at each grid point for both winter and spring. First, an interannual SND time series is computed for each season (not shown) using the area-weighted average SND over North America following Ge and Gong (2008). For each season's time series, the year with the maximum and the year with the minimum value are identified. The seasonal mean SND

at each grid point for these years is shown in Figure 2. Alaska, the Rocky Mountains and northern Canada exhibit the deepest layers (>80cm) of snow.

Atmospheric Temperature Fields:

In this study, we use global reanalysis datasets from National Centers for Environmental Prediction/National Center for Atmospheric Research (NCEP/NCAR) (Kalnay et al., 1996). We extract monthly mean temperatures at the 925 hPa level (hereafter T925) to represent lower atmosphere temperature. We derive seasonal averages from the monthly fields, for the entire extratropical (20^0N to 90^0N) Northern Hemisphere, at a spatial resolution of 2.5^o x 2.5^o. Temperatures at 850hPa and 1000 hPa levels were also extracted, and yielded qualitatively identical results as for the 925 hPa level.

Teleconnection Indices:

A winter NAO index timeseries is acquired from the National Center for Atmospheric Research (http://www.cgd.ucar.edu/cas/jhurrell/indices.data.html#naostatmon), computed as the difference in normalized sea level pressures (SLP) between Ponta Delgada, Azores and Stykkisholmur/Reykjavik, Iceland. Results (Section 3.5) using this station-based NAO index hold true when we repeated the analyses with the NAO index from Climate Prediction Center (http://www.cpc.noaa.gov/products/precip/CWlink/pna/nao.shtml#discussion), as computed through rotated principal component analysis of monthly standardized 500mb height anomalies. A winter PNA index timeseries is acquired from the National Oceanic and Atmospheric Administration (NOAA) Climate Prediction Center

(http://www.cpc.noaa.gov/products/precip/CWlink/pna/pna.shtml), computed from four regionally averaged H500 values following their modified pointwise method.

3.4 Methodology

Singular Value Decomposition Analysis (SVD):

SVD is an established method for identifying the temporal co-variability between two climatic spatial fields (Prohaska, 1976; Lanzante, 1984; Wallace et al., 1992; Cherry, 1997; Rajagopalan et al., 2000). We employ SVD on various combinations of gridded fields during the winter (DJF) and spring (MAM) seasons. Here, timeseries at each grid point have been detrended via ordinary least squares regression to remove the influence of linear trends on the explained covariance. Our SVD analysis utilizes the correlation matrix approach since the coupled fields have different units of measurements. It produces pairs of spatial patterns that explain the maximum mean-squared temporal covariance between the two fields (Bretherton et al., 1992); SVD spatial patterns in each field follow orthogonality constraints. It also generates associated pairs of temporal expansion coefficient (TC) timeseries that describe the temporal variations in the SVD spatial patterns. We present the spatial patterns as heterogeneous correlation (HC) maps. The k^{th} HC map shows Pearson correlations between the detrended timeseries at each grid point for one field and the k^{th} TC of the other field, thus describing how well the spatial pattern of one field can be explained by the k^{th} TC of another field. Non-parametric Spearman rank correlations were also examined, and the results are consistent with those using Pearson correlations (not shown).

Correlation and Partial-Correlation Analysis:

Linear Pearson correlations and partial correlations are also applied directly to various combinations of climatic data and SVD extracted TCs; only results that exceed the 95% confidence level have been reported. Partial correlations identify the remaining linear relationship between two variables after the influence of a third variable has been removed, which is useful for discerning the intervening or antecedent role of a variable in a causal link between two other variables (Blalock, 1961). The partial correlation between X and Y, given Z as a third variable, is expressed as $r_{XY|Z} = \frac{r_{XY} - r_{XZ} r_{YZ}}{\sqrt{(1 - r_{XZ}^2)(1 - r_{YZ}^2)}}$. This value approaches zero if Z is responsible for nearly all correlation between X and Y, and approaches the basic Pearson correlation value r_{XY} if the correlation between X and Y is unrelated to Z.

3.5 Results

Two analogous series of analyses are performed in section 3.5.1 and 3.5.2 to identify distinct temperature and snowfall pathways, each associated with different climate modes.

3.5.1 Temperature Pathway

Covariability between winter temperature and snow depth fields reveals the NAO signal

We start with an SVD analysis between the winter T925 and winter SND fields to evaluate the temperature pathway shown in Figure 1. The HC maps for the leading mode, which explains 31% of the total co-variability, are shown in Figure 3a, b. The winter SND pattern is mainly centered over eastern North America along with a second, less coherent region of co-variability over northwestern North America. The winter T925 pattern exhibits regions that vary in phase (out of phase) with winter SND over

Greenland, the Bering Sea and North Africa (east and central North America and northern Eurasia). Over eastern North America, we find the expected local anti-correlation of temperature and SND.

A similar analysis has been performed between the winter T925 and spring SND. The HC maps for the leading mode, which explains 29% of the total co-variability, are shown in Figure 3c, d. The spring SND covariability pattern (Figure 3c) shifts northwest to central interior North America following the poleward retreat of the snow line from winter to spring. This central interior SND covariability region is more apparent in spring than winter, since winter T925 anomalies can affect the thermal content of the winter snowpack more than its thickness. Consequently, this may make spring snowpack vulnerable to the positive temperature anomalies and may lead to the faster loss of spring SND. Overall, winter lower atmosphere temperatures exhibit notable structured covariability with both winter and spring SND over North America. Their similarities (Figure 3b, d) suggest a common climatic driver whose impact on SND is readily visible in winter and spring.

Note that the hemispheric-scale HC1 patterns of T925 (Figure 3b, d) from both analyses are similar to the spatial pattern of temperature variations associated with the NAO (Hurrell, 1996). Furthermore, Tables 1 and 2 indicate that the TC1 timeseries are highly and consistently correlated with each other and with the winter NAO. Thus an NAO signature appears in the principal co-variability between winter T925 and both winter and spring SND fields, whereby the negative NAO anomalies produce negative T925 anomalies and consequently positive SND anomalies over eastern and central parts of North America, and vice-versa.

Although the winter NAO appears to be a driving force behind winter T925 and winter-spring SND covariability, it is unlikely to physically extend as far as northwestern North America so as to affect the modest SND covariability with T925 during winter for this region indicated in Figure 3a. Thus, a different climatic driver may also be involved with the covariability between SND and T925. The PNA is a likely candidate, since it is known to exert a strong climatic influence over northwestern NA.

We also present the correlation coefficients associated with 2nd SVD mode in Tables 1 and 2. TC2 timeseries for winter SND and winter temperature are highly correlated with each other and with the winter PNA (Table 1). Table 2 does not show any TC2 relationship with the winter PNA. However, the TC1 timeseries for spring SND exhibits a significant relationship with the winter PNA as well as with the winter NAO. Note that for the 1st SVD mode between winter temperature and spring SND, the spring SND region of covariability (Figure 3c) is located northwest of the winter SND region (Figure 3a), approaching the region of known PNA influence, suggesting that a PNA signal may be present in this 1st TC.

Thus in addition to the primary NAO signature revealed in the first mode of our SVD analyses of winter T925 vs. winter-spring SND, a secondary PNA signature is also apparent. This result is consistent with GGF09, which derived a component of NA SND variability associated with the PNA mode and identified a physical pathway involving temperatures over northwestern NA. For this study, it appears clearly in the second SVD mode when winter SND is considered (Table 1), but rather vaguely in the first SVD mode with spring SND considered (Table 2). Note that SVD analysis identifies mathematically orthogonal modes of variability, but these modes may not necessarily represent

physically distinct phenomena. The same physical relationship may be reflected in more than one mode, and conversely a single mode may reflect more than one physical pathway. Similarities and differences between this study and GGF09 are discussed in Section 3.6.

Confirming the NAO–temperature pathway

To confirm that the dominant winter pattern of co-variation between the temperature and snow depth fields is associated with the NAO, we perform additional correlation and partial-correlation analyses. First, the winter 500 hPA geopotential height field is correlated against the TC1 winter T925 time series resulting from its SVD analysis with winter SND. Figure 4 shows that a strong dipole pattern results, with one center stretching from eastern North America across the sub-tropical Atlantic, and an opposing center over Greenland. This figure resembles the NAO pattern, although the areas of correlations are more extensive. Then, gridpoint winter SND is correlated directly against the winter NAO index, as shown in Figure 5a. Significant negative correlations occur mainly over the eastern United States, largely co-located with the region of highest co-variability in the HC map between winter SND and T925 (Figure 3a) which is also correlated with the NAO (Table 1). Thus the direct linear relationship between winter SND and the NAO is consistent with the temperature pathway discerned from SVD analysis, and the eastern North America center of co-variability is reasonable since the NAO has its centers of action in the North Atlantic sector.

The results thus far indicate that the winter NAO mode anomalies result in winter SND anomalies over eastern North America, via co-located winter temperature anomalies. To confirm that temperature is a physical mechanism linking the NAO and

SND, a partial-correlation analysis is performed to determine the remaining correlation between winter gridpoint SND and the winter NAO, after removing the effect of winter temperature. We use the TC1 timeseries of winter T925 resulting from its SVD analysis with winter SND (denoted as TC1 DJF $T925_{DJF\ SND}$) to represent winter temperature, since this component of temperature variability is associated with both SND and the NAO as indicated in Table 1. The partial correlation can be represented symbolically as r(DJF SND, DJF NAO | TC1 DJF $T925_{DJF\ SND}$). The result is shown in Figure 5b, which indicates that after removing TC1 DJF $T925_{DJF\ SND}$, there is essentially no remaining correlation between the winter NAO and winter SND. Thus the portion of winter T925 variability that relates to winter SND and the winter NAO is responsible for the direct statistical relationship between them. This partial-correlation analysis confirms that during the winter season, SND over eastern North America responds to the NAO mode via variations in air temperature.

3.5.2 Snowfall Pathway

Covariability between winter snowfall and snow depth fields reveals the PNA signal

An SVD analysis is performed between the winter SNF and winter SND fields to evaluate the snowfall pathway shown in Figure 1. The HC maps for the leading mode, which explains 27% of the total co-variability, are shown in Figure 6a, b. Both patterns are centered over a broad mid-latitudinal band across North America, although the winter SND pattern is more widespread in the west than the winter SNF pattern. The two patterns vary in phase, which is reasonable since snowfall is expected to be directly related to SND.

A similar analysis has been performed between the winter SNF and spring SND. The HC maps for the leading mode, which explains 23% of the total co-variability, are shown in Figure 6c, d. Both patterns are similar to the HC1 patterns of winter SNF and winter SND (figure 6a, b), in phase, magnitude and location. The broad and seasonally consistent spatial patterns of these HC maps suggest that the driver of this observed covariability between SND and SNF occurs on a continental scale, and its influence on SND persists from winter into spring.

Table 3 and 4 indicate that the TC1s for both fields are significantly correlated with each other and with the winter PNA, but the TC2s are not significantly correlated with the winter PNA. Hence a PNA signature appears prominently in the principal co-variability between winter SNF and winter-spring SND fields, whereby the negative PNA anomalies produce positive SNF anomalies and consequently positive SND anomalies across much of North America, and vice-versa. Note that the winter PNA appears to influence snowfall variability over the eastern sector of the continent as well as the western sector. This is consistent with previous literature (for e.g. Coleman and Rogers, 2003; Sheridan, 2003) which reported a PNA influence on snowfall over eastern North America via moisture flux from the Gulf of Mexico.

The TC2s in Tables 3 and 4 do not exhibit a clear and consistent relationship with the winter PNA mode, which suggests that the PNA signature is effectively captured by the first mode of covariability between SND and SNF. Likewise, a relationship with the winter NAO mode is not apparent in either SVD mode. Isolated statistically significant correlations to winter NAO appear in SVD2 (Table 3) and SVD1 (Table 4), but they are not coherent and likely arise as artifacts of the SVD analysis. SVD identifies

mathematically distinct modes of covariability which are not necessarily physically distinct, while the general regions of known PNA and NAO influence overlap over eastern North America.

Confirming the PNA–snowfall pathway

Analogous to our approach for confirming the NAO–temperature pathway in Section 3.5.1, here we investigate this apparent PNA – snowfall pathway by correlating the winter 500hPa geopotential height field against the TC1 winter SNF time series resulting from its SVD analysis with winter SND. Figure 7 shows coherent alternating regions of strong and significant correlation centered over the Bering Sea, interior North America and the southeast US. This figure resembles the PNA pattern, although it has larger regions with significant correlations. We also correlate gridpoint winter SND directly against the winter PNA index (Figure 8a). Strong negative correlations occur over western North America, which is reasonable since the PNA pattern is primarily a Pacific sector phenomenon. This region also partially overlaps with the co-variability regions in the HC map between winter SND and SNF (Figure 6a) that are significantly correlated with the winter PNA (Table 3). Figures 6a and 8a are not expected to look exactly alike, since factors other than PNA can contribute to the winter SND and SNF covariability shown in Figure 6a, and PNA-SND relationship shown in Figure 8a can occur via mechanisms other than snowfall (e.g., as shown in GGF09). The relationship between PNA, SNF and SND is clearly not a simple one. Nevertheless the direct statistical relationship between PNA and SND in Figure 8a provides additional circumstantial evidence that the broad co-variability signal between SNF and SND shown in Figure 6a is associated in part with the PNA pattern.

The results thus far support the snowfall pathway illustrated in Figure 1, more specifically that the winter PNA mode anomalies result in winter SND anomalies over portions of North America, via co-located winter snowfall anomalies. To confirm that snowfall is a physical mechanism linking the PNA and SND, a partial-correlation analysis is performed, to determine the remaining correlation between winter gridpoint SND and the winter PNA, after removing the effect of winter snowfall. We use the TC1 timeseries of winter SNF resulting from its SVD analysis with winter SND (denoted as TC1 DJF $SNF_{DJF\ SND}$) to represent winter snowfall, since this component of snowfall variability is associated with both SND and the PNA as indicated in Table 3. The partial correlation can be represented symbolically as r(DJF SND, DJF PNA | TC1 DJF $SNF_{DJF\ SND}$). The result is shown in Figure 8b, which indicates that after removing TC1 DJF $SNF_{DJF\ SND}$, the only remaining significant and coherent correlation is found over the coastal mountain ranges of British Columbia and southern Alaska. Thus the portion of winter SNF variability that relates to winter SND and the winter PNA is responsible for most of the direct statistical relationship between them. This partial-correlation analysis confirms that during the winter season, SND over much of North America responds to the PNA mode via variations in snowfall.

Note that this PNA–snowfall pathway occurs across much of North America according to the SVD analysis shown in Figure 6, with an emphasis on western North America according to the linear and partial-correlation analyses shown in Figure 8. In contrast, the NAO–temperature pathway occurs over eastern North America, according to Figures 3 and 5. Hence there appear to be distinct physical mechanisms throughout

North America, over geographical regions that are consistent with the domain of their respective climatic drivers.

3.5.3 Confirming the independence of two pathways:

To demonstrate the distinction between the two pathways identified, a final set of partial correlations is performed. Figure 9a shows r(DJF SND, TC1 DJF $SNF_{DJF\ SND}$ | TC1 DJF $T925_{DJF\ SND}$), which represents the remaining correlation between winter gridpoint SND and winter SNF, after removing the effect of winter T925. Once again we use component of T925 variability that co-varies with SND as the intervening variable. Figure 9a exhibits the same pattern of co-variability as Figure 6a, which indicates that T925 has no bearing on SVD1 covariability between SND and SNF. In other words, the PNA–snowfall pathway is maintained after removing the contribution of the NAO–temperature pathway.

We use the same technique to remove the effect of winter SNF instead of winter T925. Figure 9b shows r(DJF SND, TC1 DJF $T925_{DJF\ SND}$ | TC1 DJF $SNF_{DJF\ SND}$), which represents the remaining correlation between winter gridpoint SND and winter T925, after removing the effect of winter SNF. Once again we use component of SNF variability that co-varies with SND as the intervening variable. Figure 9b exhibits the same pattern of co-variability as Figure 3a, which indicates that SNF has no bearing on SVD1 covariability between SND and T925. In other words, the NAO–temperature pathway is maintained after removing the contribution of the PNA–snowfall pathway.

Note also that when the PNA–snowfall pathway is removed in Figure 9b, a separate region of co-variability between SND and T925 begins to emerge prominently over northwestern North America. This is very similar to Figure 3a; though Figure 9b

exhibits a much stronger and more coherent signal. GGF09 revealed the PNA–driven SND anomalies over North America that involved both precipitation and temperature. Their PNA–precipitation pathway spanned mid-latitude North America and is entirely consistent with the PNA–snowfall pathway identified here. Their PNA–temperature pathway was centered over northwest of North America and is consistent with the secondary co-variability region between SND and air temperature revealed in Figure 3a and especially in Figure 9b. Hence our interpretation of Figure 3a and 9b is that when the winter snowfall is removed as an intervening variable, the SVD co-variability between winter SND and air temperature is refined and reveals two mechanistic pathways: one involving the NAO over eastern North America, and another involving the PNA over northwestern North America.

3.5.4 Persistence of winter snow depth anomalies into spring reveals signatures of atmospheric modes

Finally, an SVD analysis between the winter and spring SND fields is performed to identify the dominant spatio-temporal patterns of its seasonal persistence. This relationship represents the common final step in both pathways illustrated in Figure 1. Spatial patterns for the first mode (HC1; Figure 10a, b) explain 29% of the total co-variability between these two fields. Broad regions with significant covariability upwards of r = 0.9 are centered over northwest North America. As indicated in Table 5, the corresponding TC1 timeseries are highly correlated with each other. The spatial location and the temporal variability of the first mode suggest a possible signature of the PNA on the co-variability between winter SND and spring SND. However, Table 5 shows that

linear correlations between winter PNA and the SND TC1s are not significant at the 95% confidence level, although they are significant at the 90% confidence level.

The spatial patterns for second SVD mode (HC2; Figure 10c, d) are shifted slightly to the southeast, across southern Canada and the northern US, with broad regions of significant covariability upwards of r = 0.88 that explain 17% of the total co-variability. Table 5 indicates that the corresponding TC2 timeseries are highly correlated with each other, significantly correlated with the winter PNA (at 95% significance), and even more significantly correlated with the winter NAO. The signature of PNA on the co-variability between winter SND and spring SND is more apparent in this second SVD component of SND persistence than the first mode, and an NAO signature has also emerged, with negative correlations indicating inverse relationships. Thus the first two modes of seasonal SND persistence over North America span most of the continent and appear to be statistically related to major winter climate teleconnections; although the 1st mode is correlated with PNA at only 90% confidence level. Note that the PNA and NAO signals emerge from this analysis which includes only SND observations, with no input from any other fields.

3.6 Discussion and Conclusions

In this study, two prominent modes of atmospheric circulation, i.e. the NAO and the PNA, have been identified as major drivers of SND variability over North America. Lower atmospheric temperature and snowfall are used in conjunction with SND to identify spatially coherent patterns of co-variability within North America, which portray physically-based linkages between the climate modes and North American SND. These atmospheric linkages result in winter SND anomalies over North America that

subsequently persists into the spring season. Furthermore, the SVD analysis of winter vs. spring SND reveals the signature of the NAO and PNA teleconnections on SND observations: no corollary field (e.g. atmospheric circulation), and no *a priori* assumptions, are required to identify the PNA and NAO signatures in the SND observations.

Figure 11 shows a refined version of the generalized pathways in Figure 1, that incorporates the results of our investigation. The snowfall pathway (denoted by grey arrows) is attributed to the winter PNA mode, where the positive phase of the winter PNA is associated with below-normal snowfall across mid-latitude North America, and hence shallower winter–spring SND. Results of this study attribute the temperature pathway (denoted by black arrows) to the winter NAO mode, where the positive phase of the winter NAO is associated with above normal temperatures over eastern North America, and hence a thinner winter-spring snowpack. A separate temperature pathway attributed to the winter PNA mode (denoted by dashed arrows) was shown previously by GGF09 and is also supported by results presented here, where the positive phase of the winter PNA is associated with above normal temperatures over northwestern North America, and hence a thinner winter–spring snowpack. Taken together, these three pathways explain much of the SND variability throughout North America.

Note that SVD analysis simply identifies coherent co-variability between two specified variables, and does not necessarily identify physically distinct modes of variability over multiple variables. Hence the SVD spatial pattern resulting from one mode may arise from partially overlapping phenomena, and a phenomenon may be evident in more than one SVD pattern or in different SVD modes across different

variables. This helps to explain why for example the NAO–temperature pathway is clearly evident in the first mode of winter SND vs. T925 co-variability, but obscured within the second mode of winter vs. spring SND co-variability. This may also explain why the 2nd co-varying pattern of seasonal snow persistence is statistically related to the winter climate modes at 95% significance but the 1st co-varying pattern is not. Nevertheless, the clear, coherent and consistent patterns that result from the SVD analyses presented here provide compelling evidence for the aforementioned pathways.

Since the results presented here are consistent with the results of GGF09, it is informative to discuss the similarities and differences between these two studies. Both apply the DM06 dataset over the full North American spatial domain, use the same PNA index timeseries, and consider the winter–spring season. However, GGF09 used a one-parameter EOF filtering procedure on SND in order to extract its specific relationship to the PNA and the associated atmospheric pathways. In contrast, here we use two-parameter SVD analyses to identify the specific patterns of co-variability between various combinations of variables along the pathways, and statistically link them with climate teleconnections without *a priori* identifying the PNA or any particular signal as a mechanism. Hence our study complements GGF09, by broadening the suite of climate teleconnections which influence winter–spring SND variability over North America. In particular, the PNA–snowfall pathway across mid-latitude North America identified here echoes the PNA–precipitation pathway in GGF09. Moreover, a physical linkage with the winter NAO is revealed here that contributes to the second-most dominant mode of seasonal SND persistence, and is manifest as an NAO–temperature pathway over eastern North America.

Recent studies (e.g. Feldstein, 2000; Riviere and Orlanski, 2007) show that the NAO and PNA have time scales of about 10 days and intra-seasonal variability cannot be captured through the mean seasonal (winter or spring) index, as applied in this chapter. Thus, there is a future scope of research to investigate how the variations in the NAO and PNA affect SND variability at shorter time scale as opposed to inter-annual time scale.

3.7 Acknowledgements:

We thank Dr. Yan Ge for many helpful discussions and James McCreight for his help. We also acknowledge the support of Dr. David Robinson and Thomas Estillow (Rutgers University Global Snow Lab) for providing us data and for helping with any data related question. We are also thankful to National Oceanic and Atmospheric Administration (NOAA) Physical Sciences Division for providing reanalysis products. Moreover, we are grateful to the anonymous reviewers for their detailed and constructive comments and suggestions which enhanced the quality of the manuscript. This work has been partially supported by the NASA Cryospheric Sciences Division (#NNX08AQ70G).

3.8 References:

Armstrong, R. L., and E. Brun, 2008: Snow and Climate: Physical Processes, Surface Energy Exchange and Modeling. Cambridge University Press, 256 pp.

Baker, D., R. Skaggs, and D. Ruschy, 1991: Snow Depth Required to Mask the Underlying Surface. J. Appl. Meteor., 30, 387–392.

Barnston, A.G., and R.E. Livezey, 1987: Classification, Seasonality and Persistence of Low-Frequency Atmospheric Circulation Patterns. Mon. Wea. Rev., 115, 1083–1126.

Blalock, H., 1961: Causal inferences in nonexperimental research. Chapel Hill, NC, UNC Press, 193pp.

Bretherton, C.S., C. Smith, and J.M. Wallace, 1992: An intercomparison of methods for finding coupled patterns in climate data. J. Climate, 5, 541–560.

Cayan, D.R., 1996: Interannual climate variability and snowpack in the western United States. J.Climate, 9, 928-948.

Cherry, S., 1997: Some Comments on Singular Value Decomposition Analysis. J. Climate, 10, 1759–1761.

Cohen, J., 1994: Snow cover and climate. Weather, 49, 150-156.

Coleman, J.S.M., and J.C. Rogers, 2003: Ohio River Valley Winter Moisture Conditions Associated with the Pacific–North American Teleconnection Pattern. J. Climate, 16,969–981.

Dyer, J. L., and T. L. Mote, 2006: Spatial variability and trends in snow depth over North America. Geophysical Research Letters, 33(L16503): doi:10.1029/2006GL027258.

Ellis, A.W., and D.J. Leathers, 1999: Analysis of Cold Airmass Temperature Modification across the U.S. Great Plains as a Consequence of Snow Depth and Albedo. J. Appl. Meteor., 38, 696–711.

Feldstein, S.B., 2000: The Timescale, Power Spectra, and Climate Noise Properties of Teleconnection Patterns. J. Climate, 13, 4430–4440.

Ge, Y., and G. Gong, 2008: Observed Inconsistencies between Snow Extent and Snow Depth Variability at Regional/Continental Scales. J. Climate, 21, 1066–1082.

Ge, Y., and G. Gong, 2009: North American Snow Depth and Climate Teleconnection Patterns. J. Climate, 22, 217–233.

Ge, Y., G. Gong, and A. Frei, 2009: Physical Mechanisms Linking the Winter Pacific–North American Teleconnection Pattern to Spring North American Snow Depth. J. Climate, 22, 5135–5148.

Grundstein, A., 2003: A synoptic-scale climate analysis of anomalous snow water equivalent over the northern Great Plains of the USA. Int. J. Climatol., 23, 871–886.

Hartley S., and M.J. Keables, 1998: Synoptic associations of winter climate and snowfall variability in New England. Int. J. Climatol., 18, 281–298.

Hurrell, J.W., 1995: Decadal trends in the North Atlantic Oscillation: Regional temperatures and precipitation. Science, 269, 676-679.

Hurrell, J. W., 1996: Influence of Variations in Extratropical Wintertime Teleconnections on Northern Hemisphere Temperature. Geophys. Res. Lett., 23(6), 665-668.

Jin, J., N. L. Miller, S. Sorooshian, and X. Gao, 2006: Relationship between atmospheric circulation and snowpack in the western USA. Hydrol. Process., 20, 753-767.

Kalnay, E., M. Kanamitsu, R. Kistler, W. Collins, D. Deaven, L. Gandin, M. Iredell, S. Saha, G. White, J. Woollen, Y. Zhu, A. Leetmaa, R. Reynolds, M. Chelliah, W. Ebisuzaki, W. Higgins, J. Janowiak, K. Mo, C. Ropelewski, J. Wang, R. Jenne, and D. Joseph, 1996: The NCEP/NCAR 40-Year Reanalysis Project. Bull. Amer. Meteor. Soc., 77, 437–471.

Kluver, D. B., 2007: Characteristics and trends in North American snowfall from a comprehensive gridded dataset. M.S. thesis, Department of Geography, University of Delaware,159pp.

Lanzante, J.R., 1984: A Rotated Eigenanalysis of the Correlation between 700 mb Heights and Sea Surface Temperatures in the Pacific and Atlantic. Mon. Wea. Rev., 112, 2270–2280.

Leathers, D.J., B. Yarnal, and M.A. Palecki, 1991: The Pacific/North American Teleconnection Pattern and United States Climate. Part I: Regional Temperature and Precipitation Associations. J. Climate, 4, 517–528.

McCabe, G.J., and M.D. Dettinger, 2002: Primary modes and predictability of year to year snowpack variations in the western United States from teleconnection with pacific ocean climate. J. Hydrometeorology, 3, 13-25.

McFadden, J.D., and R. A. Ragotzkie, 1967: Climatological significance of albedo in central Canada. J. Geophys. Res., 72(4), 1135–1143.

Morin, J., P. Block, B. Rajagopalan, M. Clark, 2007: Identification of large scale climate patterns affecting snow variability in the eastern United States. International Journal of Climatology, 28 (3), 315-328.

Mote, P.W., 2006: Climate-driven variability and trends in mountain snowpack in western North America. J. Climate, 19 (23), 6209-6220.

Namias, J., 1985: Some empirical evidence for the influence of snow cover on temperature and precipitation. Monthly Weather Review, 113, 1542–1553.

Prohaska, J.T., 1976: A Technique for Analyzing the Linear Relationships between Two Meteorological Fields. Mon. Wea. Rev., 104, 1345–1353.

Rajagopalan, B., E. Cook, U. Lall, and B.K. Ray, 2000: Spatiotemporal variability of ENSO and SST teleconnections to summer drought over the United States during the twentieth century. J. Climate, 13, 4244–4255.

Riviere, G., and I. Orlanksi, 2007: Characteristics of the Atlantic storm-track activity and its relation with the North Atlantic Oscillation. J. Atmos. Sci., 64, 241–266.

Shepard, D., 1968: A two-dimensional interpolation function for irregularly-spaced data. Proceedings of the 1968 23rd Association for Computing Machinery National conference, 517-524.

Sheridan, S.C., 2003: North American weather-type frequency and teleconnection indices. Int. J. Climatol., 23, 27-45.

Sobolowski, S., and A. Frei, 2007: Lagged relationships between North American snow mass and atmospheric teleconnection indices.International Journal of Climatology, 27, 221-231.

Walker, G. T., and E. W. Bliss, 1932: World Weather V. Mem. Roy. Meteor. Soc., 4, 53-84.

Wallace, J.M., and D. S. Gutzler, 1981: Teleconnections in the geopotential height field during the Northern Hemisphere Winter. Mon. Wea. Rev., 109, 784-812.

Wallace, J.M., C. Smith, and C.S. Bretherton, 1992: Singular Value Decomposition of Wintertime Sea Surface Temperature and 500-mb Height Anomalies. J. Climate, 5, 561–576.

Wettstein, J.J., and L.O. Mearns, 2002: The Influence of the North Atlantic–Arctic Oscillation on Mean, Variance, and Extremes of Temperature in the Northeastern United States and Canada. J. Climate, 15, 3586–3600.

Zhang, T., 2005: Influence of the seasonal snow cover on the ground thermal regime: An overview. Rev. Geophys., 43, RG4002, doi:10.1029/2004RG000157.

Table 1: Pearson correlation coefficients between SVD temporal expansion coefficient series (TC) and the winter NAO and PNA indices. Values in bold are significant at 95% confidence level. SVD between winter temperature vs. winter snow depth.

	SVD 1		SVD 2	
	TC1 DJF T925	TC1 DJF SND	TC2 DJF T925	TC2 DJF SND
Corresponding SVD Field	**0.93**		**0.85**	
DJF PNA	-0.08	-0.07	**-0.69**	**-0.68**
DJF NAO	**-0.79**	**-0.68**	-0.21	-0.13

Table 2: Same as Table 1 except SVD between winter temperature vs. spring snow depth

	SVD 1		SVD 2	
	TC1 DJF T925	TC1 MAM SND	TC2 DJF T925	TC2 MAM SND
Corresponding SVD Field	**0.87**		**0.86**	
DJF PNA	-0.36	**-0.50**	0.33	0.37
DJF NAO	**-0.77**	**-0.66**	-0.37	-0.22

Table 3: Same as Table 1 except SVD between winter snowfall vs. winter snow depth

	SVD 1		SVD 2	
	TC1 DJF SNF	TC1 DJF SND	TC2 DJF SNF	TC2 DJF SND
Corresponding SVD Field	**0.96**		**0.96**	
DJF PNA	**-0.58**	**-0.56**	0.32	0.16
DJF NAO	-0.17	-0.22	**0.4**	0.39

Table 4: Same as Table 1 except SVD between winter snowfall vs. spring snow depth

	SVD 1		SVD 2	
	TC1 DJF SNF	TC1 MAM SND	TC2 DJF SNF	TC2 MAM SND
Corresponding SVD Field	**0.93**		**0.94**	
DJF PNA	**-0.69**	**-0.63**	0.08	0.13
DJF NAO	-0.28	**-0.41**	-0.25	-0.15

Table 5: Same as Table 1 except SVD between winter snow depth vs. spring snow depth

	SVD 1		SVD 2	
	TC1 DJF SND	TC1 MAM SND	TC2 DJF SND	TC2 MAM SND
Corresponding SVD Field	**0.94**		**0.93**	
DJF PNA	-0.37	-0.34	**-0.48**	**-0.51**
DJF NAO	0.04	-0.03	**-0.56**	**-0.56**

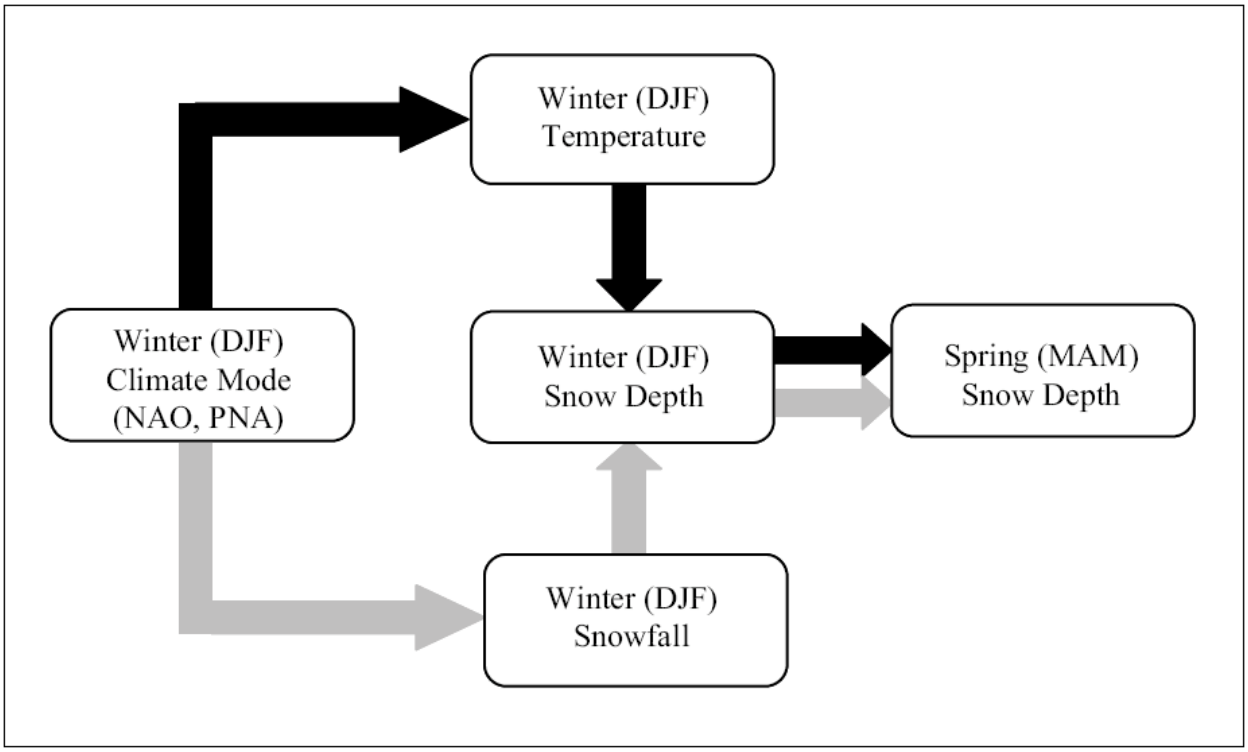

Figure 1 Generalized physical pathways to be investigated, through which winter climate modes can potentially affect snow depth over North America. Black and grey arrows represent different pathways associated with temperature and snowfall anomalies, respectively.

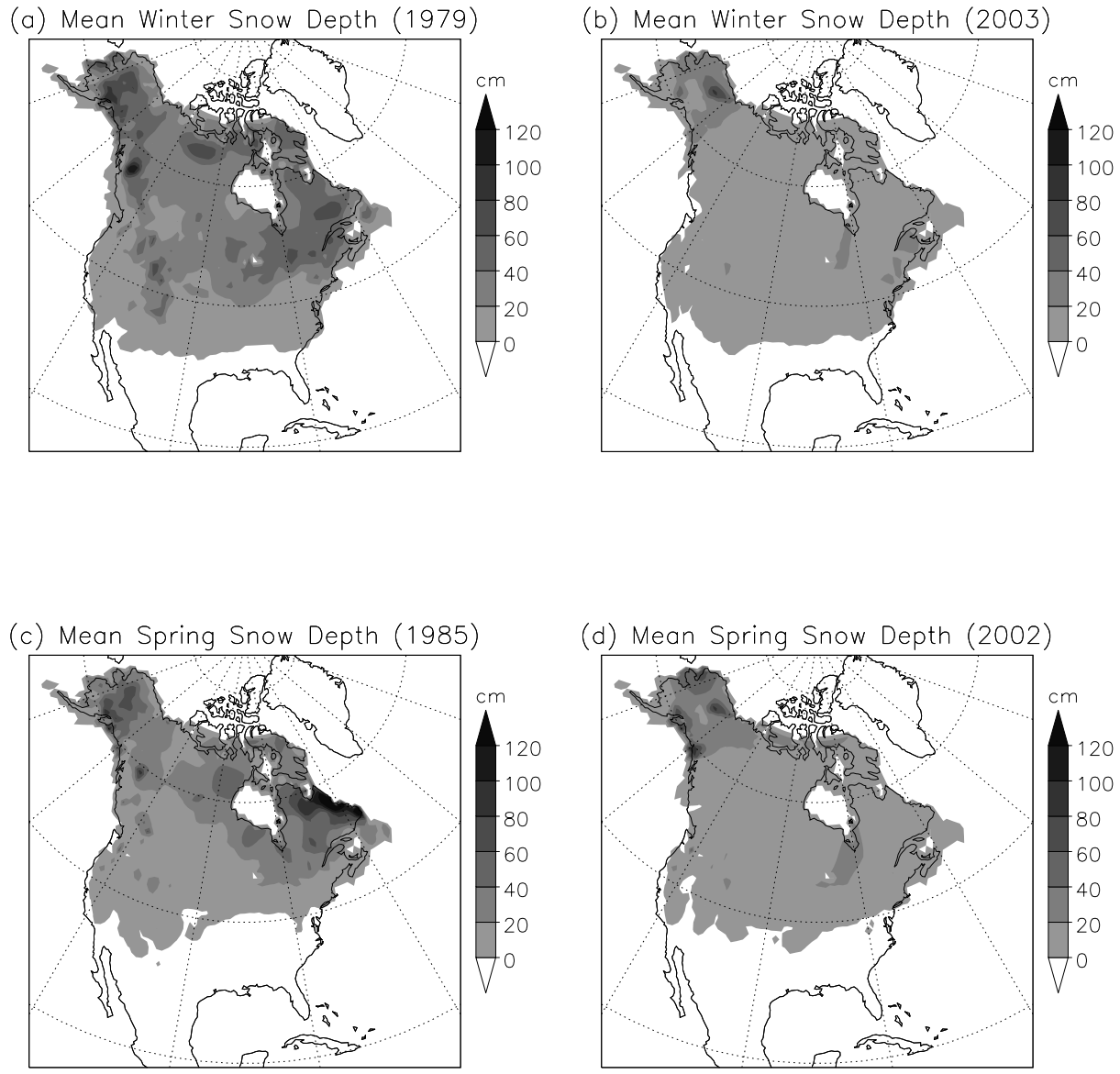

Figure 2 Mean winter (DJF) snow depth for year with the a) highest and b) lowest average North American winter snow depth. c) and d) same for spring.

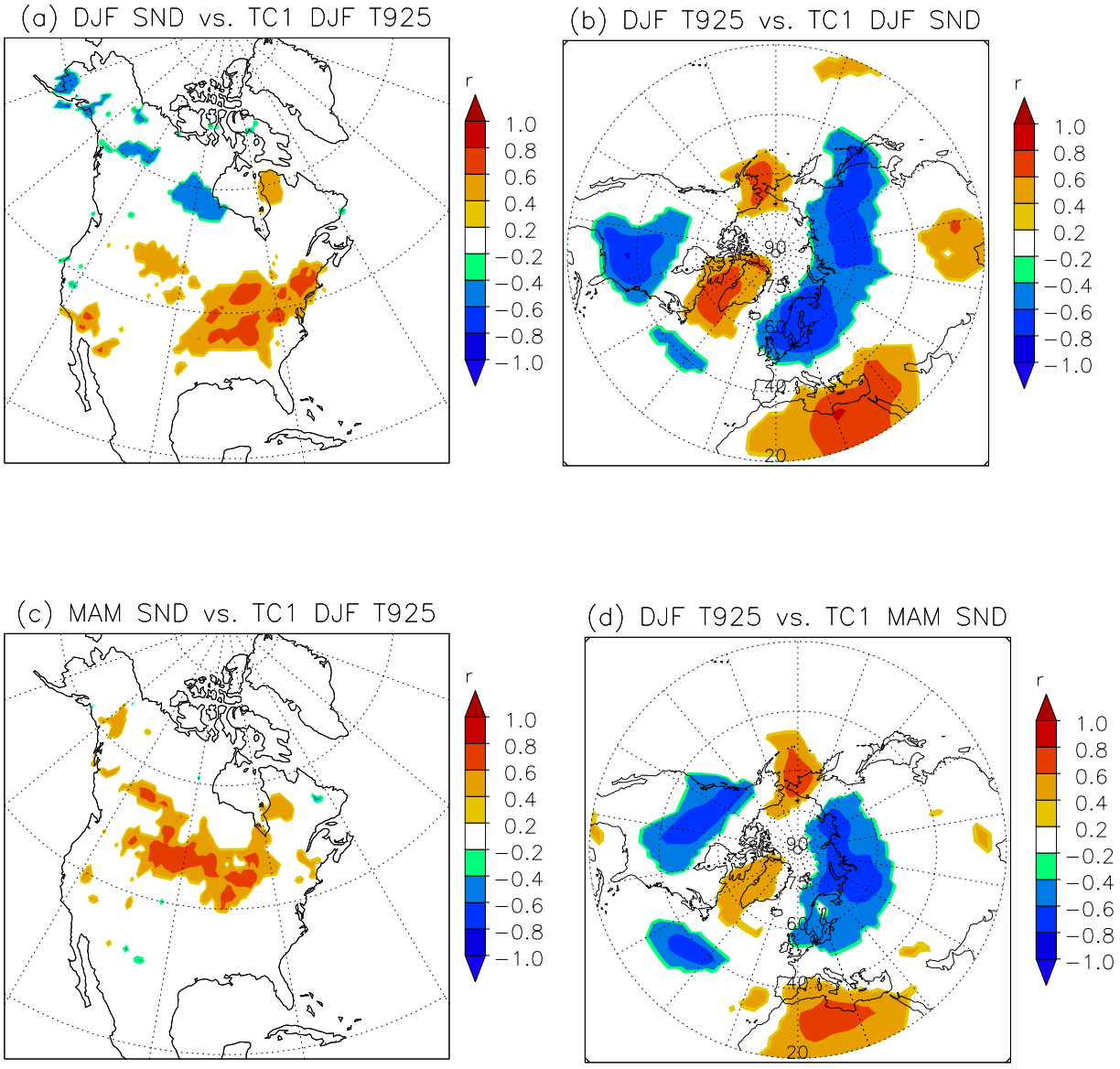

Figure 3 Heterogeneous correlation maps of the first SVD mode between winter snow depth vs. winter temperature a) SVD1 for winter snow depth. b) SVD1 for winter temperature; and same between spring snow depth vs. winter temperature c) SVD1 for spring snow depth. d) SVD1 for winter temperature. Correlation coefficients (r) significant >=95% confidence level are shown here.

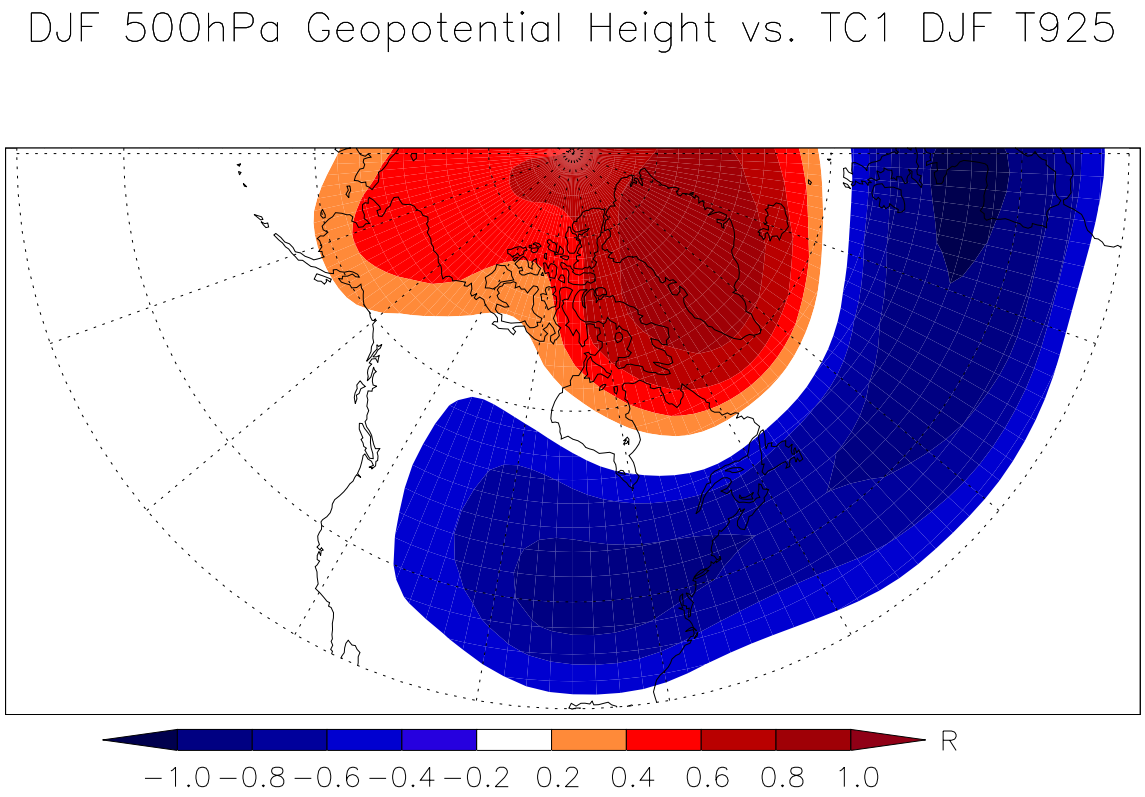

Figure 4 Linear correlation map between winter 500 hPa geopotential height field and TC1 of winter temperature resulting from an SVD analysis with winter snow depth.

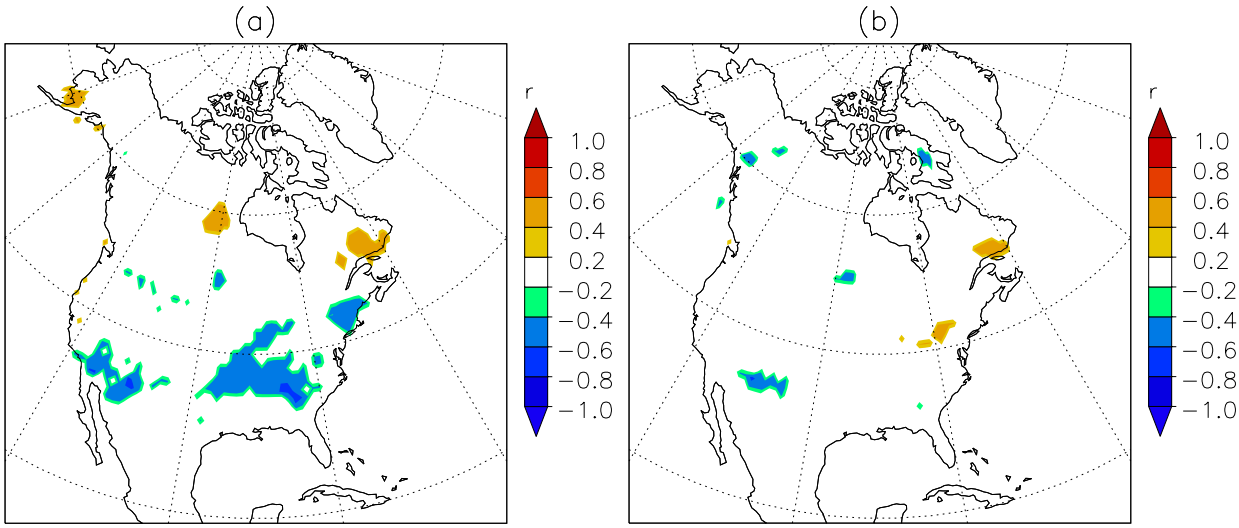

Figure 5 a) Linear correlation map between winter snow depth and the winter NAO index. b) Partial correlation map between winter snow depth and the winter NAO index, after removing the influence of TC1 DJF $T925_{DJF\ SND}$ (see section 3.5.1 for the description). Correlation coefficients significant >= 95% confidence level are shown here.

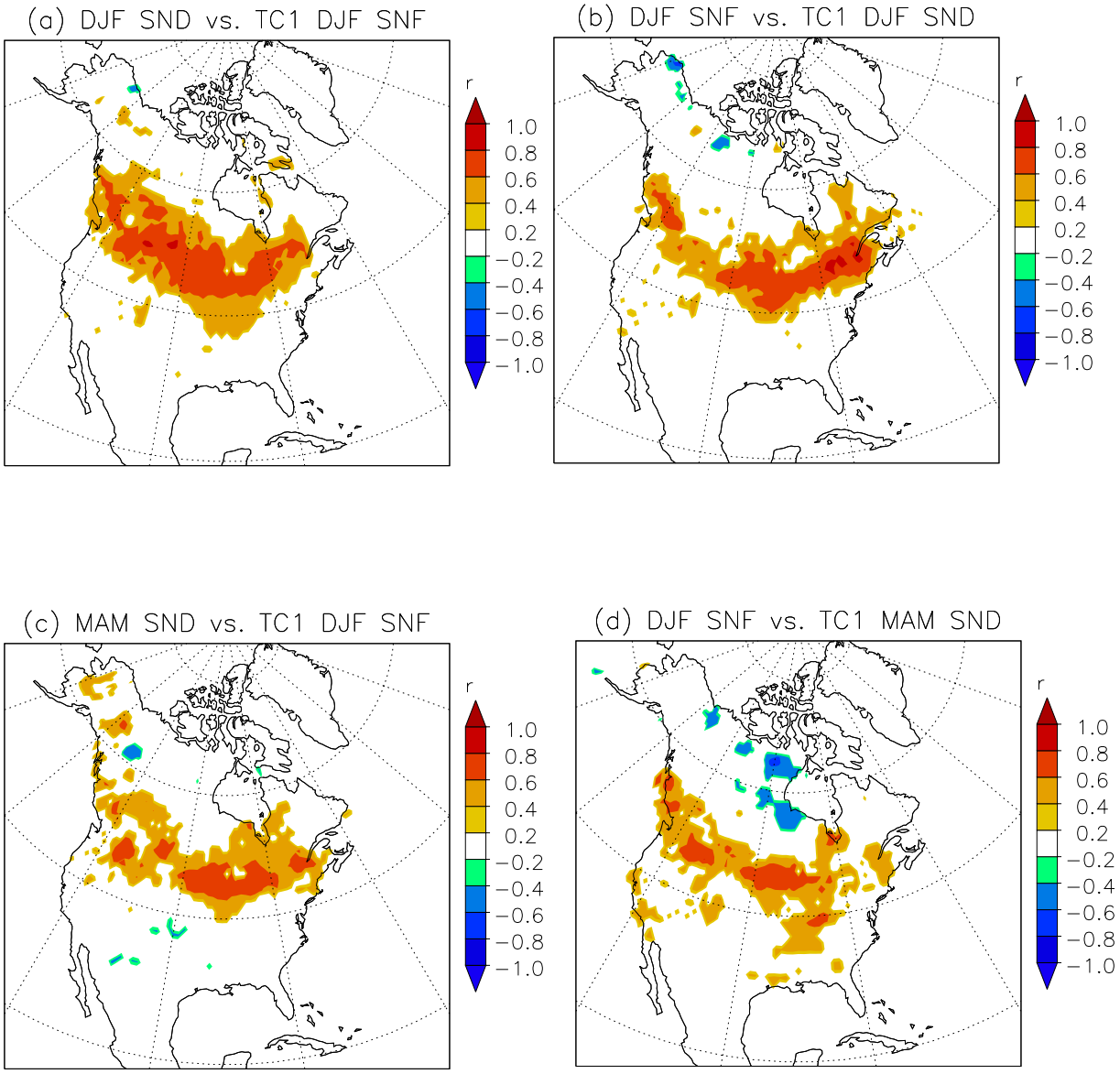

Figure 6 Heterogeneous correlation maps of the first SVD mode between winter snow depth vs. winter snowfall a) SVD1 for winter snow depth. b) SVD1 for winter snowfall; and same between spring snow depth vs. winter snowfall c) SVD1 for spring snow depth. d) SVD1 for winter snowfall. Correlation coefficients (r) significant >=95% confidence level are shown here.

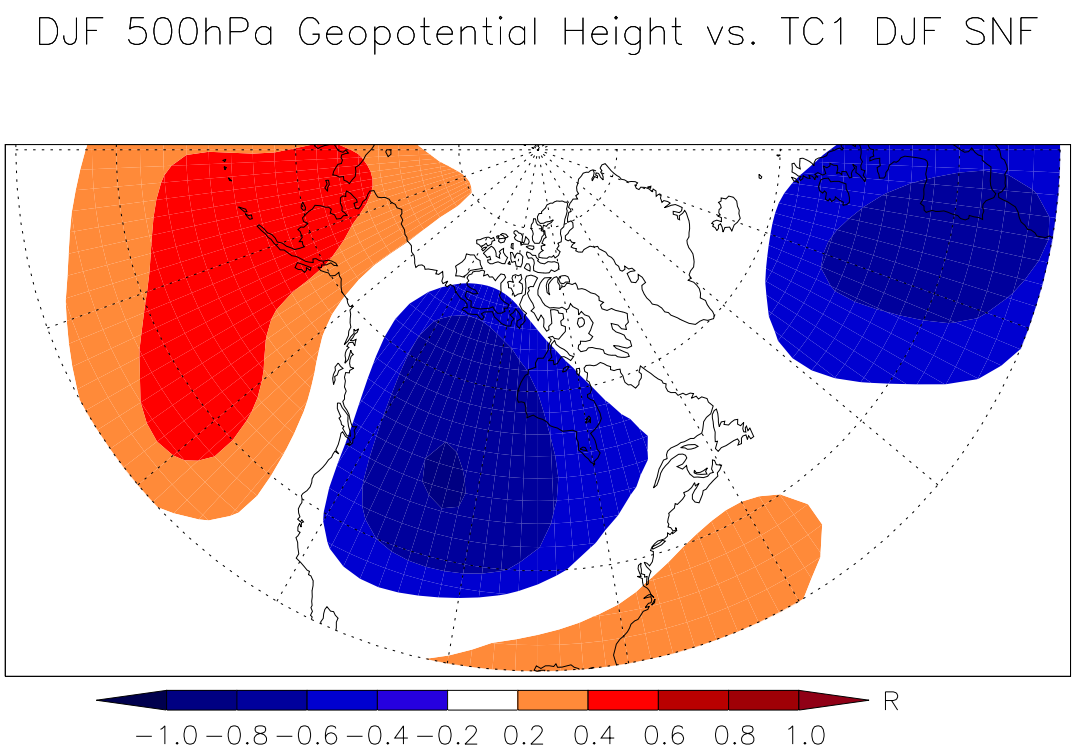

Figure 7 Linear correlation map between winter 500 hPa geopotential height field and TC1 of winter snowfall resulting from an SVD analysis with winter snow depth.

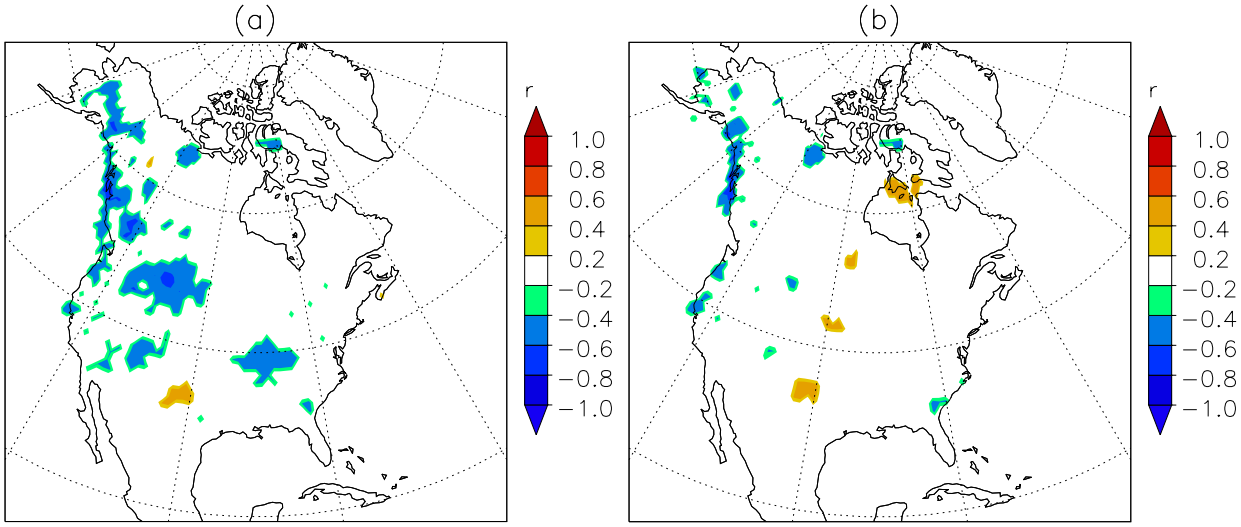

Figure 8 a) Linear correlation map between winter snow depth and the winter PNA index. b) Partial correlation map between winter SND and winter PNA index, after removing the influence of TC1 DJF $SNF_{DJF\ SND}$ (see section 3.5.2 for the description). Correlation coefficients significant >=95% confidence level are shown here.

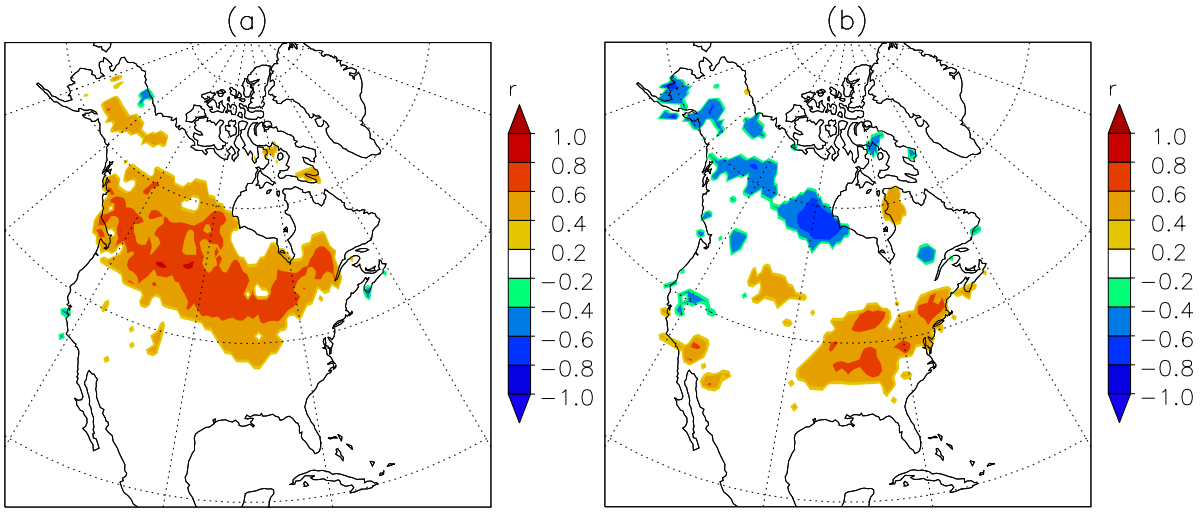

Figure 9 a) Partial correlation map between winter snow depth and TC1 DJF $SNF_{DJF\ SND}$, after removing the influence of TC1 DJF $T925_{DJF\ SND}$. b) Partial correlation map between winter snow depth and TC1 DJF $T925_{DJF\ SND}$, after removing the influence of TC1 DJF $SNF_{DJF\ SND}$. Correlation coefficients significant >=95% confidence level are shown here.

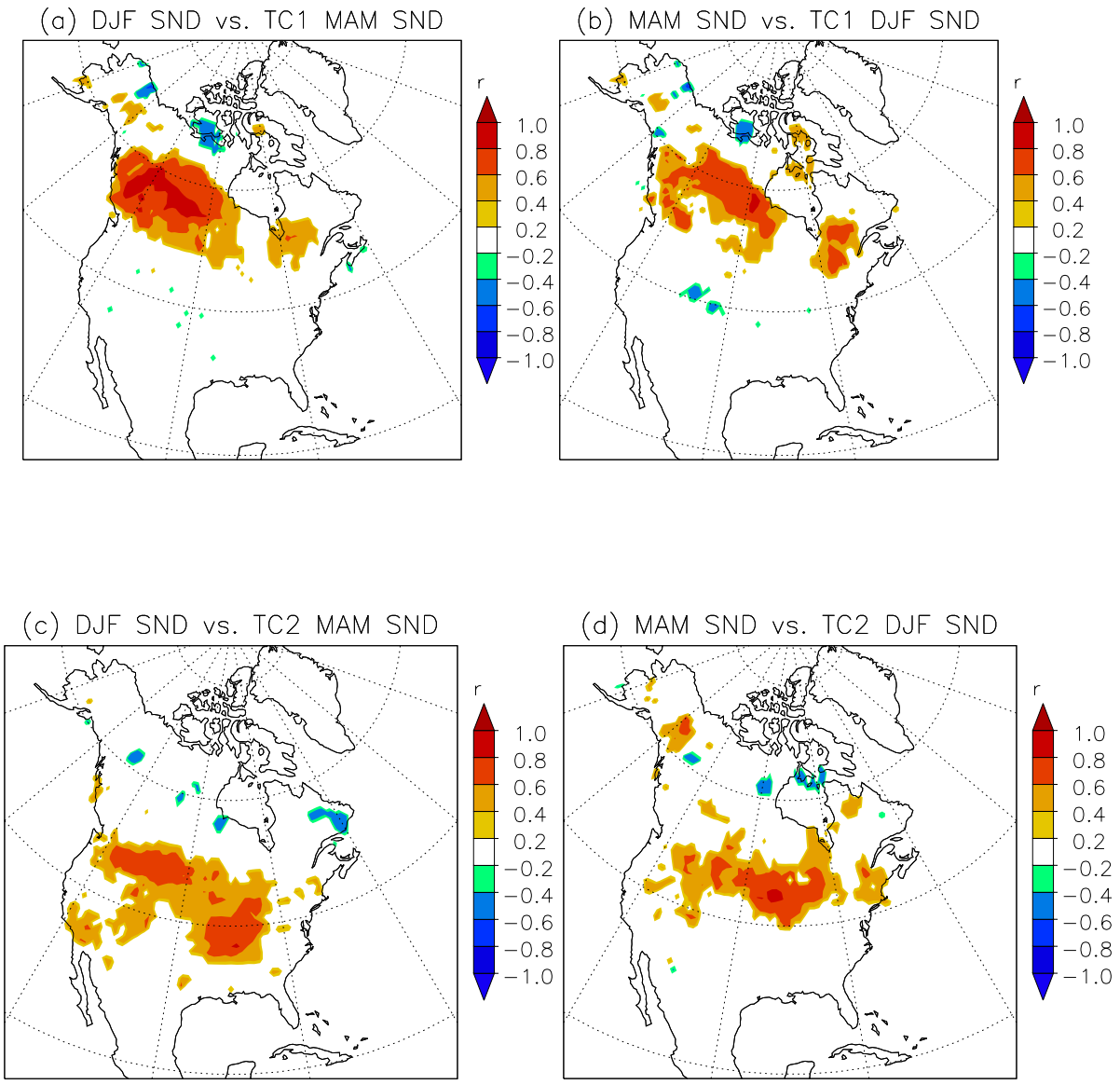

Figure 10 Heterogeneous correlation maps of the first two SVD modes between winter and spring snow depth a) SVD1 for winter snow depth. b) SVD1 for spring snow depth. c) SVD2 for winter snow depth. d) SVD2 for spring snow depth. Correlation coefficients (r) significant >=95% confidence level are shown here.

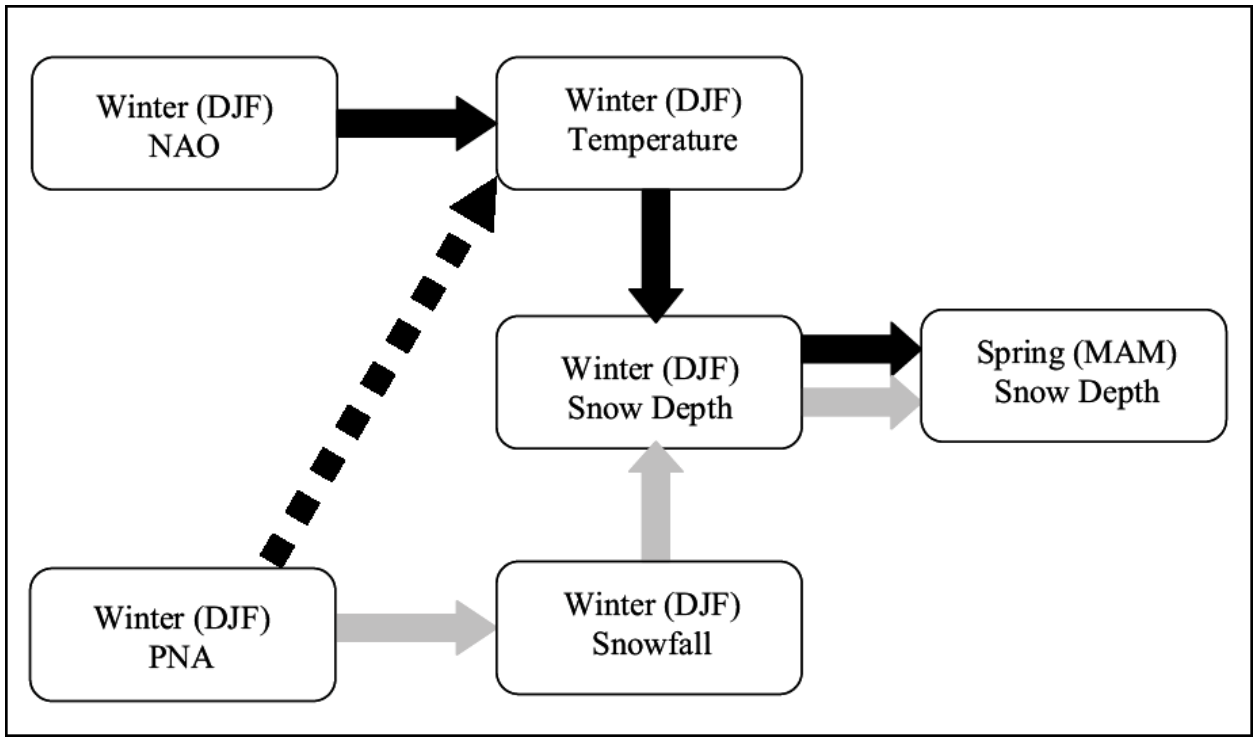

Figure 11 Refined physical pathways based on study results, through which winter climate modes affect snow depth over North America. Black, grey and dashed arrows represent distinct pathways influencing eastern, mid-latitude and northwestern regions, respectively, within North America.

Chapter 4

On The Emergence of an Arctic Amplification Signal in Terrestrial Arctic Snow Extent

Debjani Ghatak[1], Allan Frei[1,3], Gavin Gong[2], Julienne Stroeve[4], David Robinson[5]

[1] Program in Earth and Environmental Sciences, The Graduate Center, The City University of New York, New York, NY

[2] Department of Earth and Environmental Engineering, Columbia University, New York, NY

[3] Department of Geography, Hunter College, The City University of New York, New York, NY

[4] National Snow and Ice Data Center, CIRES, University of Colorado, Boulder, CO

[5] Department of Geography, Rutgers University, Piscataway, New Jersey

Part of this chapter has been published in Journal of Geophysical Research-Atmospheres as: Ghatak, D., A. Frei, G. Gong, J. C. Stroeve, D. Robinson (2010), On the emergence of an Arctic amplification signal in terrestrial Arctic snow extent, J. Geophys. Res., 115, D24105, doi:10.1029/2010JD014007.

4.1 Abstract:

The impact of declining sea ice in amplifying surface air temperatures (SAT) over the Arctic Ocean is readily visible, and this 'Arctic amplification' will become more pronounced as more sea ice is lost in the coming decades. The effect of sea ice loss on atmospheric temperatures and circulation patterns is of utmost significance as these changes will affect the terrestrial climate. Land-surface snow is vulnerable to these changes; hence, we search for any link between changes in Arctic sea ice and Northern Hemisphere snow cover. Analyses of observational datasets suggest that the increasing snow cover over Siberia during fall and early winter is correlated with the decreasing September Arctic sea ice over the Pacific sector. We also examine modeled co-variance between sea ice and snow using historical and future simulations of the Community Climate System Model (CCSM3). Results indicate the emergence of a Siberian snow signal during the last half of the twenty-first century most strongly during late winter. Moreover, CCSM3 future simulations show diminishment of snow at a hemispheric-scale outside of the Siberian region, which is correlated with the loss of Arctic sea ice. These results indicate that we may be seeing the first, albeit weak, signs of "arctic amplification" on the terrestrial Arctic snowpack; that only a weak, and therefore inconclusive signal would be expected at this time; and that the signal should strengthen over the coming decades.

4.2 Introduction:

The status of the rapidly declining Arctic sea ice has been closely monitored for more than a decade now (e.g. Cavalieri et al., 1997; Rothrock et al., 1999; Parkinson et al., 1999; Stroeve et al., 2005, 2007; Serreze et al., 2007; Comiso et al., 2008). Considering the crucial role of sea ice in the climate system, many researchers have investigated the effects of retreating sea ice on present and projected future atmospheric temperatures and circulation patterns (e.g. Honda et al., 1999; Deser et al., 2000; Magnusdottir et al., 2004; Alexandar et al., 2004; Kvamsto et al., 2004; Gerdes, 2006; Singarayer et al., 2006; Francis et al., 2009; Deser et al., 2010). One of the major impacts is already apparent in the amplification of rising surface air temperatures (SAT) over the Arctic ocean, as suggested by the concept of 'Arctic amplification' (Serreze et al., 2009). Expanding open water areas in summer allows for heating of the ocean's mixed layer and therefore a net heat gain by the ice-ocean column during summer; this subsequently leads to a delayed autumn freeze-up. The insulating effect of sea ice during autumn is then weakened due to the thinner and the smaller ice pack, which results in a large heat loss from the ocean to the atmosphere which further amplifies the atmospheric warming (Serreze and Francis, 2006; Serreze et al., 2009). Moreover, it is expected that amplified warming from the loss of the summer sea ice cover will spread over high-latitude land areas, hastening degradation of permafrost (Lawrence et al., 2008).

Model simulations indicate increased SAT over high latitudes and shifts in precipitation patterns and amounts in response to a prescribed future reduction in Arctic sea ice (Singarayer et al., 2006; Deser et al., 2010). Francis et al. (2009) also examined changes in winter precipitation due to historical summer sea ice variability through the

analysis of observational and reanalysis datasets, and suggest negative anomalies in precipitation over the Northeast Atlantic extending into northern Europe and also over much of US and Alaska.

It is reasonable to hypothesize that these changing atmospheric and terrestrial climates may play a significant role in affecting the snow over the surrounding landmasses. The impact of increased SATs on snow cover depends on whether the change in temperature crosses the freezing point. Over regions where temperatures do cross the freezing point, snowfall is partially or wholly replaced by rain, and snow melt is increased, resulting in a diminished snow pack. Over regions that remain below freezing after the warming, snowfall and snow cover are typically enhanced because of the increased moisture capacity of the atmosphere.

Considering the vulnerability of snow to the generalized warming and to the changes induced by sea ice, it is important to investigate here the observed covariance between early season snow and the preceding summer sea ice (as also mentioned in the chapter 2: Research Objectives and Approach). Furthermore, we also examine the modeled covariance between them for the historic and future time domains. We focus on fall and early winter season snow to represent the snowpack accumulation period, and the preceding September sea ice which is the month of climatological minimum sea ice cover. Since, the impact of 'Arctic amplification' is readily visible over the high-latitude region during the autumn season (Serreze et al., 2009), it is prudent to examine the land-surface snow during this season for any emerging signal of links between declining sea ice cover and snow cover. We also discuss possible physical mechanisms linking sea ice changes to snow cover.

4.3 Datasets and Methodology

4.3.1 Datasets and Model Outputs:

The spatial domain of our study spans the extratropical Northern Hemisphere. EASE-grid (Equal Area Scalable Earth Grid) snow extent data (Armstrong and Brodzik, 2005) based on NOAA-NESDIS snow charts, and sea ice concentration (Comiso, 1999) data from Scanning Multichannel Microwave Radiometer (SMMR) and Special Sensor Microwave/Imager (SSM/I) sensors, have been obtained from the National Snow and Ice Data Center (NSIDC). The use of weekly snow information provides the opportunity to compute an annual time series of the total number of weeks of autumn and early winter (defined here as October through December, OND) snow cover (SNE) for the period 1979-2007 at each grid point. The mean September sea ice field is also generated for the same 29 year time period from the sea ice concentration (SIC) dataset which has been produced using a Bootstrap algorithm. No data above 83^0 North is included during the processing of SIC data. Both SNE and SIC datasets are available at a spatial resolution of 25 km; but are regridded to 100 km resolution for our hemispheric-scale analysis. We also use a mean September Arctic sea ice extent time series available from NSIDC's Sea Ice Index (http://nsidc.org/data/seaice_index).

We use archived output from the Intergovermental Panel on Climate Change fourth assessment report (IPCC AR4), produced by the Community Climate System Model version 3 (CCSM3), a fully-coupled atmosphere-ocean general circulation model (AOGCM). Arctic sea ice variability is simulated well by this model (Holland et al., 2006; Stroeve et al., 2007). Historical simulations as well as 21^{st} century simulations from the SRESA1B scenario (Special Report on Emissions Scenarios; gradual rise to 720

ppm of atmospheric CO_2 concentrations by 2100) are utilized for this study. Model outputs for three variables, 'surface snow area fraction where land' (SNC in %, as named by IPCC), 'surface snow thickness' (SND in meter, as named by IPCC) and 'sea ice area fraction' (SIC in %, as named by IPCC) are used here (http://www-pcmdi.llnl.gov/ipcc/standard_output.html#Experiments). For both the observational data and for the model output, grid cells with less than 15% sea ice concentration have been excluded in the analysis, because 15% SIC isopleth is considered as the cutoff for ice extent (Stroeve et al., 2007). We use the ensemble mean of three runs (Runs 1, 5, and 6), which are the only ensemble members available for all fields at the time of the preparation of this manuscript.

4.3.2 Methodology:

Singular Value Decomposition Analysis (SVD) is applied here to snow and sea ice fields, where each field consists of a 29 year long time series at each grid point. SVD is a useful method to extract coupled patterns from two space-time fields and has been used in many studies (Prohaska, 1976; Lanzante, 1984; Wallace et al., 1992; Cherry, 1997; Rajagopalan et al., 2000; Stroeve et al., 2008). Here, we employ the correlation matrix approach as these two fields have different units of measurements. SVD analysis produces pairs of spatial patterns, explaining maximum mean-squared temporal covariance between two space-time fields. It also generates pairs of temporal coefficient (TC) time series describing the temporal evolutions of their corresponding spatial patterns (Bretherton et al., 1992). Negative TC time series values indicate that the pattern of variability follows the SVD result but with the signs reversed. We present the SVD results as heterogeneous correlation (HC) maps rather than SVD mode maps, where the

HC map is computed by correlating the time series at each grid point of one field with the corresponding TC of the other field. Here, we employ non-parametric Spearman correlation coefficients (ρ) to compute HC maps and report only results which exceed 95% confidence level. We also discuss results of composite analysis.

4.4 Results

4.4.1 Observational Results:

Figure 1 presents the leading mode of the SVD analysis between mean September SIC and OND SNE, which explains 31% of the covariance between the two fields. The regions of significant correlation between the SIC and SNE fields are the Pacific sector of the Arctic Ocean and northern Asia, respectively. The SNE pattern (Figure 1a) is strongest ($|\rho| > 0.7$) over the Siberia region. The SIC pattern (Figure 1b) is strongest ($|\rho| > 0.7$) over the Beaufort and Chukchi seas. Correlation pattern values for the two fields are of opposite sign, indicating an inverse relationship between SNE and SIC. The TC time series (Figure 1c) for both fields are positively correlated with each other ($r = 0.81$), indicating significant covariability. Moreover, the two TC time series exhibit an overall negative trend from positive to negative values over the study period of 1979-2007. These results indicate that the strongest covariability signal between these two fields is associated with gradually increasing snow over Siberia and declining sea ice over the Arctic Ocean.

SVD analysis between these two variables was repeated after detrending the parameter fields (Fig 2). Using ordinary least square regression, we remove the trend from the time series at each grid point for both of the original space-time fields of SNE and SIC, and then use these fields for SVD analysis. The HC maps generated from the

leading mode show no significant correlations between Siberian SNE and Arctic SIC. Thus, this set of analysis suggests that the primary pattern of correlation between two fields identified in Figure 1 is driven mainly by the trends in both fields. This does not imply any cause and effect relationship. However, because the trend is so strong, and recent sea ice coverage in the Pacific sector of the Arctic is so far below earlier values, the possibility remains that there is an influence of recent dramatically low sea ice years on Siberian snow, but that earlier "low" years were not low enough to impact the snow cover.

To evaluate the relationship further, we compute the differences in OND SNE between two nine-year composites, which consist of the nine extreme low and nine extreme high mean September sea ice extent years from the period of 1979-2007. Nine extreme high years are 1996, 1980, 1992, 1986, 1983, 1988, 1987, 1982, 1981 and nine extreme low years are 2007, 2005, 2006, 2002, 2004, 1995, 2003, 1990, 1999. This composite analysis was performed both with and without detrending the sea ice extent time series. Figure 3 presents the results for the (low SIC – high SIC) difference, i.e. the SNE response to decreasing SIC. We only show the composite difference at grid points where each of the two 9-year composites has significantly different means at significance level of 0.05 following Student's T-statistic. When the original time series is used, the composite difference (Figure 3a) indicates extended OND SNE over Siberia (as well as at scattered grid points in other regions) following low summer sea ice extent. In the composite difference map using the detrended sea ice extent time series (Figure 3b) the Siberian signal is mostly eliminated.

These sets of composite analyses confirm the results from SVD analyses that the inter-annual trends in both fields drive the relationship between Siberian snow and the Arctic sea ice. Thus, it indicates an emerging signal of climate change as opposed to a signature of inter-annual climate variability. Composite analyses based on 5-year composites produce similar conclusions.

4.4.2 Results based on modeling output:

We also performed SVD analyses on mean OND SNC and mean September SIC using CCSM3 historical and 21st century simulations. Here, the analysis is repeated using four time domains (1979-2007, 1979-2020, 1979-2050 and 1979-2080), to reveal how the leading pattern of co-variability between snow and sea ice changes as the time domain extends farther into the future. Figure 4 presents the resulting HC maps and TC time series for all four time domains. The TC time series are significantly and positively correlated with each other during each time domain (R values= 0.95, 0.95, 0.97 and 0.97 respectively for four time domains).

As one scans the four SNC patterns (Figures 4a-d), a broad region of positive correlation emerges and grows throughout the twenty-first century. During the 1979-2007 time domain, isolated SNC patterns (Figure 4a) occur mainly over Scandinavia and over mid-latitudinal areas of North America. This pattern gradually spreads over NW Europe and over the interior of North America during the 1979-2020 time period (Figure 4b). By the end of the century, most of the Northern Hemisphere is affected (Figures 4c, d), except for eastern Siberia.

During 1979-2007, the HC SIC pattern exhibits strongest positive correlations over the Atlantic sector of the Arctic (Figure 4e). This spatial pattern is different than

what has actually been observed in recent years where major ice loss has primarily occurred in the Pacific sector (Stroeve et al., 2005; Serreze et al., 2007) (see Discussion). Between 2007 and 2080 the SIC pattern spreads strongly over the Pacific sector (Figures 4f, g, h). The TC time series show negative trends during all time domains (Figures 4i-l), although in the 1979-2080 analysis (Figure 4l) the time series flattens out in later years as a result of the virtually complete disappearance of sea ice by mid-century.

Similar analysis (figure 4) has been done between mean OND SND and mean September SIC for the same four time domains because this snow metric provides information not only about the presence or absence of snow but also regarding the volume of snow. Unfortunately, observations of long-term and reliable hemispheric-scale snow depth data are not available, and therefore only SNE was used in the observational analysis. The modeled HC SIC pattern and the TC time series from the leading mode of this SVD analysis are virtually indistinguishable with the patterns presented in figures 4e-l. Therefore, we only present the HC SND pattern in figures 4m-p. These four figures (4m-p) of SND are also very similar with the figures 4a-d where SNC has been used; the only difference is that the correlated region over Siberia appears more spatially extensive in the figures (4o, p) using SND. Correlation coefficients are reversed in sign from the rest of the hemisphere over Siberia. This reversed Siberian pattern is undetectable during 1979-2007 time domain, but it emerges by mid century.

This series of SVD analyses show a gradual spreading of a climate change impact on snow across Northern Hemisphere lands during the twenty first century. The signal consists of a hemisphere-wide diminishment of snow except over Siberia where an

increase in snow depth emerges around mid-century, and this snow pattern is correlated with the decreasing sea ice over the Arctic.

In order to confirm that our results are not an artifact of increasing the number of points (n) in each successive SVD, we performed the SVD analyses between mean OND SNC and mean September SIC for four time domains that have the same number of years (n=29). The time domains are 1979-2007, 1992-2020, 2022-2050 and 2052-2080 (Figure 5). Figures 5a-d show the heterogeneous correlation maps between OND SNC vs. TC1 September SIC for the four time domains; figures 5e-h show the heterogeneous correlation maps between September SIC vs. TC1 OND SNC and figures 5i-l show TC1 time series for both fields. The snow pattern indicates that the strong correlated region appears over Scandinavia at the beginning of the century, and then spreads both over Eurasia and over North America during 1992-2020 and 2022-2050 time domains. On the other hand, sea ice pattern is very similar to the results presented in figure 4. The strong correlated region appears over the Atlantic sector of the Arctic during the 1979-2007 time domain, and then it spreads over the Pacific sector during the 1992-2020 and 2022-2050 time domains. Both snow and sea ice pattern are consistent with our results presented in figure 4 except the result for 2052-2080 time domain. The disappearance of the correlated region in figures 5d and 5h at the end of century (2052-2080) occurs because by that time the sea ice has already disappeared. This is demonstrated by the TC1 time series for both fields which flatten out during 2052-2080 time domains (fig 5l). Thus, this result is consistent with the figure 4.

We repeated SVD analysis for the identical four time domains using modeled mean winter (JFM) instead of fall (OND) SNC. As these SVD analyses have been done

between modeled JFM SNC and the preceding September SIC, the time domain is marked as 1980-2008 in figure 6a and likewise for the corresponding time periods in figures 6b-6d; though the four time domains in figure 6 are essentially same as the previous analyses. Figure 6 presents only the resulting SNC pattern, because the SIC pattern is similar to the previous SVD analysis (Figures 4e-4h). The correlated region of JFM SNC is more spatially extensive and coherent than during OND (compare Figures 6a-d to Figures 4a-d). Of particular interest is that the pattern over Siberia is more spatially extensive and has higher correlations. This result holds true when we repeat this analysis involving JFM SND. This is consistent with Deser et al. (2010) (from now on DTAL10) in which a stronger SND signal was reported over Siberia during late winter as opposed to fall/early winter.

It is interesting to note that the observation-based SVD indicates a climate change signal is already emerging in snow cover, while the model-based SVD does not reveal such a signal until the mid-21st century. It is possible that climate models lag the actual climate system in the timing of this effect, if for no reason other than their sea ice predictions, which have been shown to lag behind observed sea ice reductions (Stroeve et al., 2007). In addition, the signal in the SIC pattern based on CCSM3 model outputs is mainly over the Atlantic sector of the Arctic Ocean during the early 21st century, whereas recent sea ice losses have actually occurred mainly over the Pacific sector. Since the model has yet to capture the precursive regional sea ice loss in the early twenty first century, it is not surprising that it does not capture the consequent early twenty first century Siberian snow signal.

4.5 Discussion

We demonstrate empirically, using SVD analysis, that the primary signal of covariability between Arctic sea ice and Northern Hemisphere SNE between 1979 and 2007 consists of a decreasing trend in September SIC primarily over the Pacific sector, which is correlated to an increasing trend in fall and early winter SNE over Siberia. Composite analyses corroborate that SNE over Siberia has increased following the low summer sea ice during this time period. These relationships do not alone imply any cause and effect relationship.

These results are consistent with the spatial patterns as suggested by Bulygina et al. (2009), which shows the increase in the duration of snow cover over central Siberia (Yakutia) and Far East. Another study of the Lena River Basin shows a positive trend in monthly precipitation during winter months, specifically in November and December (Yang et al., 2002). They indicated that more winter precipitation likely results in greater snow cover and snowpack storage, and leads to the increased snowmelt run-off and stream-flow during early summer.

Next we compare the empirical results with results from analogous SVD analyses between sea ice and snow from CCSM3 twentieth to twenty first century climate simulations. We analyze model results for four different temporal domains: 1979-2007 (which coincides with our empirical analysis), 1979-2020, 1979-2050, and 1979-2080. Climate model comparisons show weaker correlations between September sea ice loss and snow over Siberia during OND (i.e. increase in snow), but the correlation becomes stronger during JFM. This signal is most prominent during the last half of the century. In addition, the model-based SVD indicates a diminished snow across all Northern

Hemisphere lands outside of Siberia during both OND and JFM, which is readily visible at hemispheric-scales even during the first half of the 21st century. This snow pattern is also correlated with the decreasing sea ice over the Arctic.

While covariance between sea ice and snow cover does not provide a cause and effect, our empirical results may be a first sign of an emerging climate change signal in high latitude snow cover. One would expect the spatial pattern of changing snow in response to a generalized warming to be similar to the climate model results: i.e. loss of snow over most regions. Existing literatures also indicates declining snow due to rising temperature. A study by Ye B. et al. (2003) suggested earlier snowmelt and streamflow changes due to regional climate warming over southern parts of Siberia. Another paper by Ye H. et al. (2008) indicates that rain-on-snow days increased over European Russia and increased air temperature is the primary attributing factor. Moreover, ACIA report showed that Arctic warming caused 10% loss of snow cover extent over the last 30 years (Hassol, 2004). Räisänen (2008) also examined changes in the projected 21st century snow water equivalent (SWE) in response to the greenhouse gas warming through the analysis of 20 global climate models output participating in the 3rd Coupled Model Intercomparison Project (CMIP3). He found SWE decreasing during winter over terrestrial regions in Northern Hemisphere, except over northernmost North America and Siberia where SWE increases, and identified -20°C isotherm in late 20th century winter (NDJFM) mean temperature as the threshold temperature for the SWE changes.

But even under a warming scenario, some areas still may exist that are sufficiently cold to maintain a snow cover. Furthermore, over such colder regions, a warmer (but still below-freezing) atmosphere would have a higher capacity for holding

water vapor, and therefore could potentially deliver more snowfall. Thus, an empirical result as shown in this chapter, showing the beginning of such a signal over Siberia would be consistent with the expectations, even if the hemisphere-wide signal of diminished snow is not yet found in our results.

Another question is whether the Siberian response identified here represents a manifestation of the terrestrial 'Arctic amplification' signal. Serreze and Francis (2006) and Serreze et al. (2009) discuss the emergence of an Arctic amplification signal over the ocean. The primary source of Arctic amplification is the additional energy introduced into the surface climate system within the Arctic Ocean basin by diminished sea ice (see Section 4.2). The question then is whether this energy input is transported into Siberia to influence snow cover.

There is modeling evidence to support this idea. DTAL10 performed two sets of Community Atmosphere Model version 3 (CAM3) experiments designed to isolate the atmospheric and terrestrial response to depleted Arctic sea ice. Their control experiment includes a repeating seasonal cycle of sea ice (concentrations and thickness) for the period 1980-1999; their perturbation experiment consists of a repeating seasonal cycle of sea ice specified from model results for a period of greatly diminished sea ice, 2080-2099. Same repeating seasonal cycle of SSTs for the period 1980-1999 was specified in both experiments, and GHG concentrations are also fixed at 1980-1999 levels in both experiments. An increase in SND over the Siberian region in response to the prescribed future loss of sea ice concentration and thickness is apparent beginning in November and reaching its maximum in March-April; thus, it is consistent with our observational results for fall and early winter SNE.

Furthermore, DTAL10 and Finnis et al. (2007) suggest some links between retreating Arctic sea ice and the terrestrial snow. DTAL10 suggests that the SND increase is a consequence of increased precipitation resulting from diminished sea ice. Finnis et al. (2007) shows a shift in cyclone-associated precipitation which is a major source of autumn and winter precipitation in mid and high latitude Northern Hemisphere lands. According to this study, high latitude regions experience increased precipitation from storms during autumn due to the availability of atmospheric moisture associated with rising temperatures. Moreover, they suggest the role of decreasing sea ice behind this thermodynamic effect on precipitation. Simmonds and Keay (2009) also indicates the significant role played by cyclone over the Arctic basin in recent years. Honda et al. (2009) also shows some mechanisms which may generate some pathways linking sea ice and snow. They show that decreasing summer sea ice thermally generates stationary Rossby waves, which strengthens the Siberian high and causes cold conditions over Eurasia. Further identification of the specific pathways linking sea ice and snow is currently under investigation.

An unfortunate aspect of this problem is that high latitude climatological observations are extremely limited, and have diminished in numbers in recent years. This is due to budgetary constraints in different countries as well as to the increasing dependence on remotely sensed observations, which cannot provide as much detail on snow cover (Brown and Armstrong, 2008). Thus, while in this chapter we point out that there is evidence consistent with the emergence of a sea ice related Arctic amplification signal in the snow cover record, it is too soon to tell. This insufficient observational

capacity of high latitude snow cover may result in the loss of a valuable early indicator of climate change.

4.6 Acknowledgements:

This work has been supported by the NASA Cryospheric Sciences Division (#NNX08AQ70G). We thank Mary Jo Brodzik from NSIDC for helping us in acquiring updated datasets, and Dr. Clara Deser for her insightful comments and suggestions. We are also thankful to the anonymous reviewers for their constructive comments.

4.7 References:

Alexander, M. A., U. S. Bhatt, J. E. Walsh, M. S. Timlin, J. S. Miller, and J. D. Scott, 2004: The atmospheric response to realistic Arctic sea ice anomalies in an AGCM during Winter. J. Climate, 17, 890-905.

Armstrong, R. L., and M. J. Brodzik, 2005: Northern Hemisphere EASE-Grid weekly snow cover and sea ice extent, Version 3, October 1966 to October 1978, http://nsidc.org/data/nsidc-0046.html. National Snow and Ice Data Center, Boulder, Colorado USA. Digital media.

Bretherton, C.S., C. Smith, and J.M. Wallace, 1992: An intercomparison of methods for finding coupled patterns in climate data. J. Climate, 5, 541–560.

Brown, R., and R. L. Armstrong, 2008: Snow-cover data: measurement, products, sources. in Snow and Climate: Physical Processes, Surface Energy Exchange and Modeling. edited by R. L. Armstrong and E. Brun, pp. 181-216 , Cambridge University Press.

Bulygina, O. N., V. N. Razuvaev, and N. N. Korshunova, 2009: Changes in snow cover over Northern Eurasia in the last few decades. Environ. Res. Lett., 4**,** 045026, 6 pp, doi: 10.1088/1748-9326/4/4/045026.

Cavalieri, D. J., P. Gloersen, C. L. Parkinson, J. C. Comiso, and H. J. Zwally, 1997: Observed Hemispheric Asymmetry in Global Sea Ice Changes. Science, 278 (5340), 1104, doi: 10.1126/science.278.5340.1104.

Cherry, S., 1997: Some Comments on Singular Value Decomposition Analysis. J. Climate, 10, 1759–1761.

Comiso, J., 1999: Bootstrap sea ice concentrations from NIMBUS-7 SMMR and DMSP SSM/I, updated 2008, october 1978 to December 2007, http://nsidc.org/data/docs/daac/nsidc0079_bootstrap_seaice.gd.html. National Snow and Ice Data Center, Boulder, Colorado USA. Digital media.

Comiso, J. C., C.L. Parkinson, R. Gersten, and L. Stock, 2008: Accelerated decline in the Arctic sea ice cover. Geophys. Res. Lett., 35, doi:10.1029/2007GL031972.

Deser, C., J.E. Walsh, and M.S. Timlin, 2000: Arctic sea ice variability in the context of recent atmospheric circulation trends. J. Climate, 13, 617-633.

Deser, C., R. Tomas, M. Alexander, and D. Lawrence, 2010: The Seasonal Atmospheric Response to Projected Arctic Sea Ice Loss in the Late Twenty-First Century. J. Climate, 23, 333–351.

Finnis, J., M. M. Holland, M. C. Serreze, and J. J. Cassano, 2007: Response of Northern Hemisphere extratropical cyclone activity and associated precipitation to climate change, as represented by the Community Climate System Model. J. Geophys. Res., 112, G04S42, doi:10.1029/2006JG000286.

Francis, J.A., W. Chan, D.J. Leathers, J.R. Miller, and D.E. Veron, 2009: Winter northern hemisphere weather patterns remember summer Arctic sea ice extent. Geophys.Res. Lett., 36, L07503, doi:10.1029/2009GL037274.

Gerdes, R., 2006: Atmospheric response to changes in Arctic sea ice thickness. Geophys.Res. Lett., 33(18), L18709.

Hassol, S. J., 2004: Impacts of a Warming Arctic: Arctic Climate Impact Assessment. 139 pp., Cambridge Univ. Press, Cambridge, U.K.

Holland, M. M., C. M. Bitz, and B. Tremblay, 2006: Future abrupt reductions in the summer Arctic sea ice. Geophys. Res. Lett., 33, L23503, doi:10.1029/2006GL028024.

Honda, M., K. Yamazaki, H. Nakamura, and K. Takeuchi, 1999: Dynamic and thermodynamic characteristics of atmospheric response to anomalous sea–ice extent in the Sea of Okhotsk. J. Climate, 12, 3347–33.

Honda, M., J. Inoue, and S. Yamane, 2009: Influence of low Arctic sea ice minima on anomalously cold Eurasian winters. Geophys. Res. Lett., 36, L08707, doi:10.1029/2008GL037079.

Kvamstø, N. G., P. Skeie, and D. B. Stephenson, 2004: Impact of Labrador sea-ice extent on the North Atlantic Oscillation. Int. J. Climatol., 24, 603–612.

Lanzante, J.R., 1984: A Rotated Eigenanalysis of the Correlation between 700 mb Heights and Sea Surface Temperatures in the Pacific and Atlantic. Mon. Wea. Rev., 112, 2270–2280.

Lawrence, D.M., A.G. Slater, R.A. Tomas, M.M. Holland, and C. Deser, 2008: Accelerated Arctic land warming and permafrost degradation during rapid sea ice loss. Geophys. Res. Lett., 35, L11506, doi:10.1029/2008GL033985.

Magnusdottir, G., C. Deser, and R. Saravanan, 2004: The effects of North Atlantic SST and sea-ice anomalies on the winter circulation in CCM3. Part I: Main features and storm-track characteristics of the response. J. Climate, 17, 857-876.

Parkinson, C. L., D. J. Cavalieri, P. Gloersen, H. J. Zwally, and J. C. Comiso, 1999: Arctic sea ice extents, areas, and trends, 1978–1996. J. Geophys. Res., 104(C9), 20, 837–20,856.

Prohaska, J.T., 1976: A Technique for Analyzing the Linear Relationships between Two Meteorological Fields. Mon. Wea. Rev., 104, 1345–1353.

Raisanen, J., 2008: Warmer climates: less or more snow? Climate Dynamics, 30, 307-319, doi: 10.1007/s00382-007-0289-y.

Rajagopalan, B., E. Cook, U. Lall, and B.K. Ray, 2000: Spatiotemporal variability of ENSO and SST teleconnections to summer drought over the United States during the twentieth century. J. Climate, 13, 4244–4255.

Rothrock, D.A., Y. Yu, and G.A. Maykut, 1999: Thinning of the Arctic sea-ice cover. Geophysical Resesearch Letters, 26(23), pp. 3469-3472.

Serreze, M. C., and J. A. Francis, 2006: The arctic amplification debate. Climatic Change, 76(3-4), 241-264, doi:1007/s10584-005-9017-y.

Serreze, M. C., M. M. Holland, and J. Stroeve, 2007: Perspectives on the Arctic's shrinking sea-ice cover. Science, 315, 1533-1536.

Serreze, M. C., A. P. Barrett, J. C. Stroeve, D. N. Kindig, and M. M. Holland, 2009: The emergence of surface-based Arctic amplification. The Cryosphere, 3, 11–19.

Simmonds, I., and K. Keay, 2009: Extraordinary September Arctic sea ice reductions and their relationships with storm behavior over 1979–2008. Geophys. Res. Lett., 36, L19715, doi:10.1029/2009GL039810.

Singarayer, J.S., J.L. Bamber, and P.J. Valdes, 2006: Twenty-first-Century climate impacts from a declining Arctic sea ice cover. J. Climate, 19, 1109-1125.

Stroeve, J. C., M. C. Serreze, F. Fetterer, T. Arbetter, W. Meier, J. Maslanik, and K. Knowles, 2005: Tracking the Arctic's shrinking ice cover: Another extreme September minimum in 2004. Geophys. Res. Lett., 32, doi:10.1029/2004GL021810.

Stroeve, J., M. M. Holland, W. Meier, T. Scambos, and M. C. Serreze, 2007: Arctic sea ice decline: faster than forecast. Geophys. Res. Lett., 34, doi:10.1029/2007GL029703.

Stroeve, J., A. Frei, J. McCreight, and D. Ghatak, 2008: Arctic sea-ice variability revisited. Annals of Glaciology, 48(1): 71-81, doi:10.3189/172756408784700699.

Wallace, J.M., C. Smith, and C.S. Bretherton, 1992: Singular Value Decomposition of Wintertime Sea Surface Temperature and 500-mb Height Anomalies. J. Climate, 5, 561–576.

Yang, D., D. Kane, L. Hinzman, X. Zhang, T. Zhang, and H. Ye, 2002: Siberian Lena river hydrologic regime and recent change. Journal of Geophysical Research-Atmospheres, 107(D23), 4694, doi:10.1029/2002JD002542.

Ye, B., D. Yang, and D. L. Kane, 2003: Changes in Lena river stream- flow hydrology: Human impacts vs. natural variations. Water Resour. Res., 39, 1200, doi:10.1029/2003WR001991.

Ye, H., D. Yang, D. Robinson, 2008: Winter rain on snow and its association with air temperature in northern Eurasia. Hydrological Processes, 22 (15), 2728 – 2736.

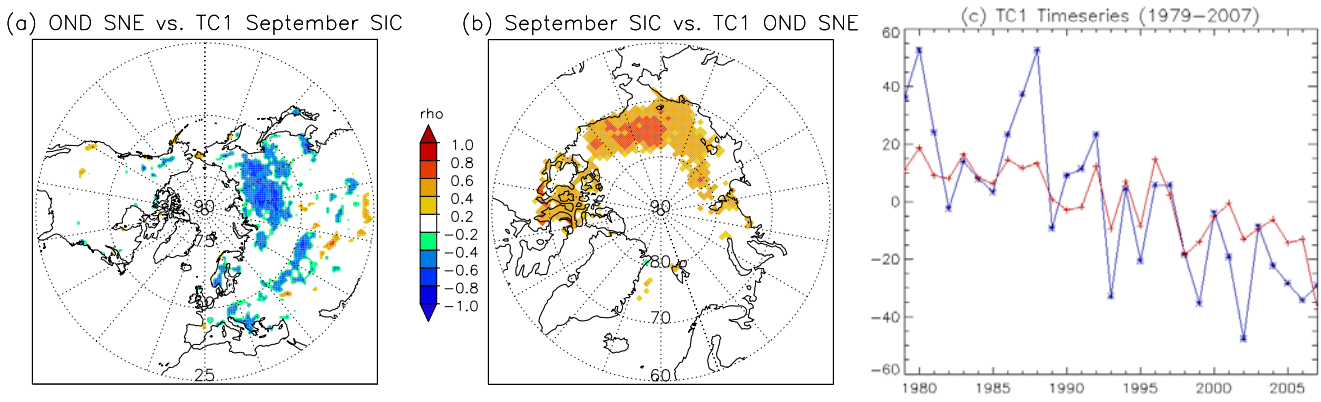

Figure 1 The first SVD mode between OND SNE and September SIC for 1979-2007 time period. Heterogeneous correlation maps: (a) OND SNE vs. TC1 September SIC and (b) September SIC vs. TC1 OND SNE; (c) TC1 time series from both fields (red=SIC, blue=SNE). Units in the y axis are arbitrary; therefore is not shown.

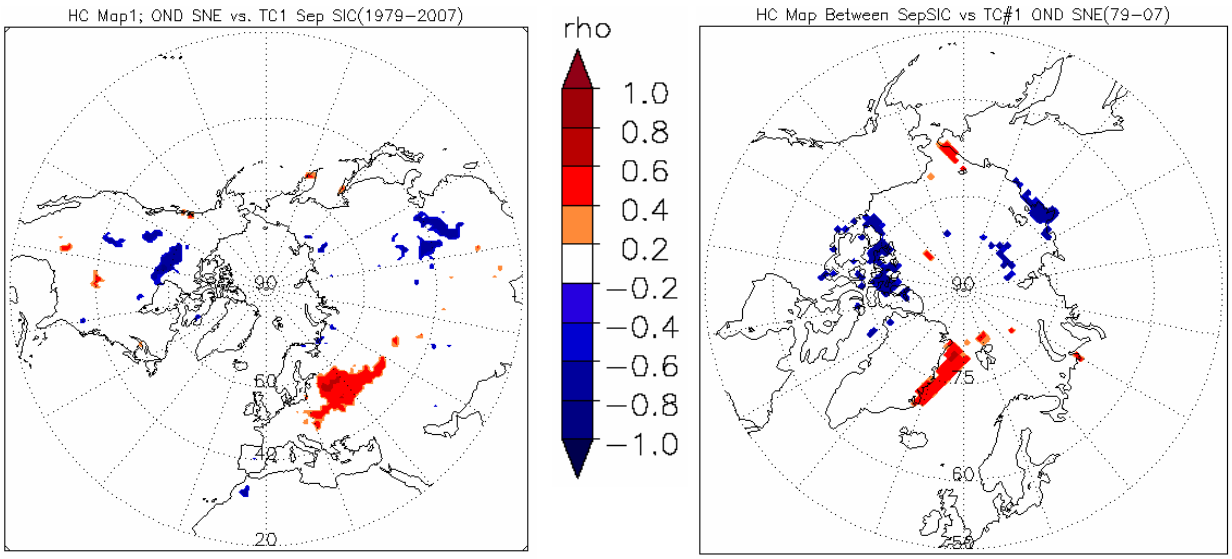

Figure 2 Same as figure 1, but SVD has been done after detrending the timeseries. Heterogeneous correlation maps: OND SNE vs. TC1 September SIC (left figure), and September SIC vs. TC1 OND SNE (right figure).

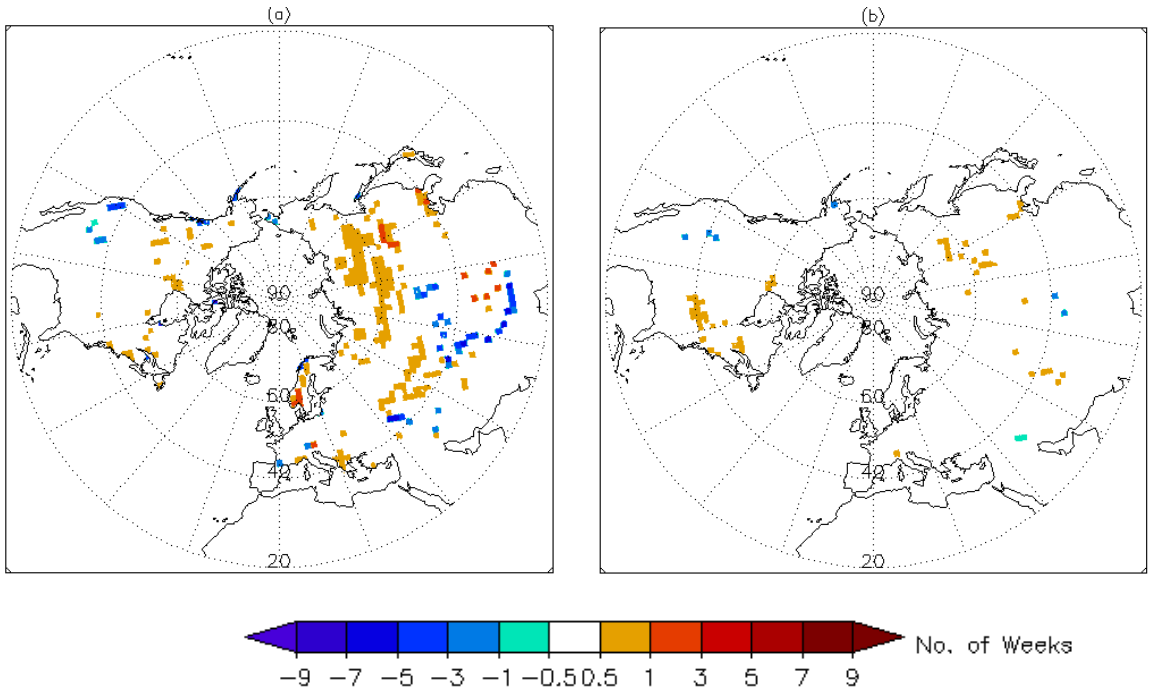

Figure 3 Difference in total number of weeks of snow cover during OND between two nine year Composites of low vs. high September sea ice extent years; a) composites based on actual time series; b) composites based on detrended time series

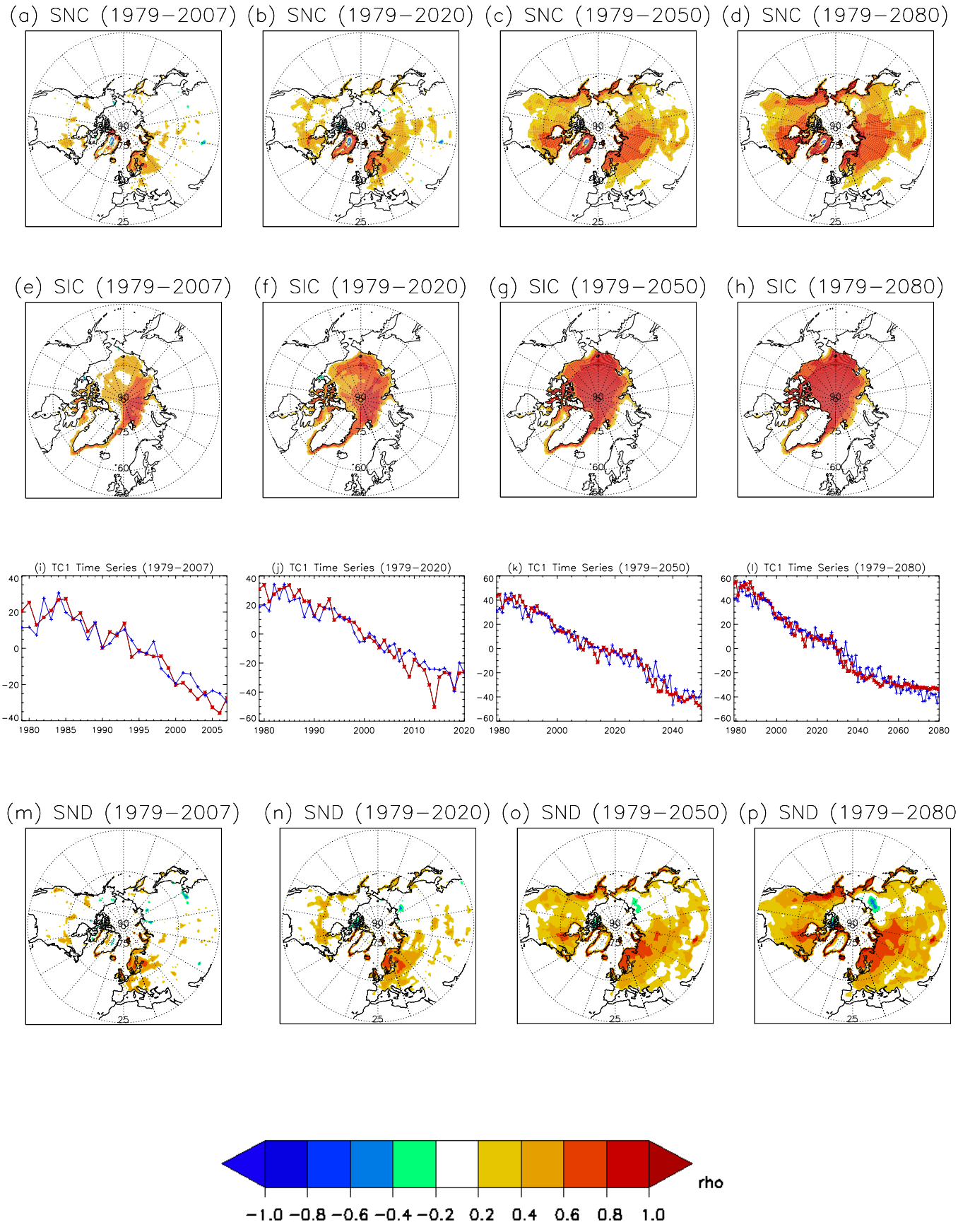
(a) SNC (1979–2007)
(b) SNC (1979–2020)
(c) SNC (1979–2050)
(d) SNC (1979–2080)
(e) SIC (1979–2007)
(f) SIC (1979–2020)
(g) SIC (1979–2050)
(h) SIC (1979–2080)
(i) TC1 Time Series (1979–2007)
(j) TC1 Time Series (1979–2020)
(k) TC1 Time Series (1979–2050)
(l) TC1 Time Series (1979–2080)
(m) SND (1979–2007)
(n) SND (1979–2020)
(o) SND (1979–2050)
(p) SND (1979–2080)
rho
−1.0 −0.8 −0.6 −0.4 −0.2 0.2 0.4 0.6 0.8 1.0

Figure 4 Leading SVD mode between OND SNC and September SIC for different time domains derived from the CCSM3 model. Heterogeneous correlation maps, (a)–(d) OND SNC vs. TC1 September SIC and (e)-(h) September SIC vs. TC1 OND SNC; (i)-(l) TC1 time series from both fields (red= SIC, blue=SNC). Similar analysis has been done between OND SND and September SIC, only shown here heterogeneous correlation maps from the leading mode for, (m)–(p) OND SND vs. TC1 September SIC

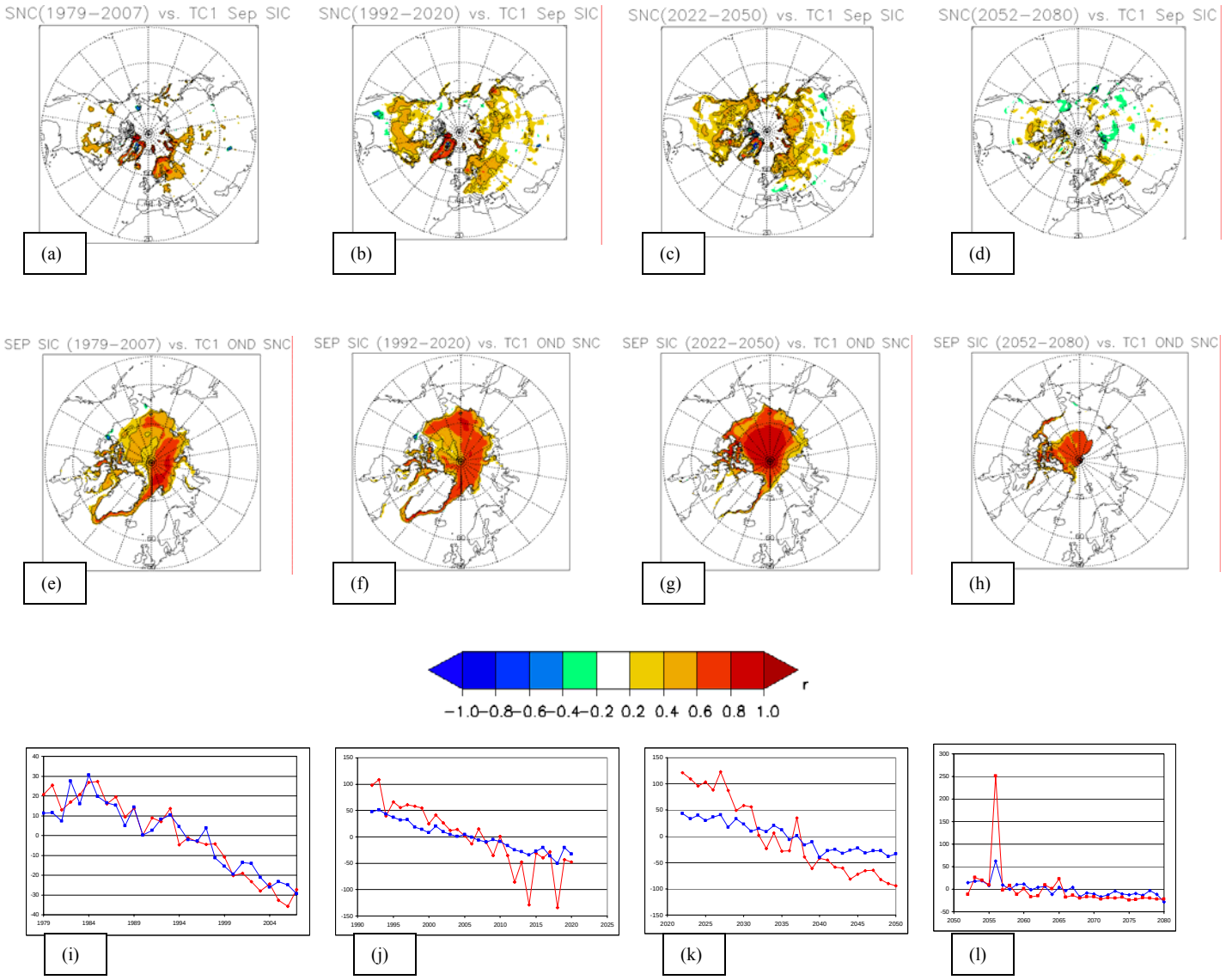

Figure 5 Leading SVD mode between OND SNC and September SIC for four time domains (1979-2007, 1992-2020, 2022-2050, 2052-2080) derived from the CCSM3 model. Heterogeneous correlation maps for different time domains, (a)–(d) OND SNC vs. TC1 September SIC and (e)-(h) September SIC vs. TC1 OND SNC; (i)-(l) TC1 time series from both fields (red= SIC, blue=SNC). Black contour lines represent the 95% confidence level.

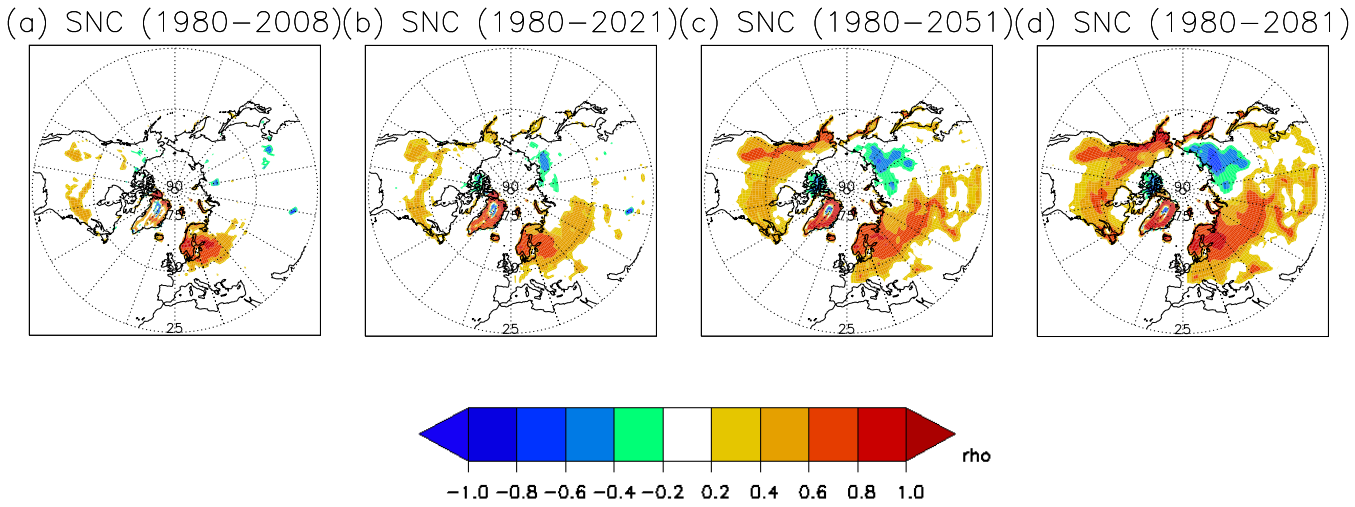

Figure 6 Heterogeneous correlation maps of the leading SVD mode between JFM SNC and September SIC for different time domains derived from the CCSM3 model; only shown here (a)–(d) JFM SNC vs. TC1 September SIC

Chapter 5

Community Atmosphere Model Version 3 (CAM3) Simulated Signature of SST and Sea Ice Forcings on the Eurasian Snow depth

Debjani Ghatak[1] and Allan Frei [1,2]

[1] Program in Earth and Environmental Sciences, The Graduate Center, The City University of New York, New York, NY

[2] Department of Geography, Hunter College, The City University of New York, New York, NY

5.1 Abstract:

In recent years, changing pan-Arctic atmospheric and terrestrial climates threaten to alter temperature and precipitation regimes over Eurasia, and therefore make Eurasian snow cover vulnerable to these changes. In order to determine the potential response of snow to the rapidly retreating Arctic sea ice, a suite of Community Atmospheric Model version 3 (CAM3) experiments are analyzed. These experiments isolate the high latitude surface forcings due to the sea surface temperature and sea ice variations from that of the direct atmospheric radiative forcings. Comparisons of four specific CAM3 experiments suggest that a significant snow response emerges over the Eurasian landmasses, which is generated due to a key role played by the high-latitude surface forcings. East Eurasia, north of Yeneisy and Lena river basins, experiences an opposite trend in snow depth to that of the Scandinavian region. Increasing snow pack is observed over the east, whereas the negative trend is observed over western Eurasia. Modeling results indicate that fall and early winter warming along with the increase in atmospheric water vapor and precipitation lead to these changes in the snow pack. Average temperature remains below-freezing under warming scenario over Siberia, which facilitates the thickening of the snow pack. Conversely, the significant warming over Scandinavia where average temperatures begin closer to 0^0C, leads to the thinning of the snow pack.

5.2 Introduction

Changes in the Pan-Arctic environment are under deep-scrutiny for its immense impact on the global climate (Hassol, 2004). Land-surface snow over the high latitude regions of Eurasia is not an exception, and has been changing gradually (Ye et al., 1998; Clark et al., 1999; Frei and Robinson, 1999; Brown, 2000; Ye, 2001; Ye and Ellison, 2003; Ye B. et al., 2003; Hassol, 2004; Iijima et al., 2007; Brown and Mote, 2009; Bulygina et al., 2009; Ghatak et al., 2010; McCabe and Wolock, 2010). General circulation model simulations suggest that in response to increasing greenhouse gases, snow water equivalent (SWE) will decrease by 60% to 80% over most of the mid-latitudinal regions of the Northern Hemisphere (Barry et al., 2007), but that SWE will increase over Siberia (Barry et al., 2007; Räisänen, 2008).

A detailed picture of recent changes in snow over Russia for the period of 1966-2007 based on 820 station observations, reveals that snow cover duration decreased over the northern regions of European Russia, whereas it increased over central Siberia (Yakutia) and Far East (Bulygina et al., 2009). Positive trend in winter-averaged snow depth is observed over western half of the Russian Federation and the highest negative trend is found over the mountainous regions of southern Siberia.

While over most regions snow decreases in response to a generalized warming over Eurasia (Ye B. et al., 2003; Hassol, 2004; Ye H. et al., 2008), some areas still may have more snow (Bulygina et al., 2009; Ghatak et al., 2010). Ghatak et al. (2010) investigated observed changes in snow by analyzing autumn and early winter total number of weeks of snow cover from the satellite observation for the period of 1979-2007, and examined how this co-varies with the retreating Arctic sea ice loss. Moreover,

they suggest that the snow over Eurasia (e.g. Siberian region) can also be affected by the changing atmospheric and terrestrial climates induced by Arctic sea ice loss; but this signal is inconclusive in the present observational evidences and may strengthen over time (Ghatak et al., 2010). The observational evidence for a Siberian snow signal associated with varying sea ice reported in the 4th chapter and by Ghatak et al. (2010) is consistent with the modeling studies by Deser et al. (2010). But, the causal link between the changing observed snow over Siberia and the decreasing Arctic sea ice is still not clear to us.

In this chapter, the causal linkage between snow and sea ice has been investigated through analyzing model outputs from specific experiments which are designed to isolate the impact of changing sea ice from a generalized warming trend. Therefore, our first objective is to identify the relative roles of surface forcings, versus the effects of radiative forcings in generating the changes in snow pack. Our second objective is to investigate the physical mechanisms of the changes in snow. Details of the experiments and model outputs are discussed in section 5.3; results are shown in section 5.4 and conclusions are in section 5.5.

5.3 Model Outputs and Experiments:

We chose Community Atmospheric model version 3 (CAM3), an atmospheric model of the Community Climate System model (CCSM3) which is a fully-coupled general-circulation model. Details about the CAM3 is reported in Collins et al. (2006); whereas, the strength and weakness of the CAM3 in simulating the mean state of climate and intra-seasonal, inter-annual variability are discussed in Hurrell et al. (2006).

Moreover, Deser and Phillips (2009) showed that the observed pattern of sea level pressure and 500hPa geopotential height trends have been well simulated by CAM3.

We analyze model outputs from four different CAM3 experiments, which have been specifically designed to isolate the impacts of Arctic Sea surface temperature (SST) and Arctic sea ice loss from the effects of radiative forcings. These experiments have been accomplished in National Center of Atmospheric research (NCAR) at T42 horizontal resolution (2.8° latitude X 2.8°longitude) and more information can be obtained from http://www.cesm.ucar.edu/working_groups/Variability/experiments.html. Four experiments are (1) 'IPCC_AMIP', (2) 'Vanilla_AMIP', (3) 'RADATM' and (4) 'TOGA' (as named in the archive); we keep these names in this chapter as 'IPCC', 'Vanilla', 'RADATM' and 'TOGA'. Details of these experiments are discussed by Deser and Phillips (2009) and summarized here as follows (table 1). IPCC is forced by the observed, time-evolving atmospheric chemical composition (greenhouse gases, tropospheric and stratospheric ozone, sulfate and volcanic aerosols), solar output, global SSTs and sea ice concentration during 1950-2008. Vanilla is forced by the observed, time-evolving global SSTs and sea ice concentration during 1950-2008; the atmospheric chemical composition and solar output have been kept at 1990 level. RADATM is forced by the observed time-evolving atmospheric chemical composition and solar output during 1950-2008, but only with the mean seasonal cycle of SSTs and sea ice concentration. TOGA is forced by only the tropical (20^{0}N-20^{0}S) observed, time-evolving SSTs during 1950-2000. Climatological seasonal cycle of SSTs and sea ice have been used polewards of 20° in TOGA and the atmospheric chemical composition and solar output have been

kept at 1990 level. We use mean of 5 ensembles for each experiment and for all variables in our analyses.

Model outputs for all experiments except TOGA are available for the period of 1950-2008; TOGA ends in 2000. In section 5.4, we will discuss how we compare TOGA with the other experiments despite their different time domains. Our temporal domain of analysis includes winters 1979/1980-2007/2008, which overlaps with the period of satellite observations. Thus, this helps us to understand how the historic simulations can be compared with the observed variability. The spatial domain of the analysis is extra-tropical region of the Northern Hemisphere (beyond 20^0 N); though our area of interest is mainly Eurasia. We analyze monthly mean snow depth ('SNOWDP' in meter), surface air temperature ('TS' in degree Celsius), specific humidity at the surface level ('QBOT' in gm/kg), precipitation (mm/day), horizontal and meridional wind fields at the surface level ('UBOT' and 'VBOT' in m/s) for the extended winter season, starting from the months of October to March.

5.4 Results

5.4.1 Results from Trend Analysis

Spatio-temporal changes in SNOWDP:

In order to examine the spatio-temporal changes in simulated SNOWDP field in all these four experiments, the linear trend analyses of mean monthly SNOWDP from October to March for each of the four experiments (figures 1-4) are shown. Trends significant at 90% confidence level are shown through the black contours (figures 1-4). The time domain of the trend analyses for the months of October, November and December is 1979-2007 and for the months of January, February and March is 1980-2008

for IPCC, Vanilla and RADATM. The time domain for TOGA is 1979-2000 for the months of October, November and December, and 1980-2000 for the months of January, February and March.

Trend analyses of SNOWDP as simulated by the IPCC experiment (includes both surface and radiative forcings) show mainly a dipole pattern of positive and negative trends over the east and west of the Eurasian continent which remains consistent over the winter season (figure 1). Positive trend emerges over the northern Yenisey and Lena river basins during November (figures 1b). The significant pattern becomes more spatially extensive and strong over the winter (figures 1b-f). On the other hand, strong and significant negative trend appears mainly over the Scandinavian region extending eastward up to the west of Ob river basin along with a pattern over south-western Siberia (figures 1b-f).

A similar spatial pattern of trend in monthly SNOWDP is also seen for the Vanilla experiment (forced by surface boundary conditions only) (figure 2). The main difference with IPCC (figure 1) is that the spatial pattern of positive trend is much more widespread towards south over land areas in Vanilla experiment (figures 2e-f); though the significant pattern is still centered over the Yenisey and Lena basin areas. Another difference is that the significant and spatially extensive positive trend emerges late in the winter compared to IPCC experiment (compare figures 1 and 2).

Similar trend analysis of the mean monthly SNOWDP as simulated by the RADATM experiment (forced by the radiative forcings only) and TOGA (forced by tropical SSTs only) (figures 3, 4) show no coherent and significant trends over the Eurasian continent. Trend maps generated from the TOGA experiment help us to

understand if the trends in Vanilla experiment (figure 2) are due partly to the SST forcings from the tropics. As TOGA experiment goes only till 2000, it is important to compare Vanilla trend for the same time domain as TOGA. Therefore, the trend of mean March SNOWDP from Vanilla computed for the period of 1980-2000 has been shown (figure 5). This is consistent with the figure 2f which shows the trend for the period of 1980-2008. Now, if figure 5 is compared with the trends in mean March SNOWDP from TOGA (figure 4f), no tropical SST forcings is found. The reason of showing March SNOWDP for this comparison is that the Vanilla trend is maximized spatially during March.

In summary, these trend analyses indicate that the SNOWDP increases over central and eastern Siberia (over northern Yenisey, Lena river basin) and decreases over Scandinavian region in only those experiments which include high latitude surface boundary forcings (IPCC and Vanilla). The spatial pattern of positive trend in SNOWDP is consistent with the observational findings as discussed in chapter 4, which shows that increasing snow over Siberia during fall and early winter is correlated with the loss of summer Arctic sea ice. Our next goal is to identify the physical mechanisms leading to this dipolar pattern of SNOWDP with a focus on the centers of actions, i.e. Scandinavia and Siberia.

Spatio-temporal changes in Surface Temperature:

In order to explain the changes in SNOWDP over Eurasia, we examine the surface air temperature (TS) field as SNOWDP is partially function of temperature. Figures 6a-f show monthly TS trend plots for IPCC experiment. An extensive warming trend is readily visible over the Arctic Ocean as well as over the Eurasian landmasses

during October (figure 6a). Moreover, the strongest warming trend (0.2° C/year) is prominent over the East Siberian Sea (figure 6a), and is associated with the huge summer ice loss over the East Siberian Sea (Serreze et al., 2009). During November, the significant pattern is spatially reduced, and remains over most of the Arctic Ocean and also over the east Eurasia (figure 6b). The region with positive temperature trend shifts westward over the Eurasian landmasses during December (figure 6c). Subsequently, the significant warming trend disappears from the land and persists only over the Atlantic sector of the Arctic Ocean during rest of the winter (figures 6d-f).

Similar trend analysis has been done on mean monthly TS for Vanilla experiments, which produces similar warming trends (figures 7a-f). The only difference with the IPCC experiment is the appearance of a strong warming over the Eurasian landmasses during mid and late winter (compare figures 6d-f with figures 7d-f). On the other hand, trend analyses of monthly TS fields for RADATM experiment show no significant trend (figures 8a-f).

In summary, a strong warming over the Arctic Ocean and over Eurasian landmass is apparent in IPCC and Vanilla experiments, mainly during October. RADATM with no surface boundary forcings fails to generate this signal. Thus, this indicates that the surface forcings play a major role in this Arctic-wide warming, and is consistent with the observed 'Arctic amplification' (Serreze et al., 2009). Serreze et al. (2009) show that the surface based Arctic warming is most pronounced during autumn due to the loss of summer (September) sea ice; winter warming is still not prominent. Furthermore, feedback generated due to the sea ice loss affect the Arctic greater than the lower latitudes (Serreze et al., 2009). Results shown here are consistent with Serreze et al.

(2009) and since these CAM3 experiments are forced by the observed time-evolving forcing fields (atmospheric composition, solar output and surface forcing), they are able to produce this surface-based pan-Arctic warming as observed in recent years.

Spatio-temporal changes in Specific Humidity:

Similar trend analyses have been employed on the mean monthly fields of surface specific humidity (QBOT) from three different experiments. Figures 9a-f show trend in QBOT for IPCC (only trends significant at 90% confidence are plotted). Significant positive trends in QBOT are apparent over the whole Arctic Ocean and the Eurasian landmasses during October (figure 9a). The strongest trend is observed over the East Siberian Sea and also over a zonal band stretching from Scandinavia to the southern Siberia (figure 9a). The area of significant trends is spatially reduced during November when it remains only over the ocean and over east Eurasian (figure 9b). Subsequently, the significant trend shifts towards western Eurasia and over the Atlantic and then gradually disappears from the land (figure 9c-f).

Trend in Vanilla QBOT (figures 10a-f) is very similar with the IPCC (figures 9a-f); the only difference is the emergence of significant trend over the landmasses in Vanilla during mid and late winter. There is no significant trend present in RADATM (figures 11a-f). Please note that the trend in QBOT follows the TS pattern for all three experiments (compare figures 9-11 with figures 6-8) and their spatial pattern of changes over the winter is almost identical. This is intuitive as the rising temperature leads to the increase in atmospheric water vapor content. During fall, an arctic wide warming associated with diminished sea ice cover delays the ice formation and leaves open water (Serreze et al., 2009), which facilitates the positive trend in specific humidity.

Spatio- temporal changes in Precipitation:

Significant changes in TS and QBOT may affect the precipitation. Therefore, the spatio-temporal pattern of changes in precipitation has been investigated here (figures 12-14). Figure 12 shows the trend plots as simulated in IPCC and significant increase in precipitation is found over the Arctic Ocean and also over the Siberia during October (figure 12a). During December, the major pattern of positive trend is centered over the Atlantic side of the Arctic Ocean and also over the European Arctic coast (figure 12c). During late winter (February and March), positive trend is found over the Pacific side of the Arctic and Pacific coast (figure 12e-f). Negative trend emerges over Scandinavia during late winter (fig 12f).

Figure 13 shows the trend plots of precipitation as simulated in Vanilla. During October, the positive trend pattern over the Arctic is very similar with the IPCC pattern (figure 13a). Significant positive trend in precipitation is mainly over the landmasses during late winter (figures 13d-e). Trend analyses of precipitation do not show any coherent pattern in RADATM. Significant precipitation pattern is not as widespread as the TS and QBOT pattern.

In conclusion, these sets of trend analyses show that the Arctic wide warming during fall and early winter spreads over Eurasian landmasses extending from Scandinavia to Siberian regions. An increase in atmospheric water vapor content is also observed in the model simulations over the same region. Significant increase in precipitation is found over Siberia during October and over Scandinavia during mainly December. Scandinavia also experiences negative trend in precipitation during late winter. Consequently, these changes in TS, QBOT and precipitation over Scandinavia

and Siberia, which are mainly driven by the surface forcings of SST and sea ice, may lead to the changes in SNOWDP.

5.4.2 Regional Analysis:

In order to understand the mechanisms of the opposite SNOWDP response as found in section 5.4.1, these two regions are examined thoroughly. For this purpose, we choose Siberian region as the area between the latitudes 60^0 N and 75^0 N and the longitudes between 95^0E and 135^0 E (Figure 15a). This region shows increasing SNOWDP in the trend plots. Scandinavian region is chosen as the area between the latitudes 58^0 N -70^0N and the longitudes between 10^0E - 50^0 E (figure 15b), which exhibits loss of SNOWDP.

Siberian Region:

Area-weighted average monthly temperature time series for the time period 1979/1980-2007/2008 show warming over the Siberian region during fall and winter in both IPCC and Vanilla simulations (figures 16a-b). Monthly TS timeseries from RADATM (figure 16c) do not show any trend, which is consistent with the results of trend analyses (section 5.4.1). Table 2 shows the regression coefficients of the best fit trend lines (using the least squares method) and their corresponding significance levels. The maximum warming occurs during October (0.08ºC/Year). Moreover, figures 16a-b indicate that monthly average temperatures over this region during fall and winter season remain below 0^0C. Thus, the atmospheric condition still facilitates snowfall and snow accumulation during fall and winter over this region.

The area-weighted total monthly specific humidity (QBOT) time series for fall and winter also shows a significant positive trend for both IPCC and Vanilla simulations (figures 17a-b). The maximum trend is observed during Oct (Table 3) and is much higher than the other winter months. In contrast, there is no significant trend for RADATM, as is also suggested by the trend analyses (figure 17c).

We also examine wind patterns over this region. For this purpose, we divide this region in two parts (a) north (65° N- 70° N; 110°E- 135°E) and (b) south (60° N- 65° N; 110°E- 135°E) (figures 18a-b). We calculate the frequency of each wind direction from the monthly wind direction fields for the 1979/1980-2007/2008 time domain and then plot the distribution of wind directions as the fraction of monthly total. The prevailing monthly-mean wind direction varies between south-westerly to westerly over the whole Siberian region (both northern and southern parts) (Figure 19, 20); though it is less variable over the southern part. Northerly winds also seen during mid and late winter. We repeat this analysis for the time domain 2000/2001-2007/2008 in order to identify any potential changes in recent wind pattern (figures 21-22). The frequency of west-south-westerly wind is increased in recent years. These analyses suggest that the dominant pattern of monthly wind is continental type. Advection of ocean air mass cannot be captured through these types of analyses using monthly wind fields.

In conclusion, while temperature and atmospheric water vapor both increase during fall and early winter over this region, the average monthly-mean temperature remains well below freezing. These conditions are favorable for increased snowfall and SNOWDP.

Scandinavian Region:

Similar sets of analyses have been done for the Scandinavian region (figure 15b). Significant positive trend is apparent in the area-weighted average monthly temperature timeseries during fall and winter (figures 23a-b and table 2) for both IPCC and Vanilla and the maximum trend is found in October. Moreover, figures 23a-b indicate that the average monthly temperature over this region during October remains above freezing during 1979-2007 time domain and November temperature also sometimes exceeds freezing level. RADATM doesn't show any trend, as is also suggested by the trend analyses. Significant trend is also observed in the area-weighted total monthly QBOT time series for fall and winter and the maximum trend is found during December for IPCC (figures 24a-b, table 3). Increased precipitation is observed during this month (figure 12c). Furthermore, the wind is much more variable over this region compared to the Siberian region (figure 25). It ranges between 90° - 270° and becomes more variable even northerly during late winter (February and March); though the dominant mode of direction is south and south-westerly (figure 25a-b).

Meteorological conditions over this region favor the advection of warm, maritime air masses, resulting in increased availability of atmospheric water vapor content. In contrast to the Siberian region, atmospheric warming resulting in more frequent above-freezing temperatures favor more frequent rain (rather than snow) and melt events, both of which tend to reduce SNOWDP.

5.5 Conclusions

In this chapter, we examine the spatio-temporal changes in SNOWDP in a suite of four CAM3 experiments which is designed to isolate the impacts of surface forcings from

the direct impacts of atmospheric radiative forcings. IPCC experiments (which include both radiative and surface forcings) and Vanilla experiments (which include only surface forcings) generate a dipolar trend pattern in the SNOWDP field over Eurasia. Positive trends in SNOWDP emerge over the north Yenisey and Lena river basins and negative trends appear over Scandinavia. RADATM (which includes radiative forcings only) and TOGA (which includes tropical SST forcings) experiments fail to produce this SNOWDP responses, suggesting that the changes in SNOWDP are by high-latitude surface forcings. The TOGA experiment indicates that tropical SST variations are not responsible for this SNOWDP response; rather, high latitude surface forcings play the key role. The spatial pattern of the SNOWDP response is consistent with results from chapter 4, where observational datasets suggest that in the real climate system, decreased summer Arctic sea ice may be related to increased snow over Siberia during fall and early winter, and that this signal should strengthen over time.

Significant and strong warming is found not only over the Arctic Ocean but also over the Eurasian landmasses in IPCC and in Vanilla experiments, mainly during fall. This warming is triggered by the surface forcings, as is suggested by the suite of experiments. In other words, positive feedback due to the loss of sea ice plays the key role in warming over the Arctic and over Eurasia. This result is also consistent with the recent surface-based warming observed over the Arctic and is consistent with the 'Arctic amplification' (Serreze et al., 2009; see chapter 4). Furthermore, this study shows that the rising temperature is associated with the increasing atmospheric water vapor content over the Arctic and also over the Eurasian landmasses. The spatial pattern of increased specific humidity is almost identical with the spatial pattern of warming. More open water over

the Arctic Ocean due to the loss of summer sea ice under a warm atmosphere may cause the increase in the specific humidity. Furthermore, increased precipitation is also found over the Arctic, but the significant pattern is not as widespread as the pattern of TS and QBOT. A recent study reveals that CCSM3 21st century simulations under SRESA1B scenario suggests the ~20% increase in the annual mean moisture convergence over the Arctic and ~95% of these changes results from the thermodynamic factors (Skific et al., 2009).

Then we examine the Scandinavia and Siberian regions (as identified here in figures 15a-b) in order to identify the physical mechanisms responsible for the opposite SNOWDP trends. Area-weighted average temperatures increase over both regions during fall and early winter. In spite of significant warming, average temperatures over Siberian region remain below-freezing during October to March. On the other hand, average temperatures over Scandinavia exceed the freezing level during October and November. More frequent above-freezing temperatures over Scandinavia favor more precipitation falling as rain and more frequent melting, both of which will tend to reduce SNOWDP. Conversely, over Siberia, below-freezing temperature even under a warming scenario causes the meteorological conditions favorable to increased snowfall and SNOWDP.

5.6 Acknowledgement:

We are thankful to Dr. Clara Deser for providing us the CAM3 model outputs and for her valuable suggestions. We are grateful to Adam Philips for his immense cooperation in acquiring the model outputs and in explaining all our questions. We also appreciate the useful discussion with Dr. Imtiaz Rangwala regarding the processing of model output over a region.

5.7 References:

Barry, R. G., R. Armstrong, T. Callaghan, J. Cherry, S. Gearhead, A. Nolin, D. Russell, and C. Zockler, 2007:. Snow, in Global Outlook for Ice and Snow. pp. 39-62, UNEP (Ed.), Nairobi, Kenya.

Brown, R.D., 2000: Northern hemisphere snow cover variability and change, 1915-1997. J. Climate, 13(13), 2339-2355.

Brown, R. D., and P. W. Mote, 2009: The response of Northern Hemisphere snow cover to a changing climate. Journal of Climate, 22, 2124–2145.

Bulygina, O. N., V. N. Razuvaev, and N. N. Korshunova, 2009: Changes in snow cover over Northern Eurasia in the last few decades**.** Environ. Res. Lett., 4, 045026, 6 pp, doi: 10.1088/1748-9326/4/4/045026.

Clark, M.P., M.C. Serreze, and D. A. Robinson, 1999: Atmospheric control on Eurasian snow extent. Int. J. Climatol, 19, 27–40.

Collins, W. D., and Coauthors, 2006: The Community Climate System Model Version 3 (CCSM3). J. Climate, 19, 2122–2143.

Deser, C., and A.S. Phillips, 2009: Atmospheric Circulation Trends, 1950-2000: The Relative Roles of Sea Surface Temperature Forcing and Direct Atmospheric Radiative Forcing. J. Climate, 22, 396-413, doi:10.1175/2008JCLI2453.1

Deser, C., R. Tomas, M. Alexander, and D. Lawrence, 2010: The Seasonal Atmospheric Response to Projected Arctic Sea Ice Loss in the Late Twenty-First Century. J. Climate, 23, 333–351.

Frei, A., and D.A. Robinson, 1999: Northern Hemisphere snow extent: Regional variability 1972–1994. Int. J. Climatol., vol. 19, pp. 1535–1560.

Ghatak, D., A. Frei, G. Gong, J. C. Stroeve, and D. Robinson, 2010: On the emergence of an Arctic amplification signal in terrestrial Arctic snow extent. J. Geophys. Res., 115, D24105, doi:10.1029/2010JD014007.

Hassol, S. J., 2004: Impacts of a Warming Arctic: Arctic Climate Impact Assessment. 139 pp., Cambridge Univ. Press, Cambridge, U.K.

Hurrell, J. W., J. J. Hack, A. S. Phillips, J. Caron, and J. Yin, 2006: The dynamical simulation of the Community Atmosphere Model Version 3 (CAM3). J. Climate, 19, 2162–2183.

Iijima, Y., K. Masuda, and T. Ohata, 2007: Snow disappearance in Eastern Siberia and its relationship to atmospheric influences. International Journal of Climatology, 27: 169–177. doi: 10.1002/joc.1382.

McCabe, G.J., and D. M. Wolock, 2010: Long-term variability in Northern Hemisphere snow cover and associations with warmer winters. Climatic Change, v. 99, no. 1, p. 141-153.

Raisanen, J., 2008: Warmer climates: less or more snow? Climate Dynamics, 30, 307-319, doi: 10.1007/s00382-007-0289-y.

Serreze, M. C., A. P. Barrett, J. C. Stroeve, D. N. Kindig, and M. M. Holland, 2009: The emergence of surface-based Arctic amplification. The Cryosphere, 3, 11–19.

Skific, N., J.A. Francis, and J.J. Cassano, 2009: Attribution of Seasonal and Regional Changes in Arctic Moisture Convergence. J. Climate, 22, 5115–5134, DOI: 10.1175/2009JCLI2829.1.

Ye, B., D. Yang, and D. L. Kane, 2003: Changes in Lena river stream- flow hydrology: Human impacts vs. natural variations. Water Resour. Res., 39, 1200, doi:10.1029/2003WR001991.

Ye, H., 2001: Increases in snow season length due to earlier first snow and later last snow dates over north central and northwest Asia during 1937–94. Geophys. Res. Lett., 28(3), 551–554, doi:10.1029/2000GL012036.

Ye H, H. Cho, P. Gustafson, 1998: The changes of Russian winter snow accumulation during 1936–1983 and its spatial patterns. Journal of Climate, 11: 856–863.

Ye, H., and M. Ellison, 2003: Changes in transitional snowfall season length in northern Eurasia. Geophys. Res. Lett., 30(5), 1252, doi:10.1029/2003GL016873.

Ye, H., D. Yang, D. Robinson, 2008: Winter rain on snow and its association with air temperature in northern Eurasia. Hydrological Processes, 22 (15), 2728 – 2736.

Table 1 The forcing characteristics of the CAM3 experiments. Column caption shows the forcing fields and the row caption shows the name of the experiments, as used in this chapter. 'X' denotes the forcing field is used in the experiment.

	Observed, time-evolving atmospheric chemical composition and solar output	High Latitude Surface Forcings (Observed time evolving SSTs and Sea Ice Concentrations pole wards 20^0)	Tropical Surface Forcings (Observed time-evolving tropical (20^0 N-20^0S) SSTs)
IPCC	X	X	X
Vanilla		X	X
RADATM	X		
TOGA			X

Table 2 Linear Regression coefficients of monthly area-weighted average TS timeseries for Siberian and Scandinavian region are given below. Values in the bracket show the significance level and values in bold show the coefficients significant at 90% confidence interval.

	Siberian Region						**Scandinavian Region**					
	Oct	Nov	Dec	Jan	Feb	March	Oct	Nov	Dec	Jan	Feb	March
IPCC	**0.081 (0.000)**	**0.055 (0.002)**	**0.059 (0.002)**	**0.033 (0.08)**	0.008 (0.715)	-0.008 (0.642)	**0.044 (0.000)**	**0.028 (0.057)**	**0.074 (0.000)**	**0.059 (0.018)**	0.027 (0.105)	-0.007 (0.663)
VANILLA	**0.074 (0.001)**	0.029 (0.208)	**0.056 (0.037)**	0.010 (0.556)	**0.072 (0.003)**	**0.049 (0.019)**	**0.045 (0.000)**	**0.047 (0.000)**	**0.041 (0.034)**	**0.05 (0.014)**	**0.053 (0.051)**	0.006 (0.773)
RADATM	0.006 (0.595)	0.013 (0.547)	0.026 (0.164)	0.036 (0.102)	0.035 (0.153)	-0.020 (0.293)	-0.001 (0.852)	-0.011 (0.183)	0.008 (0.466)	-0.005 (0.72)	0.015 (0.248)	-0.003 (0.691)

Table 3 Linear Regression coefficients of monthly area-weighted total QBOT timeseries for Siberian and Scandinavian region are given below. Values in the bracket show the significance level and values in bold show the coefficients significant at 90% confidence interval.

	Siberian Region						**Scandinavian Region**					
	Oct	Nov	Dec	Jan	Feb	March	Oct	Nov	Dec	Jan	Feb	March
IPCC	**0.719 (0.000)**	**0.286 (0.004)**	**0.214 (0.002)**	0.093 (0.117)	-0.009 (0.912)	-0.145 (0.224)	**0.731 (0.000)**	0.343 (0.101)	**0.854 (0.000)**	**0.502 (0.030)**	0.172 (0.172)	-0.142 (0.440)
VANILLA	**0.723 (0.000)**	0.125 (0.268)	**0.187 (0.037)**	0.035 (0.510)	**0.225 (0.006)**	**0.263 (0.038)**	**0.751 (0.000)**	**0.589 (0.001)**	**0.450 (0.042)**	**0.409 (0.031)**	0.318 (0.133)	-0.002 (0.991)
RADATM	0.032 (0.799)	0.082 (0.397)	0.1 (0.144)	0.123 (0.103)	0.057 (0.472)	-0.082 (0.488)	-0.082 (0.599)	-0.315 (0.118)	0.166 (0.370)	-0.147 (0.396)	0.218 (0.258)	-0.078 (0.609)

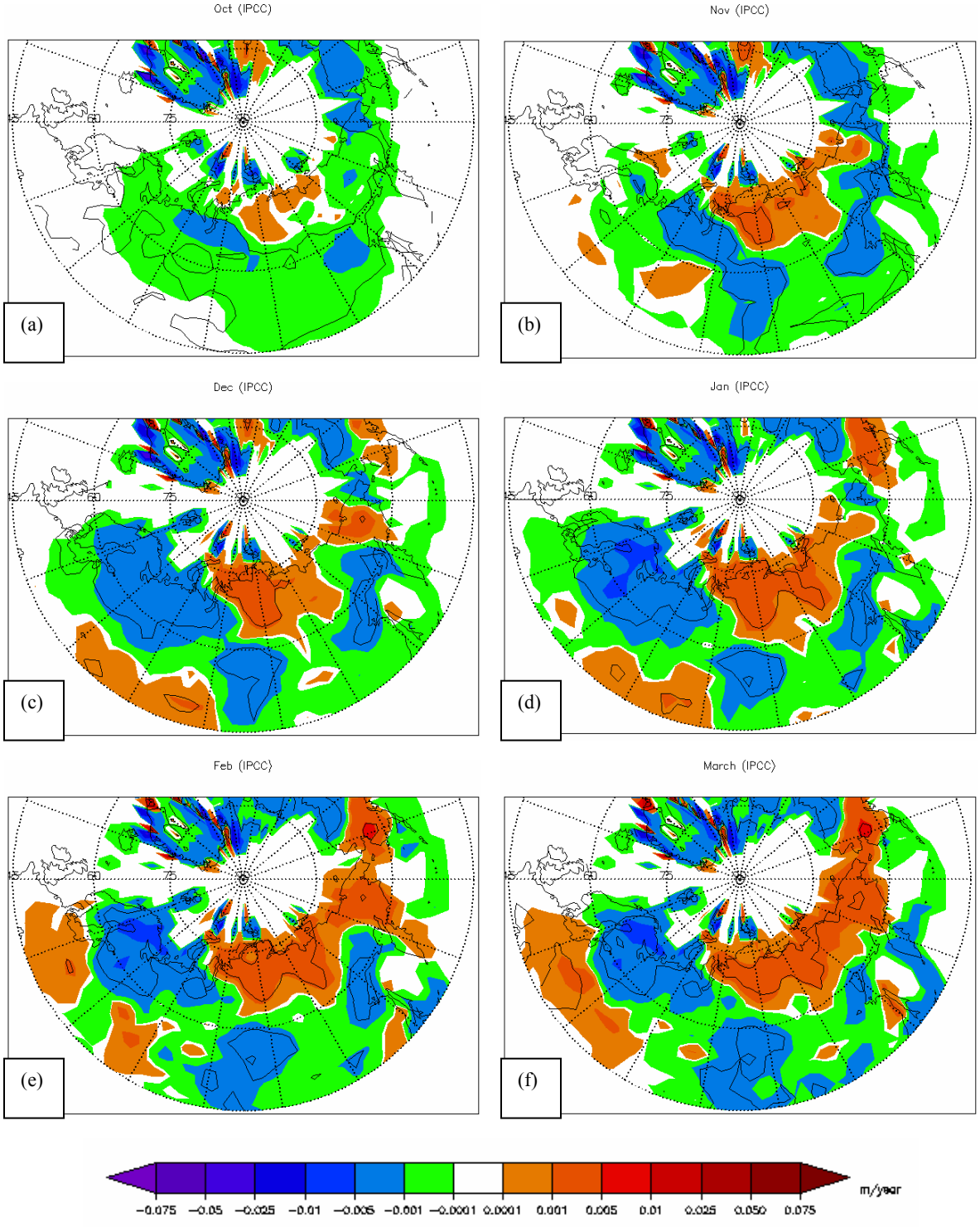

Figure 1 Linear Trend of SNOWDP from IPCC experiment for the period of 1979/1978-2007/2008 has been plotted for the month of (a) October, (b) November, (c) December, (d) January, (e) February and (f) March. Linear trend significant at 90% confidence level has been shown through the black contour.

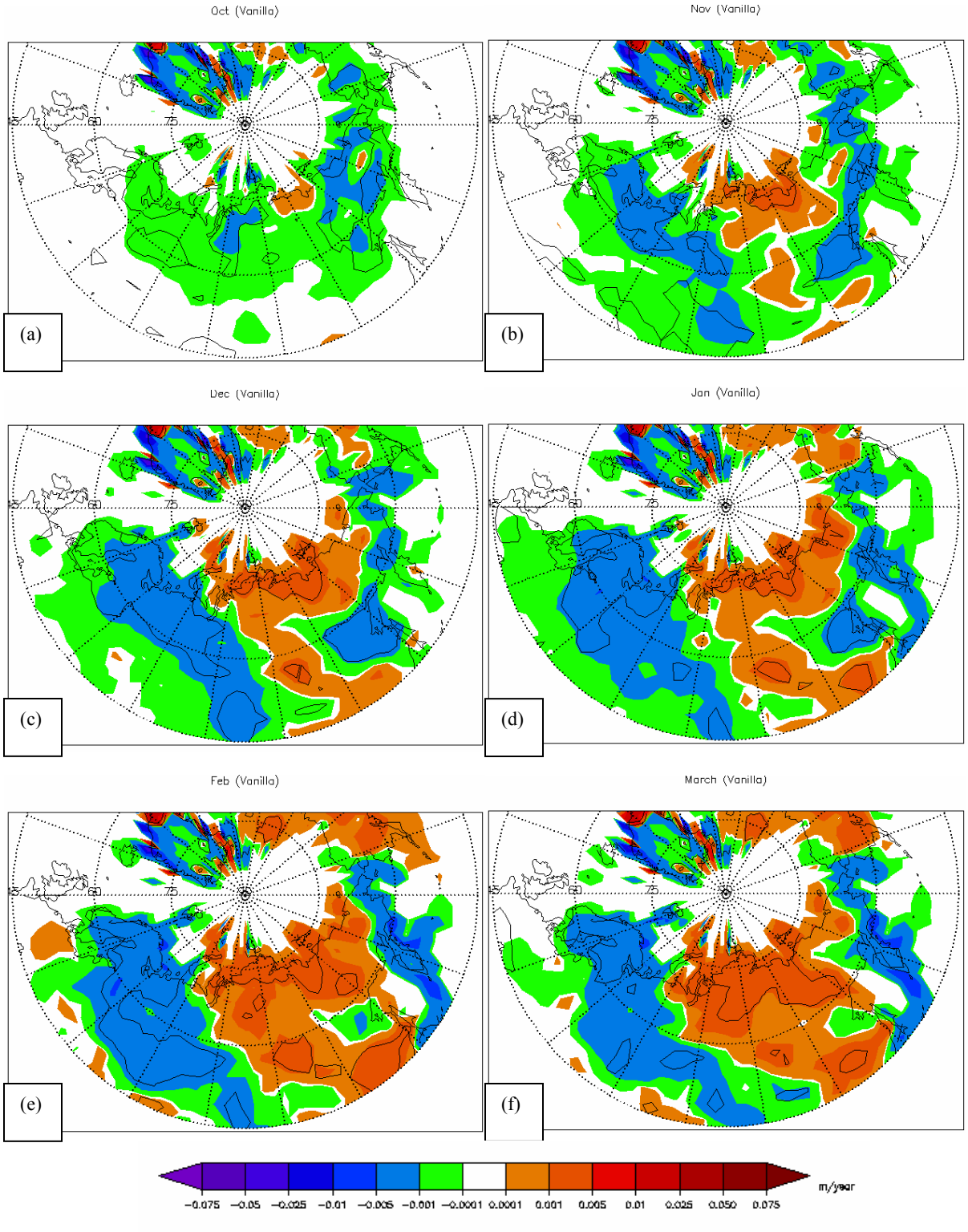

Figure 2 Same as figure 1, except for the experiment Vanilla

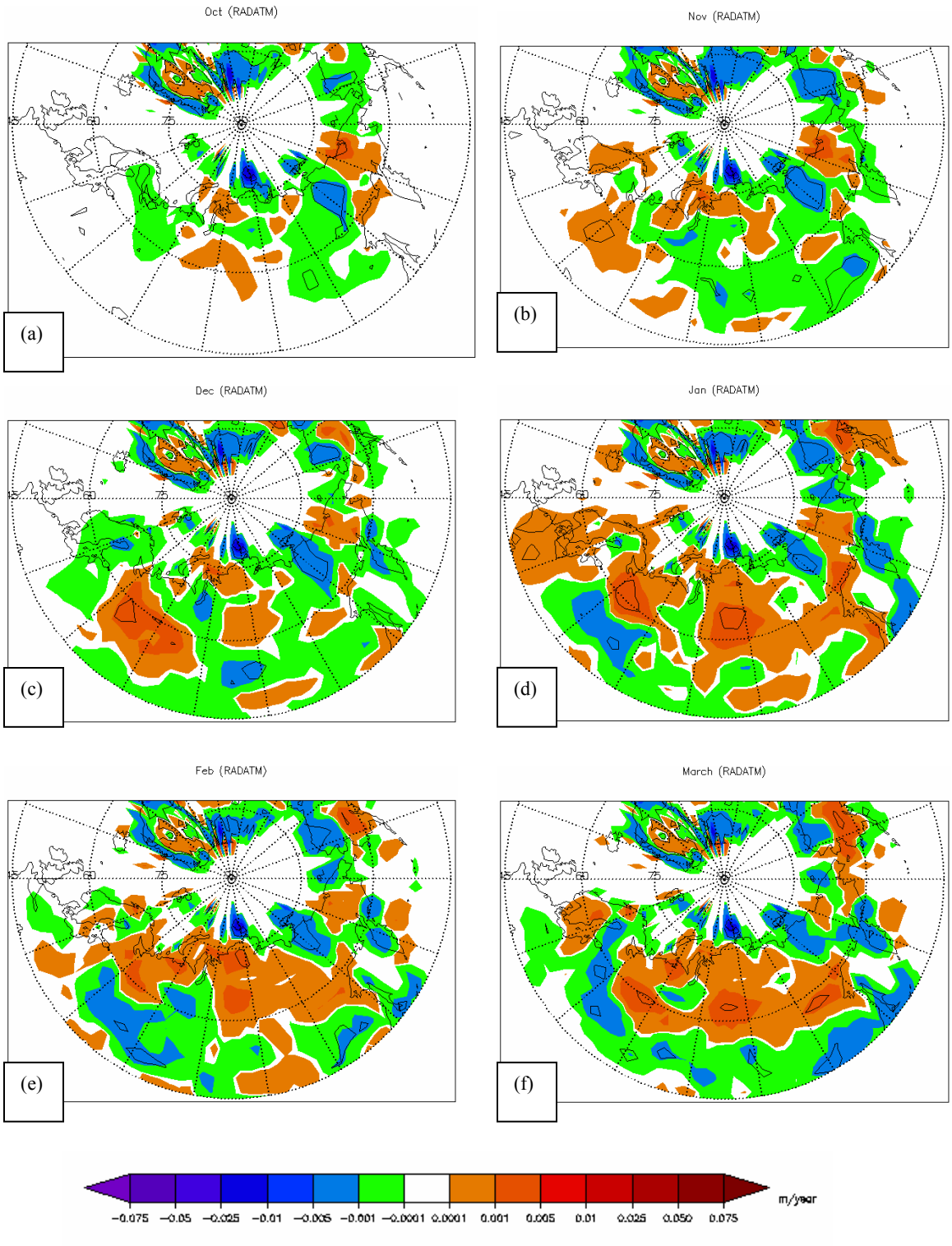

Figure 3 Same as figure 1, except for the experiment RADATM

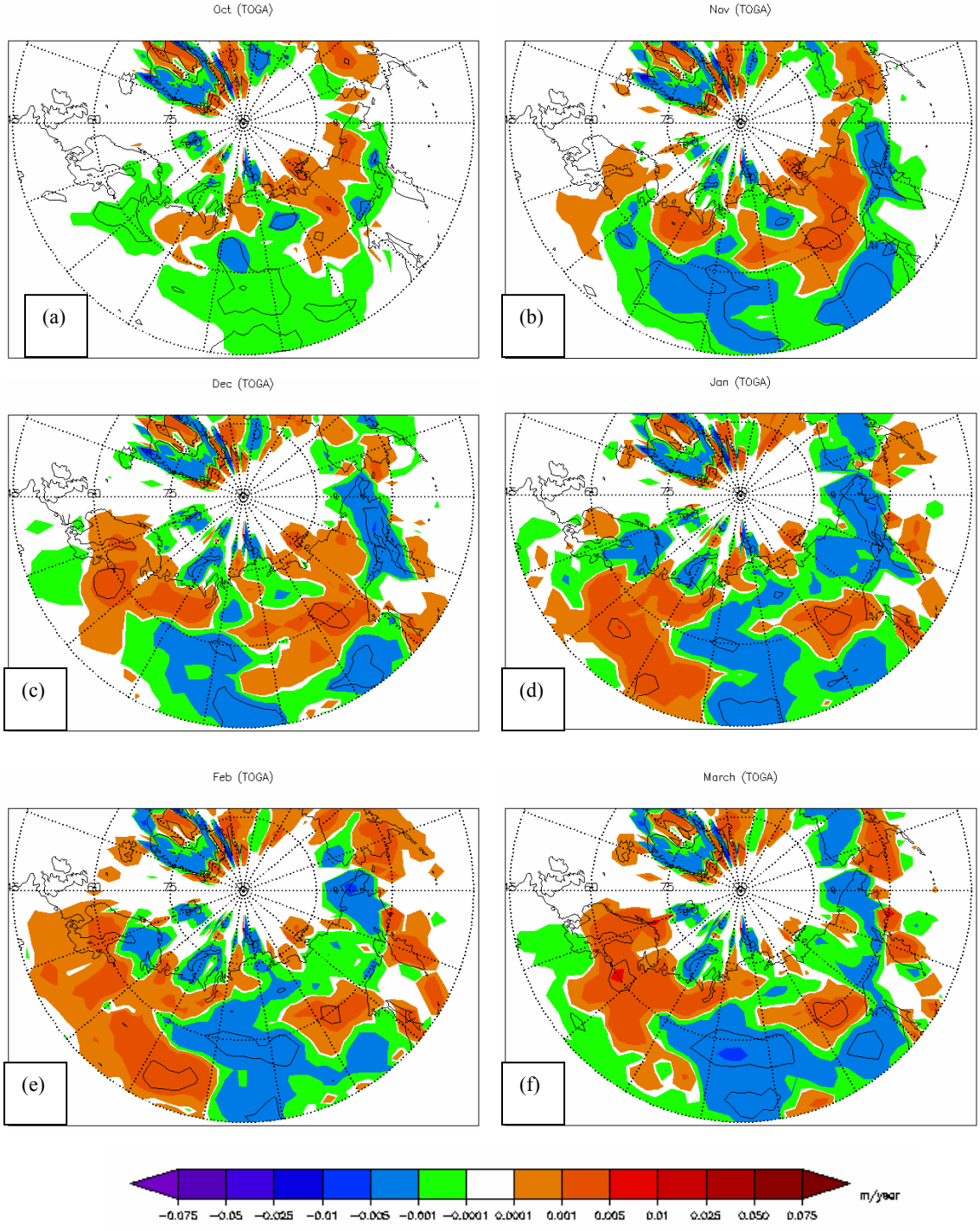

Figure 4 Same as figure 1, except for the experiment TOGA. The time domain for the trend analysis is 1979/1980-2000 (more explanation is in the text)

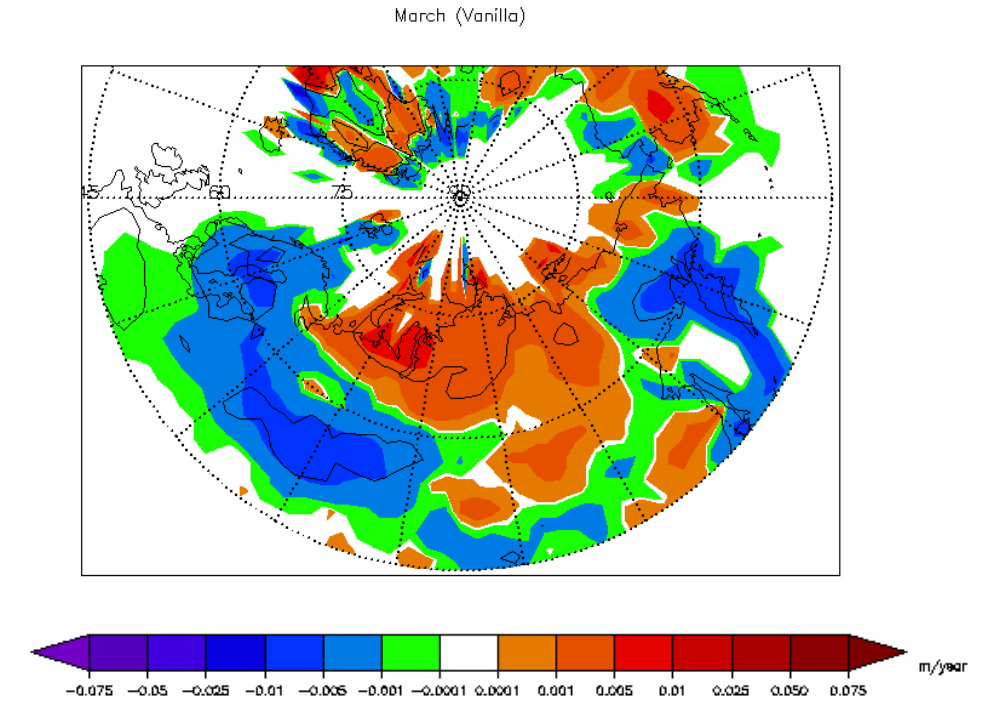

Figure 5 Same as fig 2; but only for the period 1980-2000.

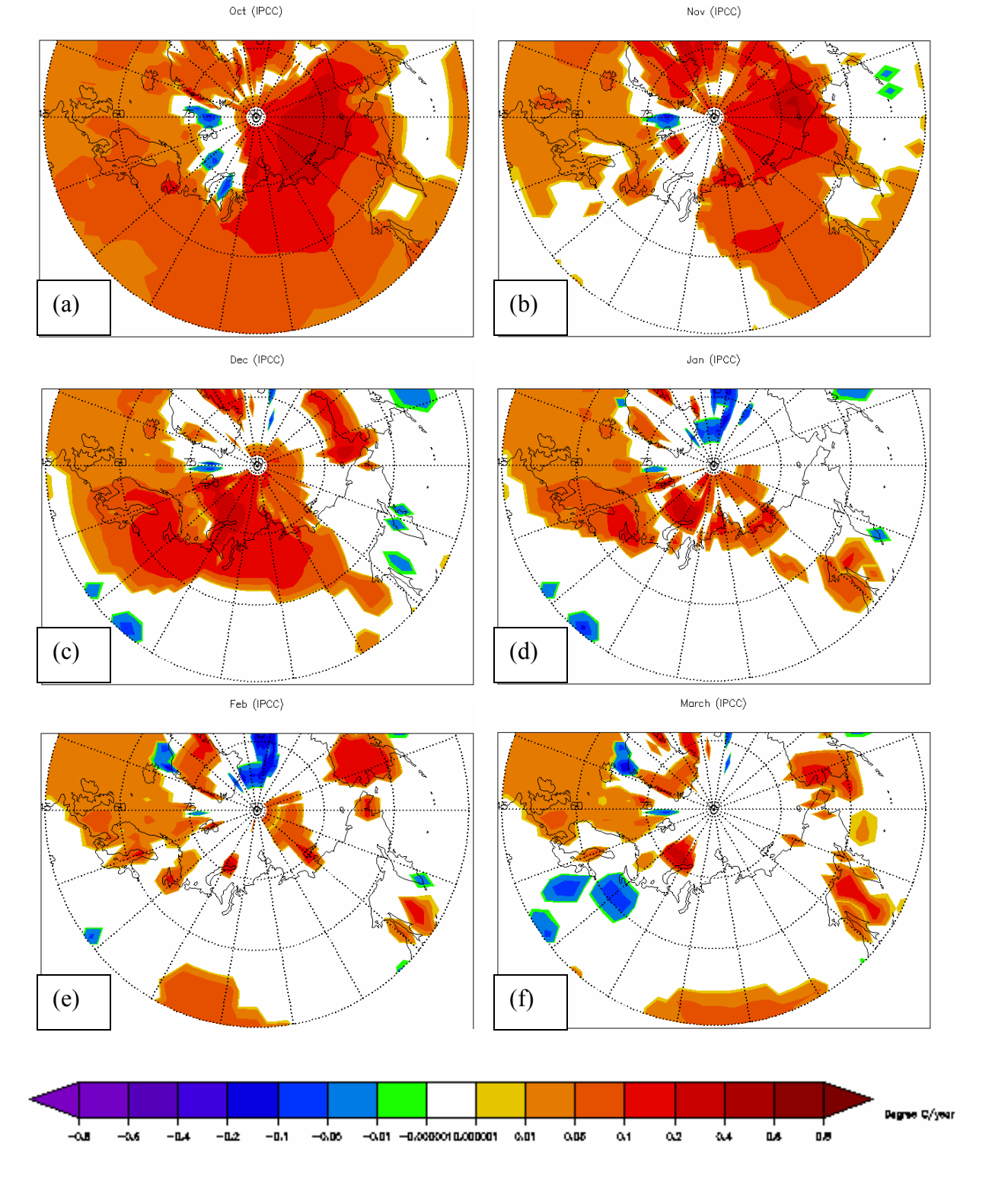

Figure 6 Linear Trend of TS from IPCC experiment for the period of 1979/1978-2007/2008, significant at 90% confidence level has been plotted for the month of (a) October, (b) November, (c) December, (d) January, (e) February and (f) March.

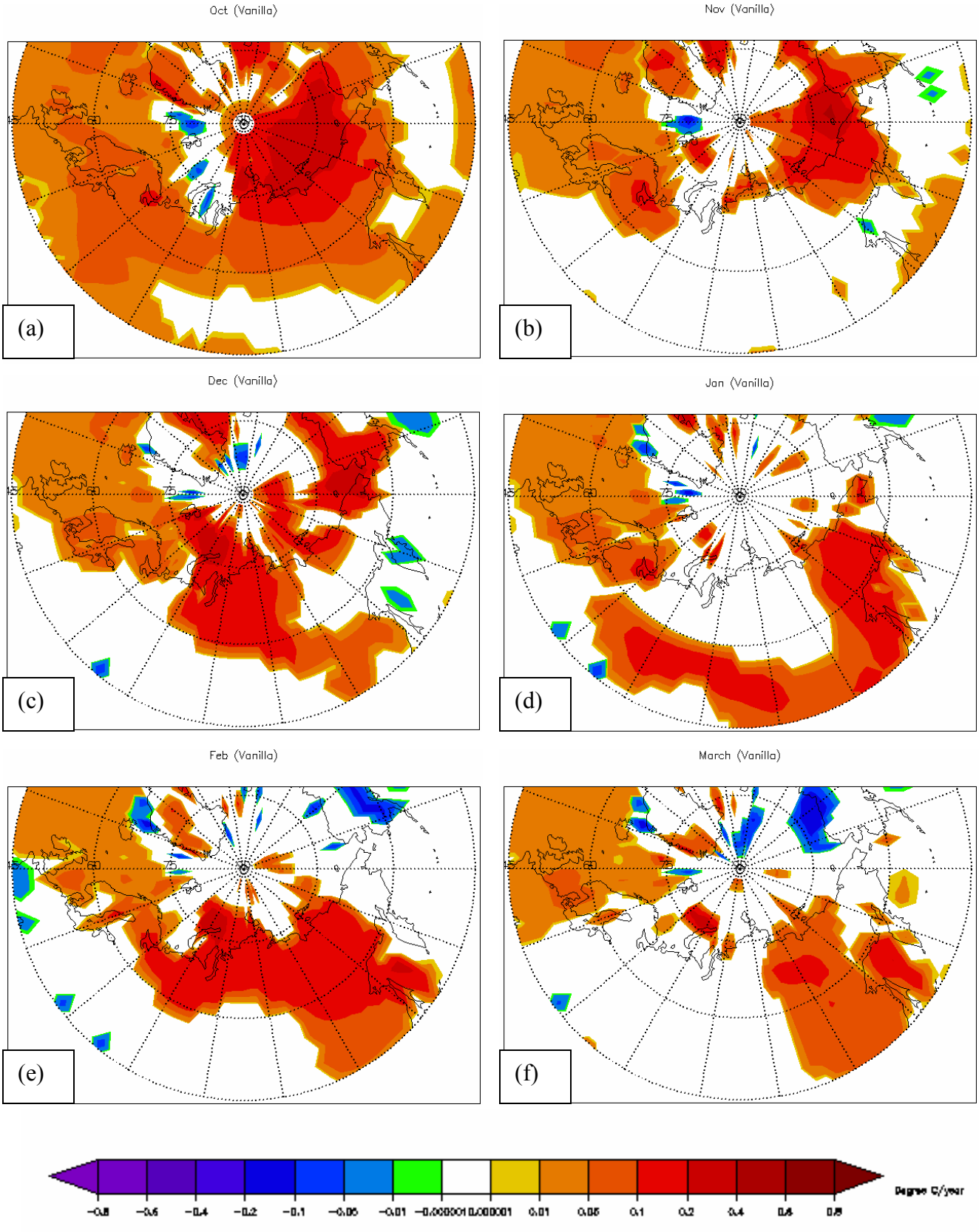

Figure 7 Same as figure 6, except for the experiment Vanilla

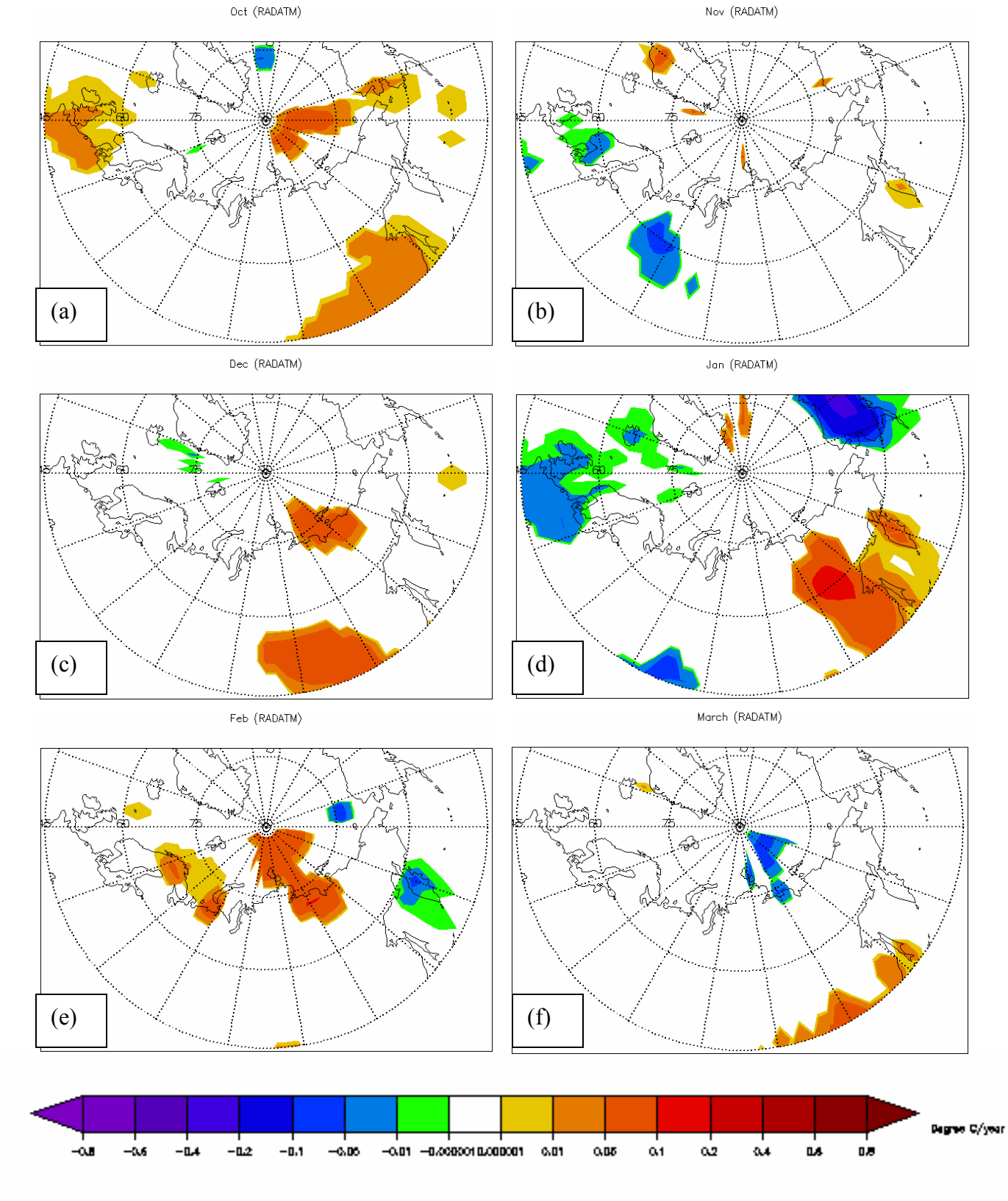

Figure 8 Same as figure 6, except for the experiment RADATM

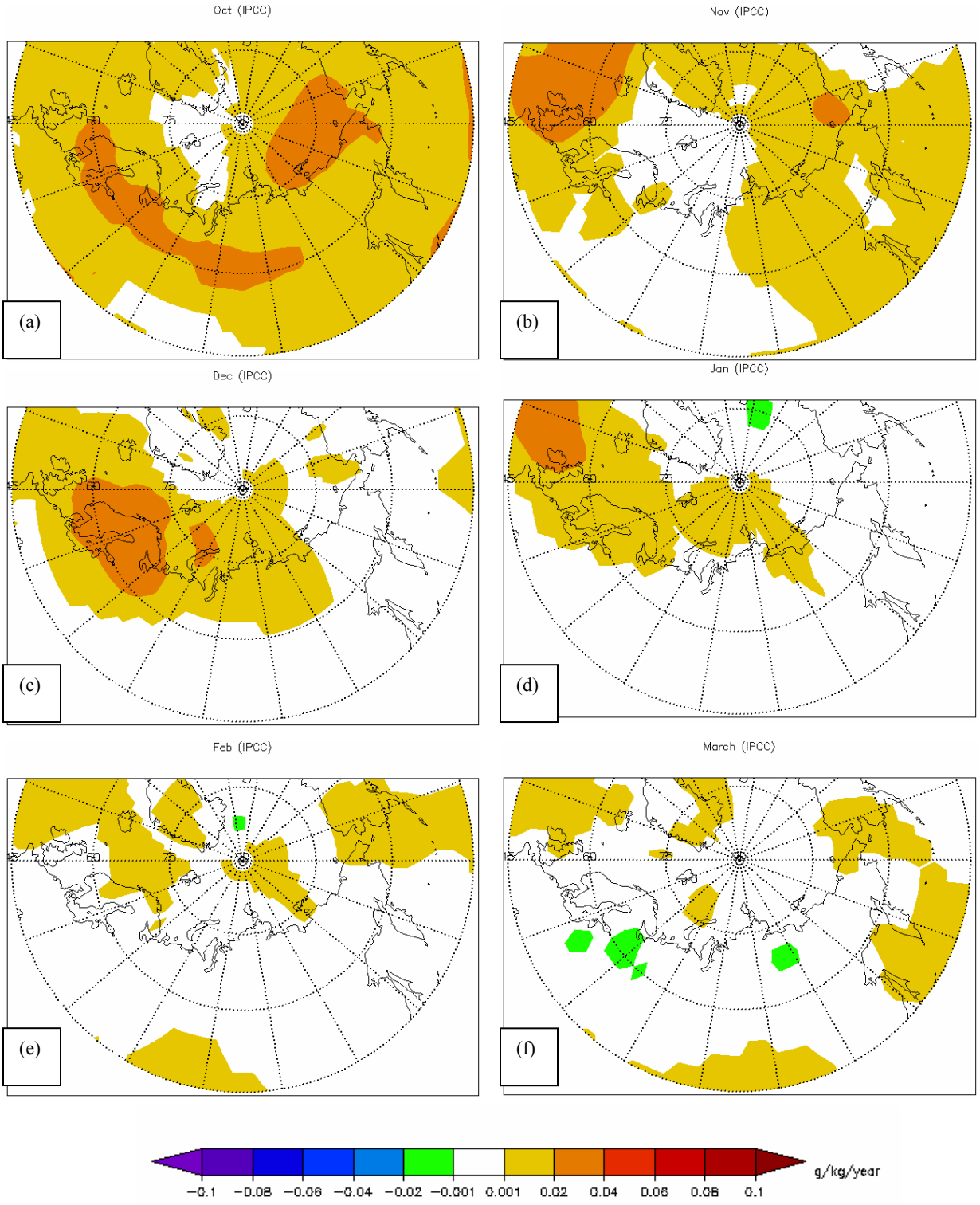

Figure 9 Linear Trend of QBOT from IPCC experiment for the period of 1979/1978-2007/2008, significant at 90% confidence level has been plotted for the month of (a) October, (b) November, (c) December, (d) January, (e) February and (f) March.

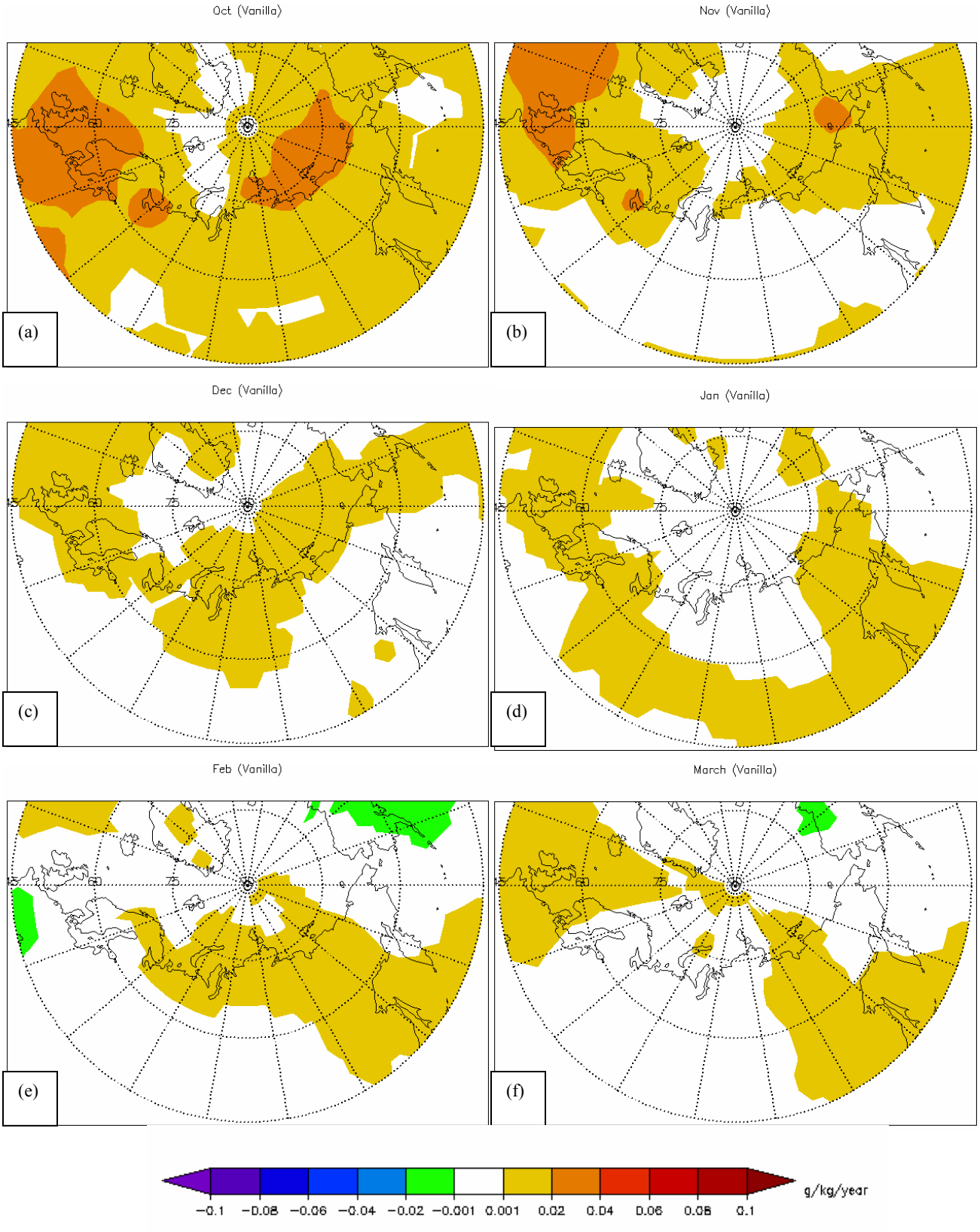

Figure 10 Same as figure 9, except for the experiment Vanilla

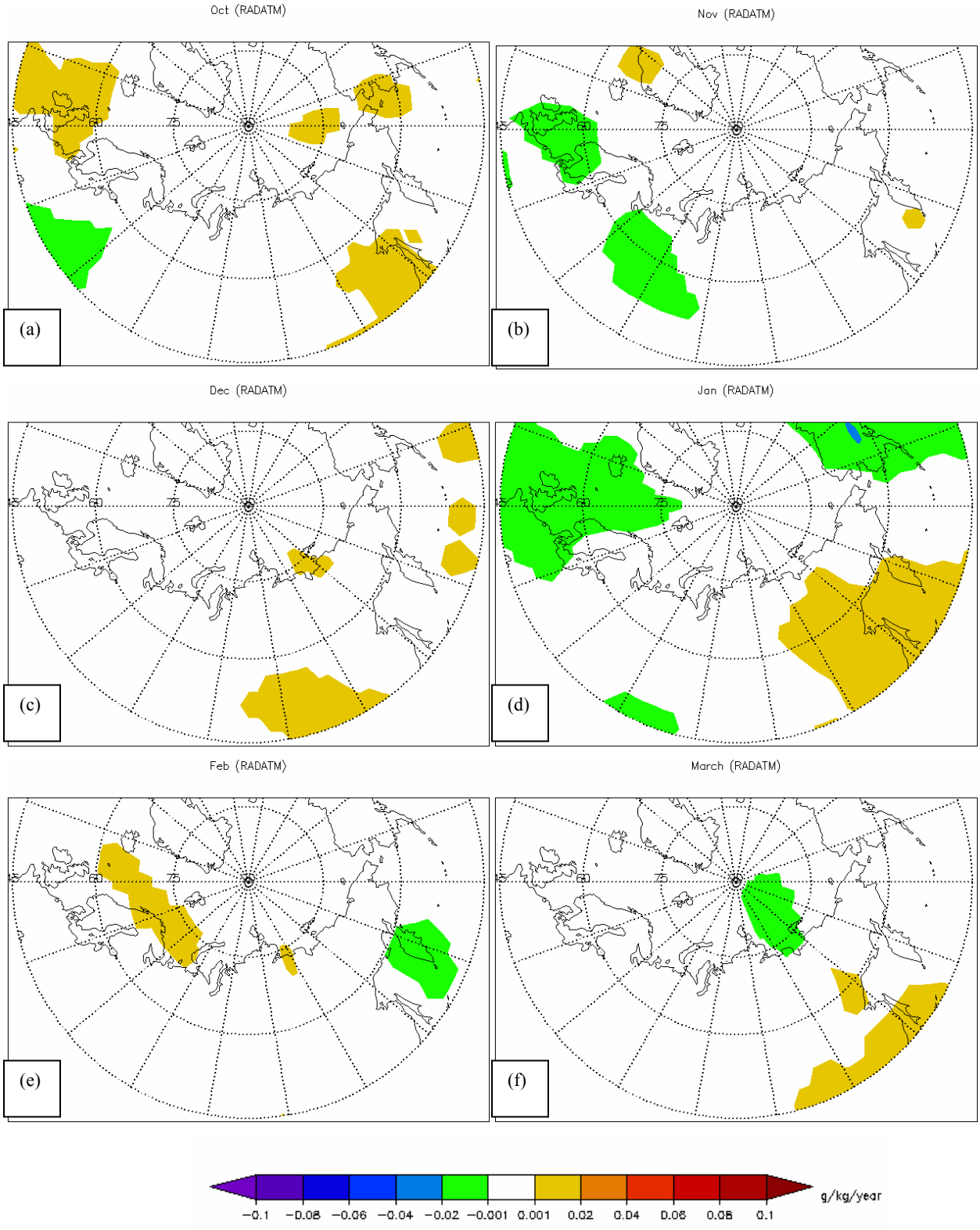

Figure 11 Same as figure 9, except for the experiment RADATM

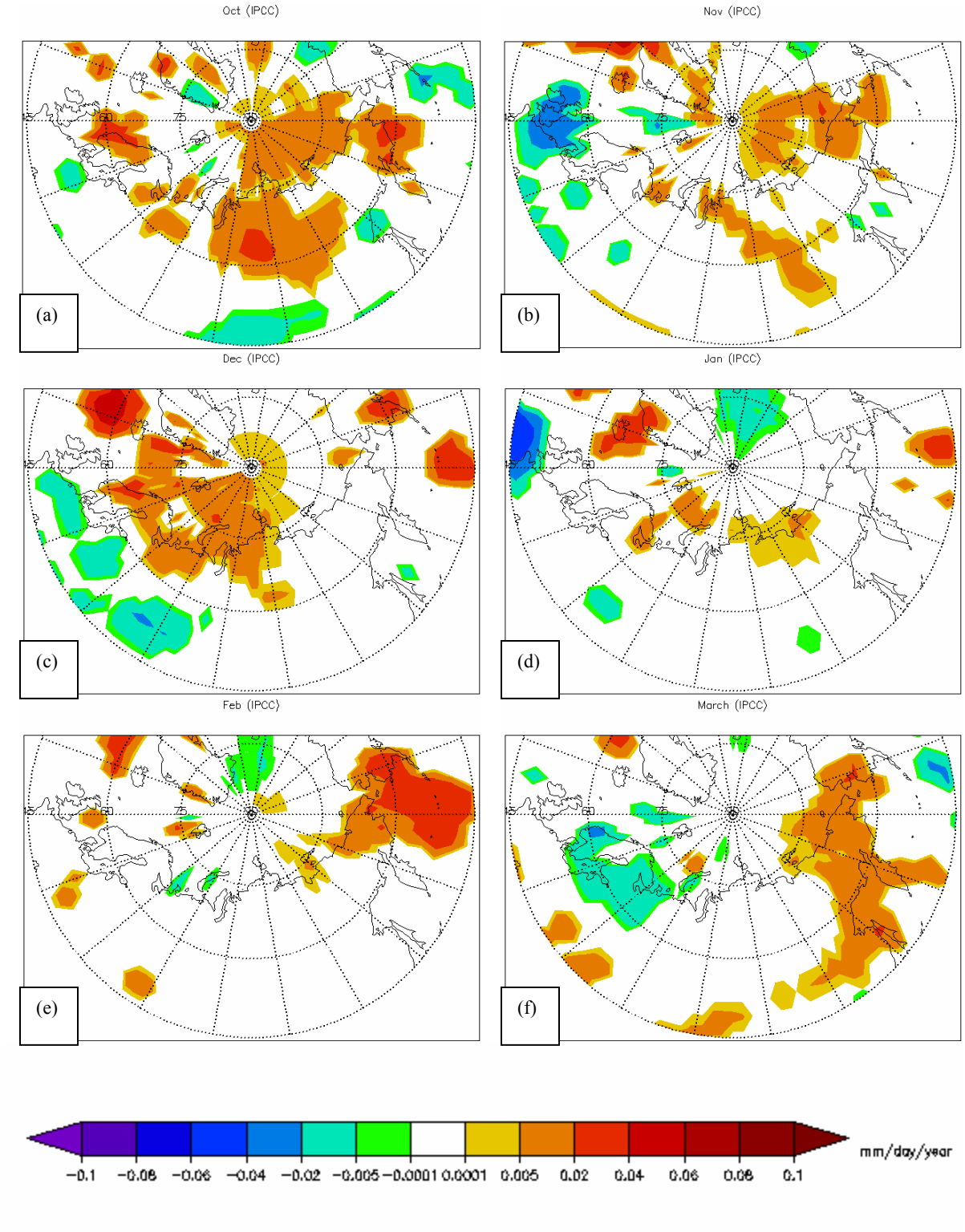

Figure 12 Linear Trend of precipitation from IPCC experiment for the period of 1979/1978-2007/2008, significant at 90% confidence level has been plotted for the month of (a) October, (b) November, (c) December, (d) January, (e) February and (f) March.

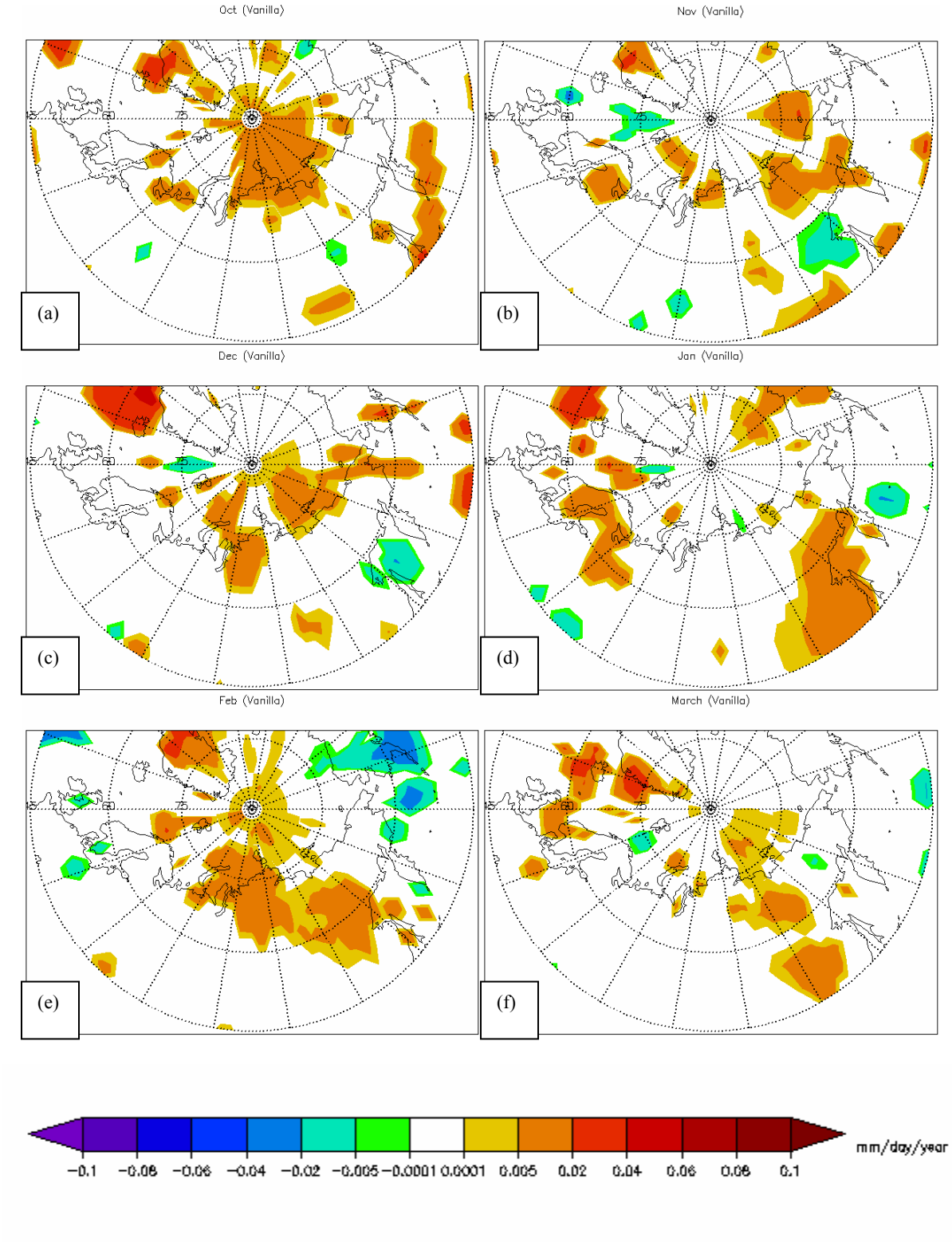

Figure 13 Same as figure 12, except for the experiment Vanilla

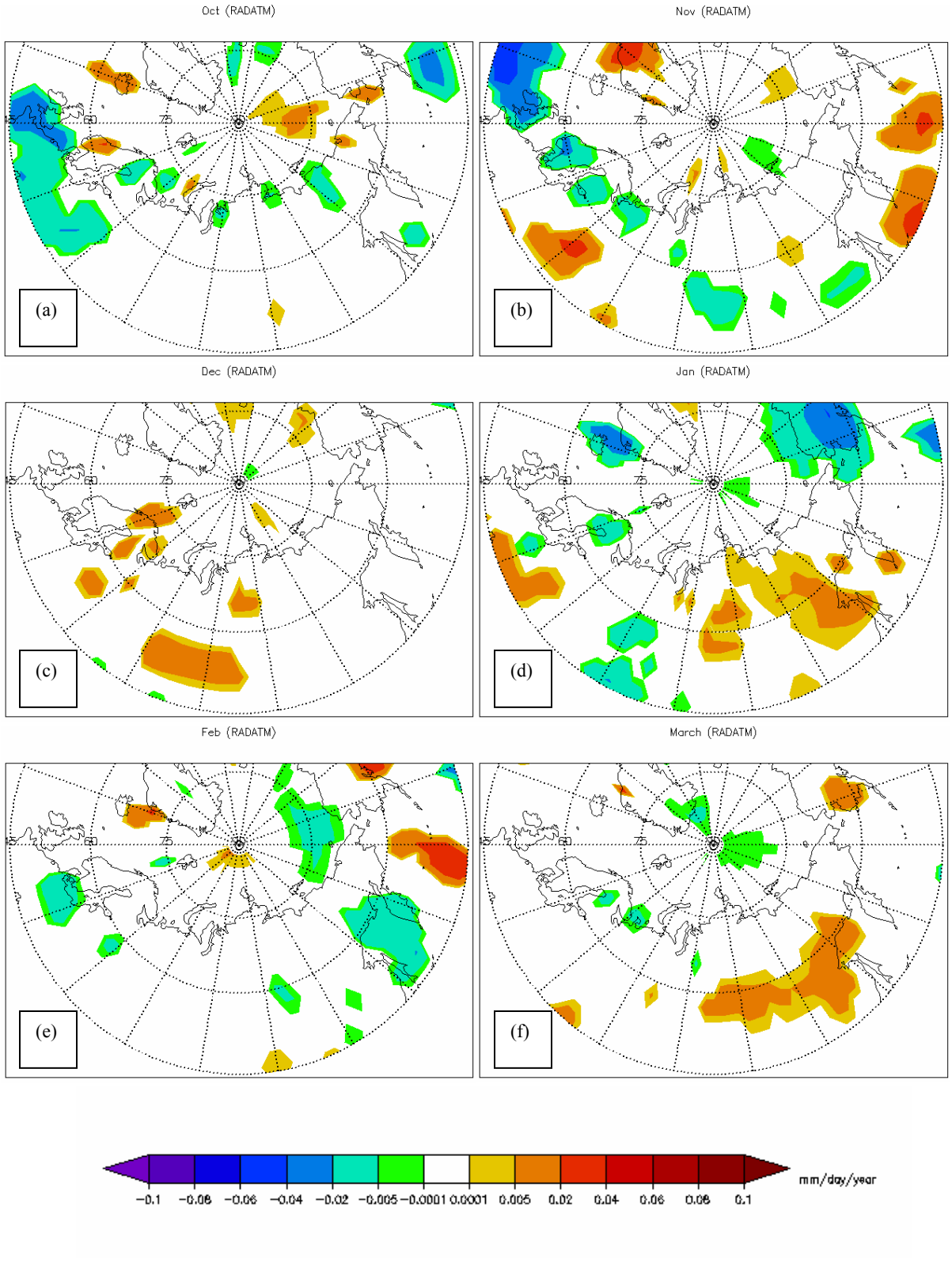

Figure 14 Same as figure 12, except for the experiment RADATM

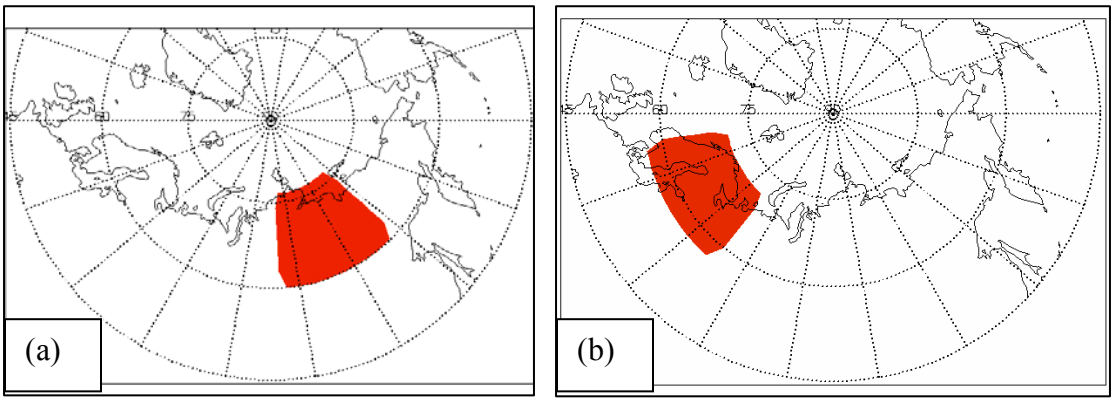

Figure 15 (a) Siberian region bounded by the latitudes 60^0 N - 75^0 N and the longitudes 95^0E - 135^0 E. (b) Scandinavian region bounded by the latitudes 58^0 N- 70^0N and the 10^0E- 50^0 E.

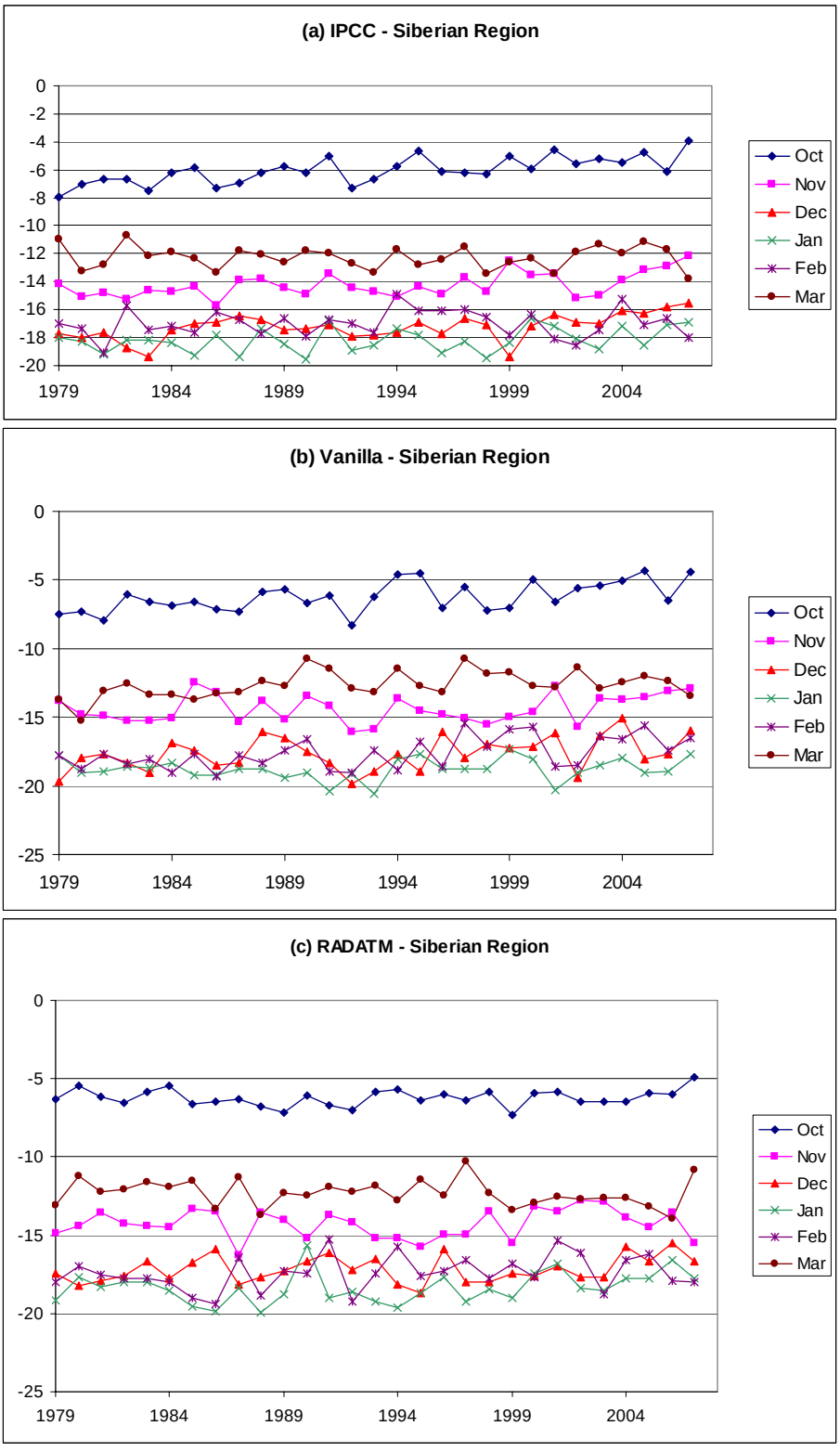

Figure 16 Area-weighted average monthly surface air temperature timeseries over the Siberian region for (a) IPCC, (b) Vanilla and (c) RADATM. X axis shows year and Y axis shows temperature in ^{0}C.

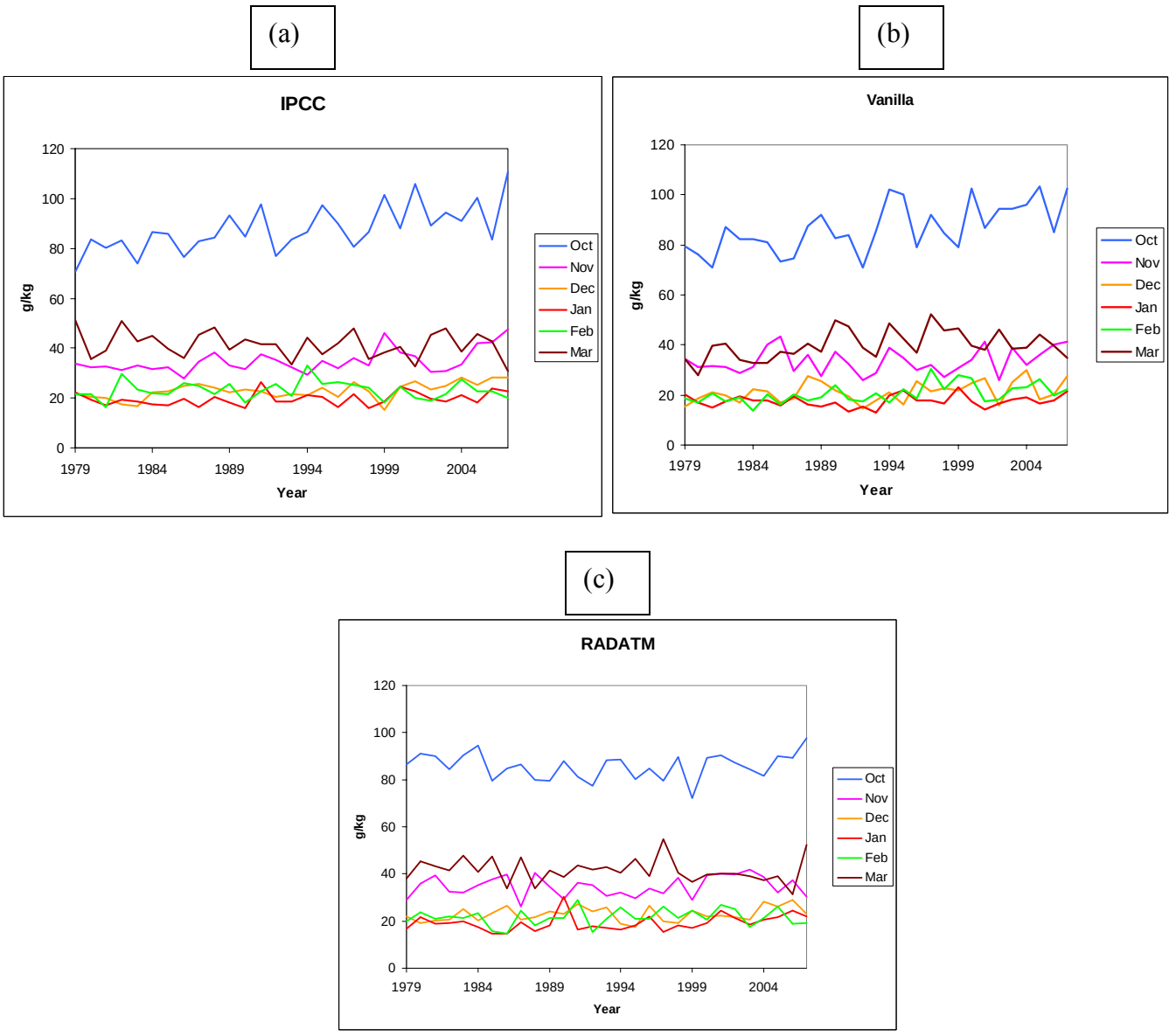

Figure 17 Area-weighted total monthly specific humidity (QBOT) timeseries over the Siberian region for (a) IPCC, (b) Vanilla and (c) RADATM

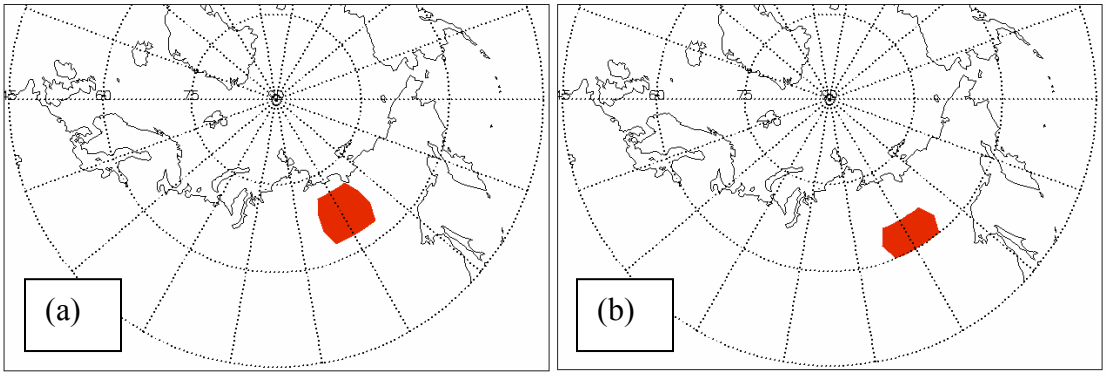

Figure 18 Siberian region is divided into two parts (a) North part (65^0 N- 70^0 N; 110^0E- 135^0E); and (b) South part (60^0 N- 65^0 N; 110^0E- 135^0E)

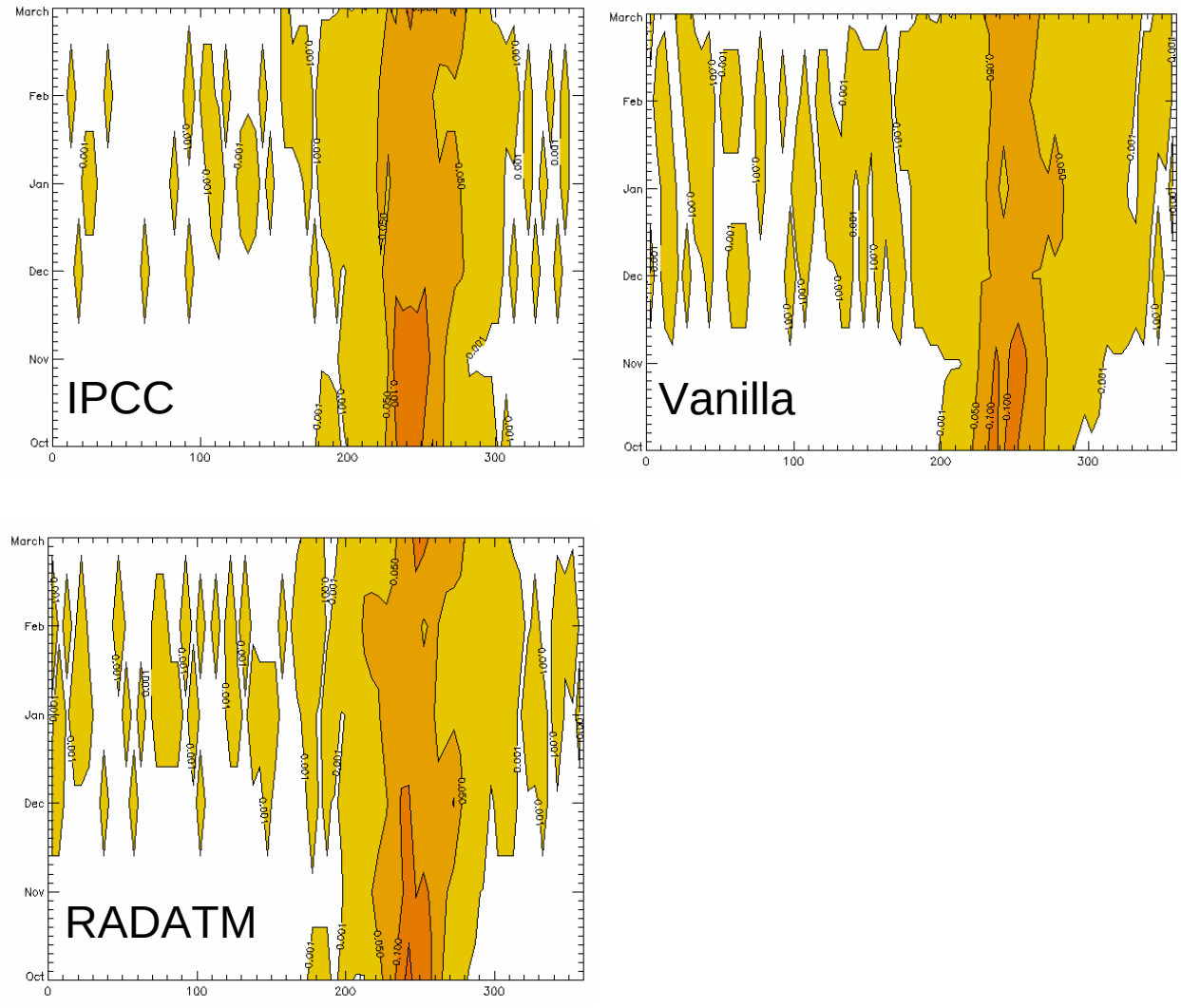

Figure 19 Distribution of monthly wind directions for each month between 1979/1980 and 2007/2008 for the northern sector of the region (65^0 N- 70^0 N; 110^0E- 135^0E). X axis shows the wind direction (degrees from north); Y axis shows months.

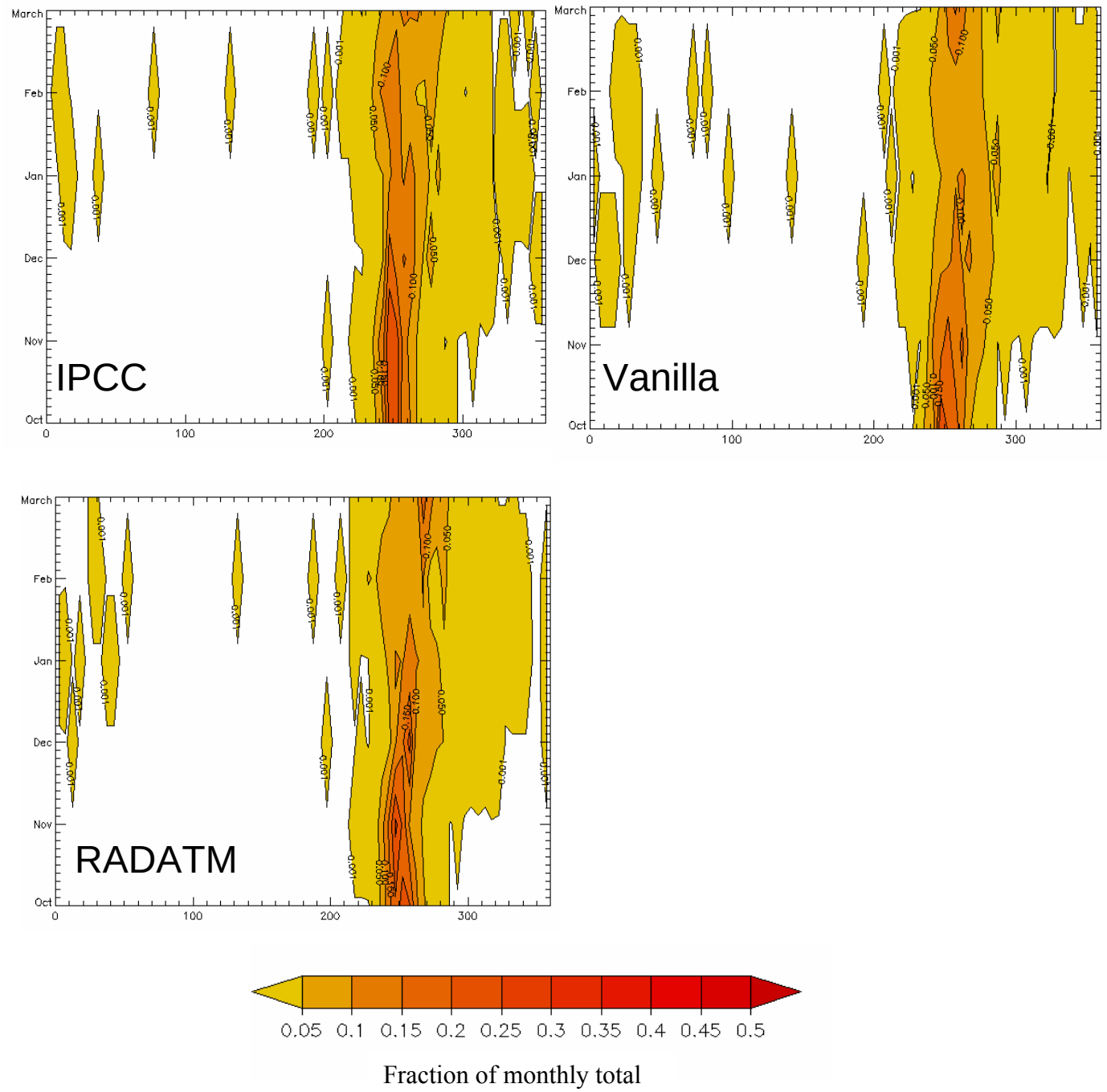

Figure 20 Same as in figure 19, but for the southern sector of the region (60^0 N- 65^0 N; 110^0E- 135^0E).

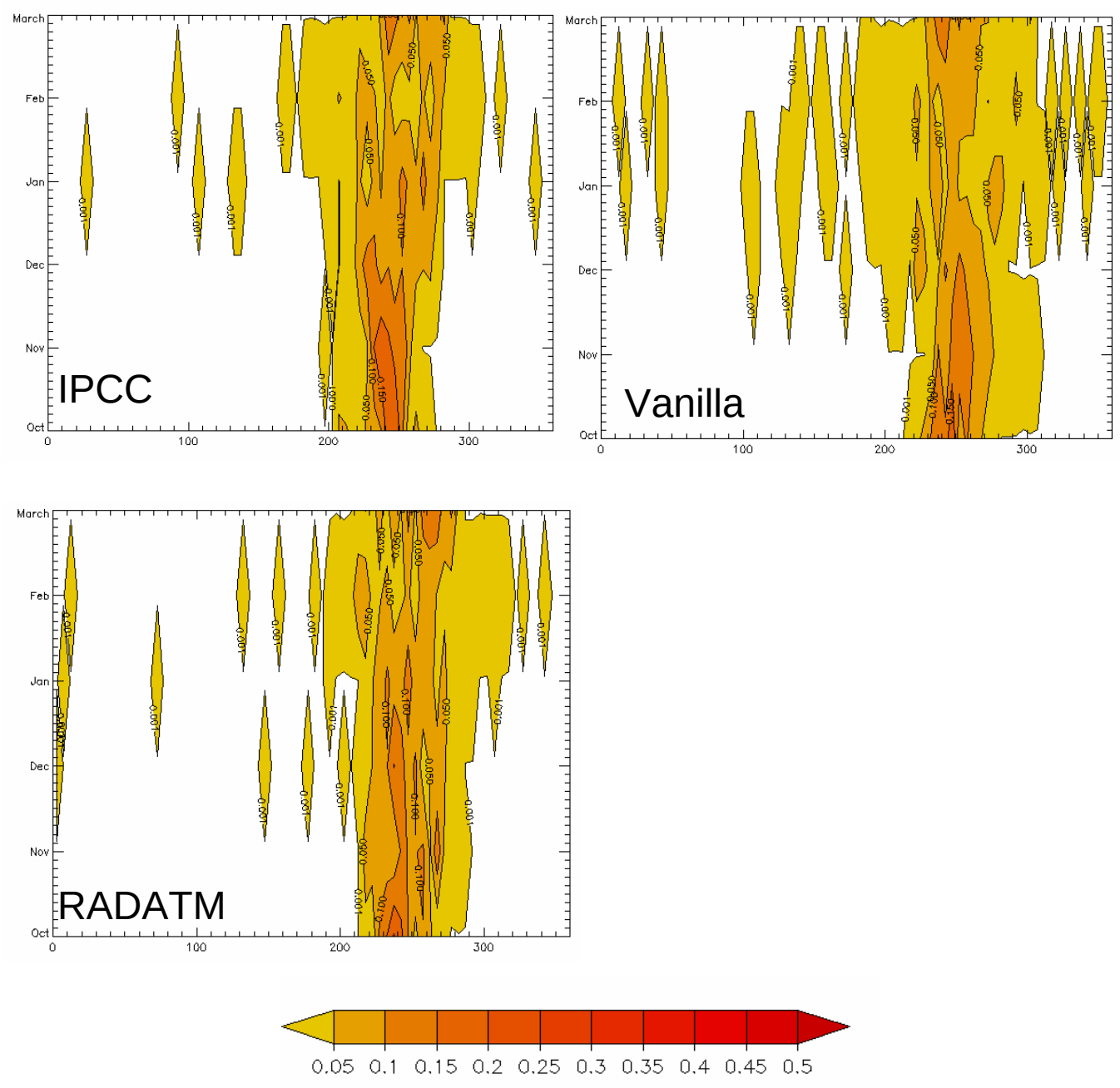

Figure 21 Same as in figure 19, but for the 2000/2001 and 2007/2008 time domain.

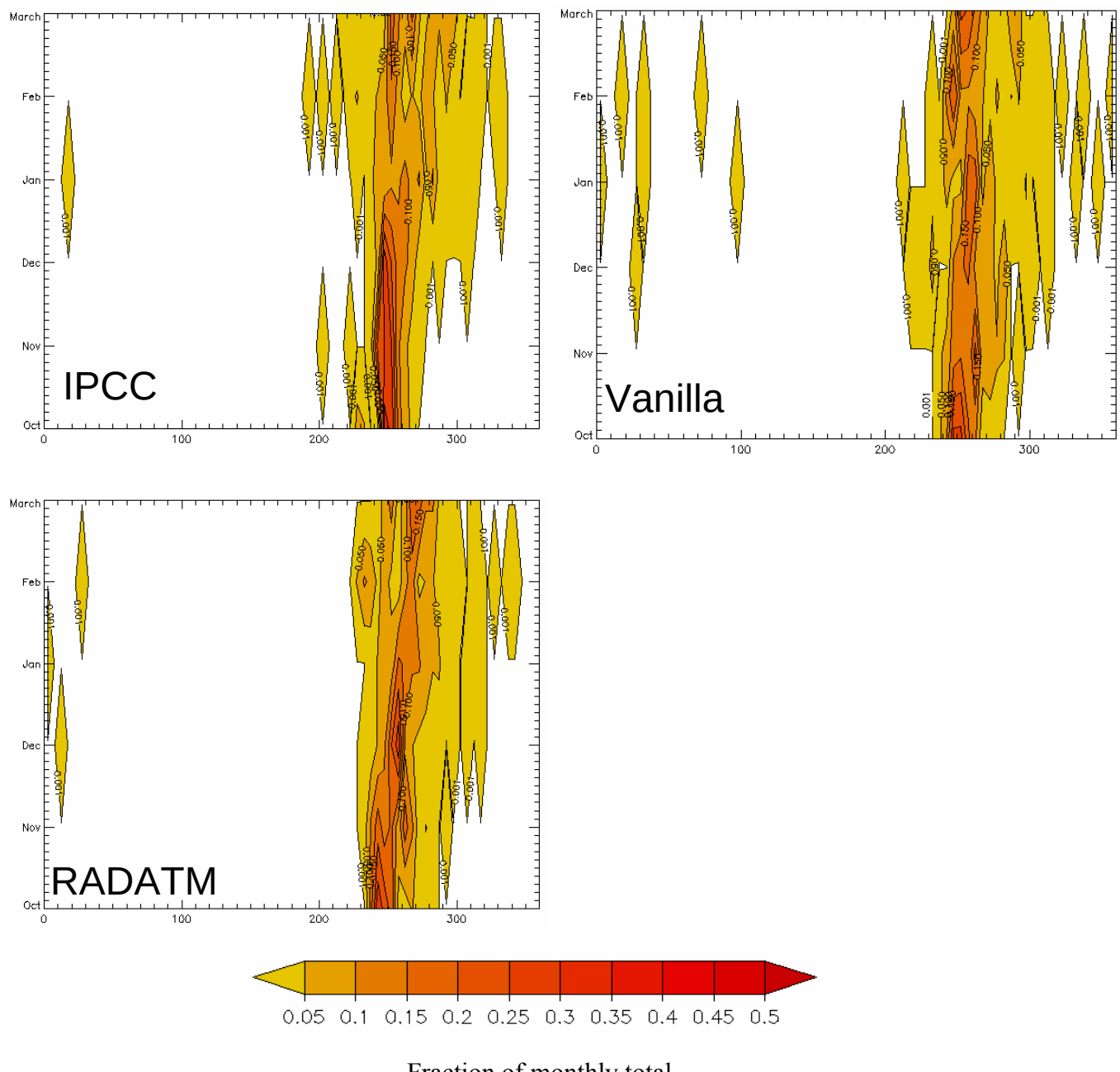

Figure 22 Same as in figure 20, but for 2000/2001 and 2007/2008 time domain.

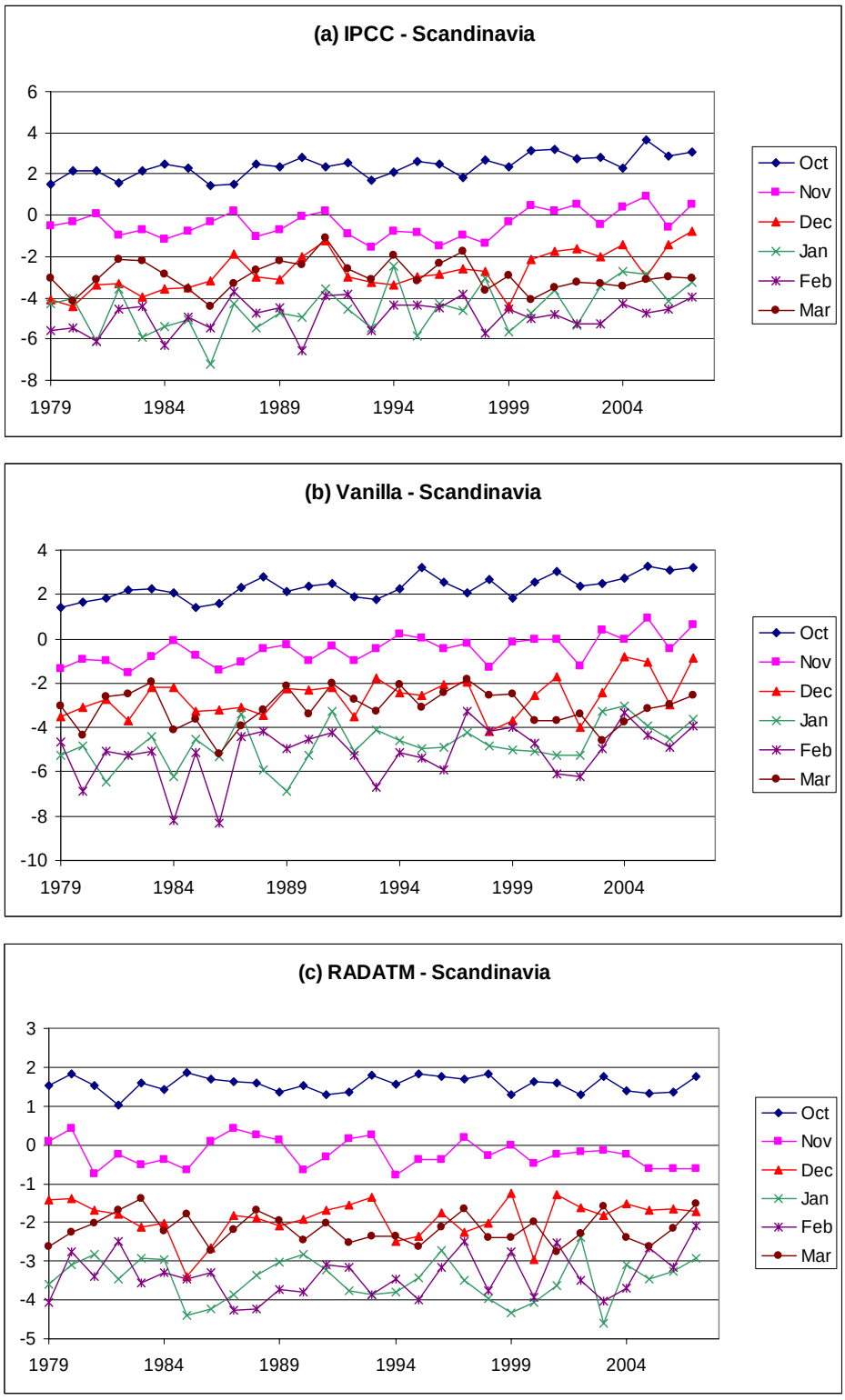

Figure 23 Same as in figure 16, but for the Scandinavian region. (a) IPCC, (b) Vanilla and (c) RADATM. X axis shows year and Y axis shows temperature in ^{0}C.

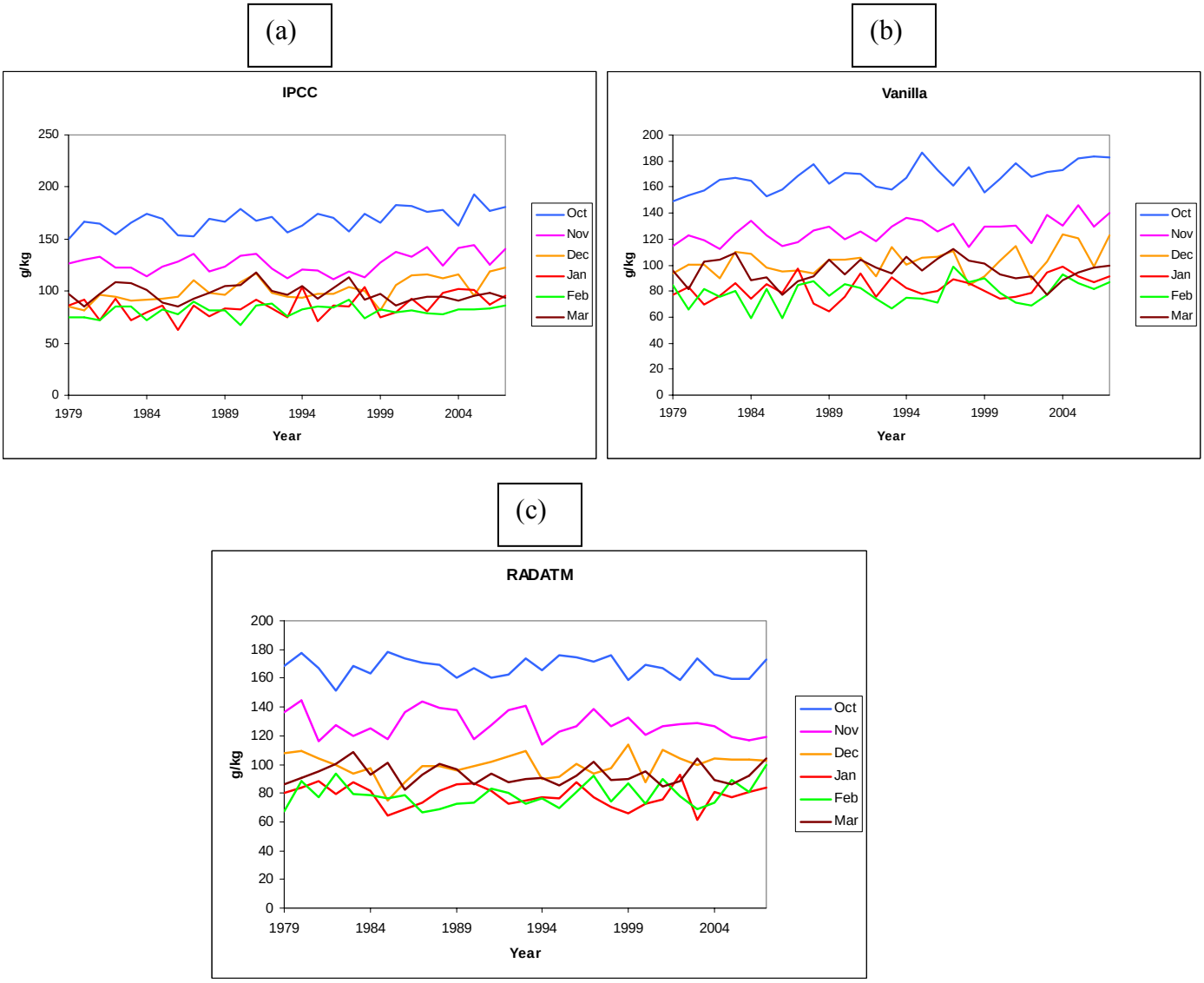

Figure 24 Same as in figure 17, but for the Scandinavian region. (a) IPCC, (b) Vanilla and (c) RADATM

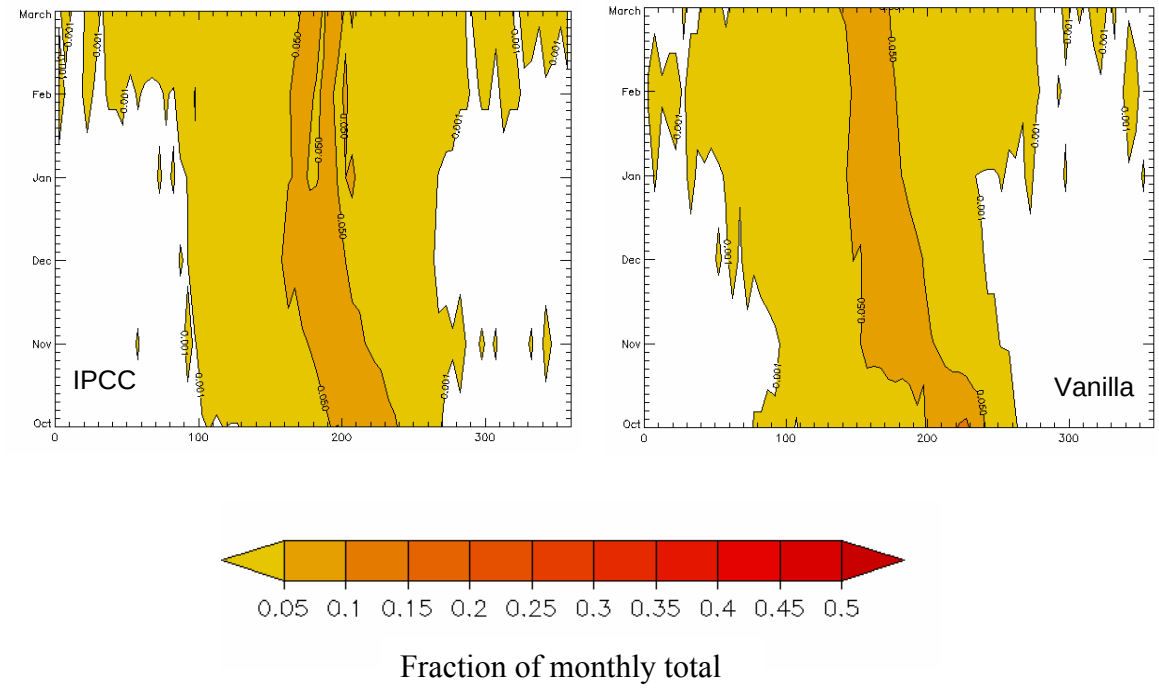

Figure 25 Same as in figure 19, but for the Scandinavian region

Chapter 6

Conclusions and Future Scope

6.1 Summary of Conclusions:

This thesis contributed to the identification of the factors causing the variations in snow at different geographical scales. The first objective of the thesis contributed to the scientific understandings of the causes of continental-scale snow depth variations, which received less attention from the scientists. This dissertation identifies that the NAO and the PNA affect the North American winter snow pack through two distinct physical pathways (temperature and snowfall), which subsequently persists into the spring season. Additionally, singular value decomposition analysis between winter and spring snow pack identifies the signatures of these two major atmospheric circulation patterns, i.e. the NAO and the PNA, in snow depth observations without any *a priori* assumptions of the driving mechanisms of snow depth variations. Temperature pathway is associated with both the NAO and the PNA, whereas the snowfall pathway is linked only to the PNA. Positive winter air temperature anomalies due to the high index phase of the NAO causes the thinning of the snow pack over eastern parts of North America. Negative winter snowfall anomalies associated with the high index phase of the PNA causes the loss of snow depth over the mid-latitudinal areas of North America. On the other hand, a decrease in snow depth over western North America has also been shown as a result of increased temperature due to the positive PNA anomalies. Influence of the PNA and the NAO has been identified as geographically distinct; the PNA influence is visible across

the continent, whereas the NAO influence is more regional over the eastern North America.

In order to fulfill the second objective, SVD analyses have been done on the observational datasets of Northern Hemisphere snow and Arctic sea ice. These results suggest that the increasing snow over Siberia during fall and early winter is correlated with the loss of summer Arctic sea ice. But the observational evidences do not imply any causation between snow and sea ice and the results suggest that the signal should strengthen over time. Similar co-variance analyses based on historic and future simulations of CCSM3 have been employed for the four time domains: 1979-2007, 1979-2020, 1979-2050 and 1979-2080. This set of analyses corroborates the Siberian signal which appears in the observational analyses. But they indicate the emergence of Siberian signal during the last half of the 21st century and most strongly during winter. The original contribution of the second objective lies in the investigation of climate change and/or sea ice related signal on Northern Hemisphere snow.

Co-variance based analyses performed for the second objective doesn't establish causation between two variables. Therefore, a suite of CAM3 experiments have been analyzed in order to establish the causal link between snow and sea ice. The results from four experiments suggest that the high latitude surface forcings due to the SST and sea ice play a major role in producing snow signal over the Eurasian landmasses. Snow depth increases over East Eurasia, specifically north of the Yeneisy and Lena river basin areas, whereas it deceases over the Scandinavian region. Modelling results indicate that the fall temperature increases over both of these regions. But the average temperature remains below-freezing over Siberian region; thus, it facilitates the snowfall and hence the

increase in snow depth. Conversely, the average fall temperature exceeds the freezing level over the Scandinavian region. The associated increase in atmospheric water vapor is also noticed here, which is favored by the advection of ocean air mass into the region. These meteorological conditions may cause the precipitation falling as rain and also increases melting; thus, these reduce the snow pack over the Scandinavian region.

6.2 Future Scope of Research:

This dissertation has made significant scientific contributions; it has generated future scopes of research as well. Few of them are discussed as follows.

Chapter 5 shows how a suite of CAM3 experiments has been useful in identifying the varied snow responses over Eurasian landmasses and the distinct causal mechanisms. This particular study requires more insight into the physical processes which are not addressed here; for e.g. the influence of simulated atmospheric circulation in generating the snow response, simulated moisture transport vectors over the pan-arctic region. Therefore, further analyses are required involving other variables from the CAM3 experiments. Since the focus of the chapter 5 has been only Eurasia, it is important to expand the spatial domain to North America as well. Additionally, new perturbation experiments will be definitely useful in order to better understand the impacts of recent climatic changes.

This thesis has focused on mainly large-scale analyses at continental and/or hemispheric-scale, which fails to capture the detail of many physical processes at more regional scale. As chapters 4 and 5 suggest a snow signal over Siberia, it is crucial to investigate the physical mechanisms at more micro or mesoscale. Therefore, it is prudent

to acquire station observations and examine the meteorological conditions at smaller geographic scale.

Ogi et al. (2003) demonstrated that the memory of winter NAO/AO is retained by the sea ice and snow cover and thus influences the subsequent summer circulation response to the winter AO/NAO. In chapter 1, it is also discussed how significant role played by AO in decreasing the summer sea ice (Rigor et al., 2002; Rigor and Wallace, 2004). Additionally, in chapter 3, we show how winter and spring snow depth responds to the winter NAO and the PNA through different mechanistic pathways. Thus, it is reasonable to hypothesize that the snow depth can play a discernible role in these apparent relationships between the winter NAO/AO and subsequent arctic sea ice/climate. In other words, a memory effect retained by snow may be a component which causes a link between the AO and the sea ice. Thus, this will contribute to establish a linkage between winter-spring snow depth and the following summer sea ice and atmospheric circulation. Chapters 4 and 5 show the changes in the observed and modeled snow in the recent years. Therefore, the feedback generated by snow, as hypothesized here will be complicated and needs further research.

6.3 References

Ogi, M., Y. Tachibana, and K. Yamazaki, 2003: Impact of the wintertime North Atlantic Oscillation (NAO) on the summertime atmospheric circulation. Geophysical Research Letters, 30: 1704, doi:10.1029/2003GL017280.

Rigor, I.G., and J.M. Wallace, 2004: Variations in the age of Arctic sea-ice and summer sea-ice extent. Geophysical Research Letters, 31: L09401, doi:10.1029/2004GL019492.

Rigor, I. G., J. M. Wallace, and R. L. Colony, 2002: Response of sea ice to the Arctic Oscillation. J. Climate, 15, 2648–2663.

Chapter 7

References

Chapter 1:

Alexander, M. A., U. S. Bhatt, J. E. Walsh, M. S. Timlin, J. S. Miller and J. D. Scott, 2004: The atmospheric response to realistic Arctic sea ice anomalies in an AGCM during Winter. J. Climate , 17, 890-905.

Alexander, M. A., R. Tomas, C. Deser, and D. L. Lawrence, 2010: The Atmospheric Response to Projected Terrestrial Snow Changes in the Late 21st Century. J. Climate, accepted.

Anisimov, O. A., and Nelson, F. E., 1996: Permafrost Distribution in the Northern Hemisphere under Scenarios of Climatic Change. Global Planetary Change, 14, 59–72.

Armstrong, R. L., and E. Brun, 2008: Snow and Climate: Physical Processes, Surface Energy Exchange and Modeling. Cambridge University Press, 256 pp.

Baker, D.G., D.L. Ruschy, R.H. Skaggs and D.B. Wall, 1992: Air temperature and radiation depressions associated with snow cover. J. Appl. Meteor., 31, 247–254.

Bamzai, A. S., and J. Shukla, 1999: Relation between Eurasian snow cover, snow depth, and the Indian summer monsoon: an observational study. Journal of Climate, 12(10), 3117-3132.

Bamzai, A. S., and L. Marx, 2000: COLA AGCM simulation of the effect of anomalous spring snow over Eurasia on the Indian summer monsoon. Q.J.R. Meteorol. Soc., 126, 2575-2584.

Barnett, T.P., L. Dumenil, U. Schlese, E. Roeckner, and M. Latif, 1989: The effect of Eurasian snow cover on regional and global climate variations. J. Atmos. Sci., 46, 661–685.

Barry, R. G., R. Armstrong, T. Callaghan, J. Cherry, S. Gearhead, A. Nolin, D. Russell, and C. Zockler, 2007: Snow, in Global Outlook for Ice and Snow. UNEP (Ed.), Nairobi, Kenya, pp. 39-62.

Bell, K.L., and Bliss, L.C., 1979: Autoecology of Kobresia bellardii: why winter snow accumulation limits local distribution. Ecological Monographs, 49, 377-402.

Brooks, P.D., M. W. Williams, and S.K.Schmidt, 1996: Microbial activity under alpine snowpacks, Niwot Ridge, Colorado. Biogeochemistry, 32, 93-113.

Brown, R.D., 2000: Northern hemisphere snow cover variability and change, 1915-1997. J. Climate, 13(13), 2339-2355.

Bürki R., H. Elsasser, B. Abegg, 2003: Climate Change -Impacts on the Tourism Industry in Mountain Areas. 1st International Conference on Climate Change and Tourism, Djerba.

Cerveny, R. S., and R. C. Balling Jr., 1992: The impact of snow cover on diurnal temperature range. Geophys. Res. Lett., 19(8), 797–800, doi:10.1029/92GL00573.

Chapin, F.S. III, M. Sturm, M.C. Serreze, J. P. McFadden, J. R. Key, A. H. Lloyd, A. D. McGuire,T. S. Rupp, A. H. Lynch, J. P. Schimel, J. Beringer, W. L. Chapman, H. E. Epstein, E. S. Euskirchen, L. D. Hinzman,G. Jia, C.-L. Ping, K. D. Tape, C. D. C. Thompson, D. A. Walker, J. M. Welker, 2005: Role of Land-Surface Changes in Arctic Summer Warming. Science, 310, 657, DOI: 10.1126/science.1117368.

Clark, M. P., and M. C. Serreze, 2000: Effects of Variations in East Asian Snow Cover on Modulating Atmospheric Circulation over the North Pacific Ocean. Journal of Climate, 13, 3700-3710.

Clark, M.P., Serreze, M.C., and Robinson, D.A., 1999: Atmospheric control on Eurasian snow extent. Int. J. Climatol. 19, 27–40.

Cohen, J., and D. Rind, 1991: The effect of snow cover on climate. J. Climate, 4,689–706.

Cohen, J., and D. Entekhabi, 2001: The influence of snow cover on Northern Hemisphere climate variability. Atmos.-Ocean, 39, 35-53.

Comiso, J., 2003: Warming trends in the Arctic from clear-sky satellite observations. Journal of Climate, 16, 3498-3510.

Comiso, J.C., 2006: Abrupt decline in the Arctic winter sea ice cover. Geophys. Res. Letts., 33(L18504), 5 pp.

Comiso, J. C., C. L. Parkinson, R. Gersten, and L. Stock, 2008: Accelerated decline in the Arctic sea ice cover. Geophys. Res. Lett., 35, L01703, doi:10.1029/2007GL031972.

Derksen, C., K. Misurak, E. LeDrew, J. Piwowar, and B. Goodison, 1997: Relationship between snow cover and atmospheric circulation, central North America, winter 1988. Ann. Glaciol., 25, 347– 352.

Derksen, C., R. Brown, and A. E. Walker, 2004: Merging conventional (1915-92) and passive microwave (1978-2002) estimates of snow extent and water equivalent over central North America. Journal of Hydrometeorology, 5, 850-861.

Derksen, C., A. E. Walker, B. E. Goodison, and J. W. Strapp, 2005: Integrating in situ and multiscale passive microwave data for estimation of subrid scale snow water equivalent distribution and variability. IEEE Transactions on Geoscience and Remote Sensing, 43(5), 960-972.

Derksen, C., M. Sturm, G. E. Liston, J. Holmgren, H. Huntington, A. Silis, and D. Solie, 2009: Northwest Territories and Nunavut snow characteristics from a subarctic traverse: implications for Passive Microwave remote sensing. Journal of Hydrometeorology, 10, 448-463, doi: 10.1175/2008JHM1074.1.

Deser, C., J.E. Walsh, and M.S. Timlin, 2000: Arctic sea ice variability in the context of recent atmospheric circulation trends. J. Climate, 13, 617-633.

Deser, C., G. Magnusdottir, R. Saravanan, and A. Phillips, 2004: The effects of North Atlantic SST and sea ice anomalies on the winter circulation in CCM3. Part II: Direct and indirect components of the response. J. Clim., 17, 877– 889.

Deser, C., R. A. Thomas, and S. Peng, 2007: The transient atmospheric circulation response to North Atlantic SST and sea ice anomalies. J. Clim., 20, 4751– 4767.

Deser, C., R. Tomas, M. Alexander, and D. Lawrence, 2010: The Seasonal Atmospheric Response to Projected Arctic Sea Ice Loss in the Late Twenty-First Century. J. Climate, 23, 333–351.

Dewey, Kenneth F., 1977: Daily Maximum and Minimum Temperature Forecasts and the Influence of Snow Cover. Mon. Wea. Rev., 105, 1594–1597.

Dey, B. and O. S. R. U. Kumar, 1983: Himalayan winter snow cover area and summer monsoon rainfall over India. Journal of Geophysical Research, 88(C9): 5471-5474.

Dyer, J. L., and T. L. Mote, 2006: Spatial variability and trends in snow depth over North America. Geophysical Research Letters, 33(L16503): doi:10.1029/2006GL027258.

Ellis, A.W., and D.J. Leathers, 1999: Analysis of cold airmass temperature modification across the U.S. Great Plains as a consequence of snow depth and albedo. J. Appl. Meteor., 38(6), 696.

Fiona, Lo, and Martyn P. Clark, 2002: Relationships between Spring Snow Mass and Summer Precipitation in the Southwestern United States Associated with the North American Monsoon System. J. Climate, 15, 1378–1385.

Foster, J., M. Owe, A. Rango, 1983: Snow Cover and Temperature Relationships in North America and Eurasia. J. Climate Appl. Meteor., 22, 460–469.

Francis J.A., E. Hunter, 2006: New Insight Into the Disappearing Arctic Sea Ice. EOS Trans. Am. Geophys. Union, 87, 509.

Francis, J.A., W. Chan, D.J. Leathers, J.R. Miller, and D.E. Veron, 2009: Winter northern hemisphere weather patterns remember summer Arctic sea ice extent. Geophys.Res. Lett., 36, L07503, doi:10.1029/2009GL037274.

Frei, A. and G. Gong, 2005: Decadal to century scale trends in North American snow extent in coupled Atmosphere-Ocean General Circulation Models. Geophysical Research Letters, 32: L18502, doi:10.1029/2005GL023394.

Frei, A., D.A. Robinson, and M.G. Hughes, 1999: North American Snow Extent: 1900-1994. Int. J. Climatol., 19, 1517–1534.

Ge, Y., and G. Gong, 2008: Observed Inconsistencies between Snow Extent and Snow Depth Variability at Regional/Continental Scales. J. Climate, 21, 1066–1082.

Ge, Y., and G. Gong, 2009: North American Snow Depth and Climate Teleconnection Patterns. J. Climate, 22, 217–233.

Ge, Y., G. Gong, and A. Frei, 2009: Physical Mechanisms Linking the Winter Pacific–North American Teleconnection Pattern to Spring North American Snow Depth. J. Climate, 22, 5135–5148.

Gerdes, R., 2006: Atmospheric response to changes in Arctic sea ice thickness. Geophys.Res. Lett., 33(18), L18709.

Gong, G., D. Entekhabi, and J. Cohen, 2003: Modeled Northern Hemisphere winter climate response to realistic Siberian snow anomalies. J. Clim., 16, 3917– 3931.

Gong, G., D. Entekhabi, and J. Cohen, 2004: Orographic Constraints on a Modeled Siberian Snow – Arctic Oscillation Teleconnection Pathway. Journal of Climate, 17: 1176-1189.

Groisman, P. Y., T. R. Karl and R. W. Knight, 1994: Observed Impact of Snow Cover on the Heat Balance and the Rise of Continental Spring Temperatures. Science, 263: 199-200.

Gutzler, David S., Richard D. Rosen, 1992: Interannual Variability of Wintertime Snow Cover across the Northern Hemisphere. J. Climate, 5, 1441–1447.

Gutzler, David S., and P. Preston, 1997: Evidence for a relationship between spring snow cover in North America and summer rainfall in New Mexico. Geophys. Res. Lett., 24, 2207–2210.

Gutzler, David S., 2000: Covariability of Spring Snowpack and Summer Rainfall across theSouthwest United States. J. Climate, 13, 4018–4027.

Hahn, D. G. and J. Shukla, 1976: An apparent relationship between eurasian snow cover and indian monsoon rainfall. Journal of the Atmospheric Sciences, 33: 2461-2462.

Hassol, S. J., 2004: Impacts of a Warming Arctic: Arctic Climate Impact Assessment. 139 pp., Cambridge Univ. Press, Cambridge, U.K.

Hawkins, T. W., A. W. Ellis, J. A. Skindlov and D. Reigle, 2002: Intra-annual Analysis of the North American snow cover - monsoon teleconnection: seasonal forecasting utility. Journal of Climate, 15, 1743-1753. DOI: 10.1175/1520-0442(2002)015<1743:IAAOTN>2.0.CO;2.

Holland, M.M., C.M. Bitz, 2003: Polar amplification of climate change in coupled models. Clim Dyn., 21, 221-232, doi:10.1007/s00382-003-0332-6.

Holland, M. M., C. M. Bitz, and B. Tremblay, 2006: Future abrupt reductions in the summer Arctic sea ice. Geophys. Res. Lett., 33, L23503, doi:10.1029/2006GL028024.

Hurrell,J.W., 1995: Decadal trends in the North Atlantic Oscillation: Regional temperatures and precipitation. Science,269,676-679.

IPCC, Third Assessment Report ,Climate change, 2001.Cambridge University Press.

Jones, H. G. and J. Pomeroy, W., 1999: The ecology of snow and snow-covered systems: summary and relevance to Wolf Creek, Yukon Wolf Creek Research Basin: hydrology, ecology, environment, Proc. Workshop (Whitehorse, Yukon, Mar. 1998) ed J W Pomeroy and R J Granger, pp 1–14.

Kierkus, W. T. and W. G. Colborne, 1989: Diffuse solar radiation - daily and monthly values as affected by snow cover. Solar Energy, 42(2), 143-147.

Kripalani, R. H., S. V. Singh, A. D. Vernekar and V. Thapliyal, 1996: Empirical study on nimbus-7 snow mass and indian summer monsoon rainfall. International Journal of Climatology, 16: 23-34.

Kukla, G. & D.A. Robinson, 1981: Accuracy of operational snow and ice charts. 1981 IEEE International Geoscience and Remote Sensing Symposium Digest, 974-987.

Kumar, A. and F. Yang, 2003: Comparative influence of snow and SST variability on extratropical climate in northern winter. J. Climate, 16(13), 2248-2261.

Kvamstø, N. G., P. Skeie, and D. B. Stephenson, 2004: Impact of Labrador sea-ice extent on the North Atlantic Oscillation. Int. J. Climatol., 24, 603–612.

Leathers, D.J., and D.A. Robinson, 1993: The association between extremes in North American snow cover extent and United States temperature. J. Climate, 6, 1345–1355.

Lindsay R.W., J. Zhang, 2005: The Thinning of Arctic Sea Ice, 1988–2003: Have We Passed a Tipping Point? J. Clim., 18, 4879-4894.

Magnusdottir, G., C. Deser, and R. Saravanan, 2004: The effects of North Atlantic SST and sea-ice anomalies on the winter circulation in CCM3. Part I: Main features and storm-track characteristics of the response. J. Climate, 17, 857-876.

Marshall, S., R.J. Oglesby, and A.W. Nolin, 2003: The predictability of winter snow cover over the western United States. J. Climate, 16, 1062– 1073.

Matsui, T., V. Lakshmi, E. E. Small., 2005: The Effects of Satellite-Derived Vegetation Cover Variability on Simulated Land–Atmosphere Interactions in the NAMS. Journal of Climate, 18:1, 21-40.

McCabe, G. J., and D.R. Legates, 1995: Relationships between 700 hPa height anomalies and 1 April snowpack accumulations in the western USA. International Journal of Climatology, 15: 517–530. doi: 10.1002/joc.3370150504.

McClelland, J. W., R. M. Holmes, B. J. Peterson, and M. Stieglitz, 2004: Increasing river discharge in the Eurasian Arctic: Consideration of dams, permafrost thaw, and fires as potential agents of change. J. Geophys. Res., 109, D18102, doi:10.1029/2004JD004583.

McClelland, J. W., S. J. De´ry, B. J. Peterson, R. M. Holmes, and E. F. Wood, 2006: A pan-arctic evaluation of changes in river discharge during the latter half of the 20th century. Geophys. Res. Lett., 33, L06715, doi:10.1029/2006GL025753.

Meier, W., J. Stroeve, F. Fetterer, K. Knowles, 2005: Reductions in Arctic sea ice cover no longer limited to summer. Eos, Transactions of the American Geophysical Union 86(36): 326, doi:10.1029/2005EO360003.

Mote, Thomas L., 2008: On the Role of Snow Cover in Depressing Air Temperature. J. Appl. Meteor. Climatol., 47, 2008–2022. doi: 10.1175/2007JAMC1823.1.

Namias, J., 1985: Some empirical evidence for the influence of snow cover on temperature and precipitation. Monthly weather review, 113: 1542-1552.

Nelson Frederick E., O. A. Anisimov, N. I. Shiklomanov, 2001: Subsidence risk from thawing permafrost. Nature, 410, 889-890, doi:10.1038/35073746.

Parkinson, C. L., D. J. Cavalieri, P. Gloersen, H. J. Zwally, and J. C. Comiso, 1999: Arctic sea ice extents, areas, and trends, 1978-1996. Journal of Geophysical Research – Oceans, 104(C9): 20,837.

Payette, S., A. Delwaide, M. Caccianiga, and M. Beauchemin, 2004: Accelerated thawing of subarctic peatland permafrost over the last 50 years. Geophys. Res. Lett., 31, L18208, doi:10.1029/2004GL020358.

Peterson Bruce J., R. M. Holmes, J. W. McClelland, C. J. Vörösmarty, R. B. Lammers, A. I. Shiklomanov, I. A. Shiklomanov, and S. Rahmstorf, 2002: Increasing River Discharge to the Arctic Ocean. Science, 298 (5601), 2171, DOI: 10.1126/science.1077445.

Polyakov I.V., et al., 2005: One more step toward a warmer Arctic. Geophys. Res. Lett., 32, L17605.

Raisanen, J., 2008: Warmer climates: less or more snow? Climate Dynamics, 30, 307-319, doi: 10.1007/s00382-007-0289-y.

Rawlins M A, Serreze M C, Schroeder R, Zhang X, and McDonald K C, 2009: Diagnosis of the record discharge of Arctic-draining Eurasian Rivers in 2007. Environ. Res. Lett., 4 045011.

Rayner, N. A., D. E. Parker, E. B. Horton, C. K. Folland, L. V. Alexander, D. P. Rowell, E. C. Kent, and A. Kaplan, 2003: Global analysis of sea surface temperature, sea ice, and night marine air temperature since the late nineteenth century. Journal of Geophysical Research, 108(D14): 4407, doi 4410.1029/2002JD002670.

Rigor, I.G., and J.M. Wallace, 2004: Variations in the age of Arctic sea-ice and summer sea-ice extent. Geophysical Research Letters, 31: L09401, doi:10.1029/2004GL019492.

Rigor, I.G., R.L. Colony, and S. Martin, 2000: Variations in Surface Air Temperature in the Arctic from 1979-1997. J. Climate, 13, 5, 896 - 914.

Rigor, I. G., J. M. Wallace, and R. L. Colony, 2002: Response of sea ice to the Arctic Oscillation. J. Climate, 15, 2648–2663.

Robinson, D. A., 1993: Hemispheric snow cover from satellites. Annals of Glaciology, 17: 367-371.

Robinson, D.A., 1999: Northern Hemisphere snow extent during the satellite era. Preprints: Fifth Conference on Polar Meteorology and Oceanography, Dallas, TX. American Meteorological Society, 255-258.

Robinson, D.A., and A. Frei, 2000: Seasonal variability of northern hemisphere snow extent using visible satellite data. Professional Geographer , 51, 307-314.

Robok A., and M. Mu, 2003: Land surface conditions over Eurasia and Indian summer monsoon rainfall. J. Geophys. Res., 108(D4), 4131.

Rothrock D. A , J. Zhang, 2005: Arctic Ocean sea ice volume: What explains its recent depletion? J. Geophys. Res., 110, C01002.

Rothrock, D.A., Y. Yu, G.A. Maykut, 1999: Thinning of the arctic sea-ice cover, Geophys. Res. Lett., 26(23), 3469-72.

Rothrock, D. A., J. Zhang, and Y. Yu, 2003: The arctic ice thickness anomaly of the 1990s: A consistent view from observations and models. J. Geophys. Res., 108(C3), 3083, doi:10.1029/2001JC001208.

Sankar-Rao, M., K. M. Lau, and S. Yang, 1996: On the relationship between eurasian snow cover and the asian summer monsoon. International Journal of Climatology, 16: 605-616.

Saunders, M. A., Q. Qian, and B. Lloyd-Hughes, 2003: Summer snow extent heralding of the winter North Atlantic Oscillation. Geophysical Research Letters, 30: 1378, doi:1310.1029/2002GL016832.

Seierstad, I. A., and J. Bader, 2008: Impact of a projected future Arctic sea ice reduction on extratropical storminess and the NAO. Clim. Dyn., doi10.1007/s00382-008-0463-x, in press.

Serreze M., and Barry R.G., 2005: The Arctic Climate System. Cambridge University press.

Serreze, M. C., J. E. Walsh, F. S. Chapin III, T. Osterkamp, M. Dyurgerov, V. Romanovsky, W. C. Oechel, J. Morison, T. Zhang and R. G. Barry, 2000: Observational Evidence of Recent Change in the Northern High-Latitude Environment. Climatic Change, 46: 159-207.

Serreze M.C., M. M. Holland, J. Stroeve, 2007: Perspectives on the Arctic's Shrinking Sea-Ice Cover. Science, 315: 1533-1536, DOI:10.1126/science.1139426.

Serreze, M. C., A. P. Barrett, J. C. Stroeve, D. N. Kindig, and M. M. Holland, 2009: The emergence of surface-based Arctic amplification. The Cryosphere, 3, 11–19.

Sewall, J. O., 2005: Precipitation shifts over western North America as a result of declining Arctic sea ice cover: The coupled system response. Earth Interact., 9, 1–23.

Singarayer, J.S., J.L. Bamber, and P.J. Valdes, 2006: Twenty-first-Century climate impacts from a declining Arctic sea ice cover. J. Climate, 19, 1109-1125.

Steele M., T. J. Boyd, 1998: Retreat of the cold halocline layer in the Arctic Ocean. J. Geophys. Res., 103, 10419.

Stroeve, J. C., M. C. Serreze, F. Fetterer, T. Arbetter, W. Meier, J. Maslanik, and K. Knowles, 2005: Tracking the Arctic's shrinking ice cover: Another extreme September minimum in 2004. Geophysical Research Letters, 32, doi:10.1029/2004GL021810.

Stroeve J., M. M. Holland, W. Meier, T. Scambos, M. Serreze, 2007: Arctic sea ice decline: Faster than forecast. Geophys. Res. Lett., 34, L09501, doi:10.1029/2007GL029703.

Tedesco, M., and J. Miller, 2007: Northern Hemisphere snow-covered area mapping: optical versus active and passive microwave data. IEEE Geoscience and Remote Sensing Letters, 4(2): 221-225.

Thompson, D. W. J., and J. M. Wallace, 1998: The Arctic Oscillation signature in the wintertime geopotential height and temperature fields. Geophys. Res. Lett., 25, 1297– 1300.

Wagner, J.A., 1973: The influence of average snow depth on monthly mean temperature anomaly. Mon. Wea. Rev., 101(8), 624-626.

Walsh, J. E., D. R. Tucek, M. R. Peterson, 1982: Seasonal Snow Cover and Short-Term Climatic Fluctuations over the United States. Mon. Wea. Rev., 110, 1474–1486.

Walsh, John E., W. H. Jasperson, B. Ross, 1985: Influences of Snow Cover and Soil Moisture on Monthly Air Temperature. Mon. Wea. Rev., 113, 756–768.

Wang, M., and J. E. Overland, 2009: A sea ice free summer Arctic within 30 years? Geophys. Res. Lett., 36, L07502, doi:10.1029/2009GL037820.

Williamson, S., M. Ruth, K. Ross and D. Irani, 2008: Economic impacts of climate change on New Jersey. The Center for Integrative Environmental Research (CIER) at the University of Maryland,19pp .

Wu, P., R. Wood, and P. Stott, 2005: Human influence on increasing Arctic river discharges. Geophys. Res. Lett., 32, L02703, doi:10.1029/2004GL021570.

Yang, D., Y. Zhao, R. Armstrong, D. Robinson, and M.-J. Brodzik, 2007: Streamflow response to seasonal snow cover mass changes over large Siberian watersheds. J. Geophys. Res., 112, F02S22, doi:10.1029/2006JF000518.

Yasunari, T., A. Kitoh, and T. Tokioka, 1991: Local and remote responses to excessive snow mass of Eurasia appearing in the northern spring and summer climate: A study with the MRI GCM. J. Meteor. Soc. Jpn., 69, 473– 487.

Zhang, T., et al., 2005: Spatial and temporal variability in active layer thickness over the Russian Arctic drainage basin. J. Geophys. Res., 110, D16101, doi:10.1029/2004JD005642.

Zhang, X., and J. E. Walsh, 2006: Towards a seasonally ice-covered ArcticOcean: Scenarios from the IPCC AR4 simulations. J. Clim., 19, 1730–1747.

Zhu, C., Dennis P. Lettenmaier, Tereza Cavazos, 2005: Role of Antecedent Land Surface Conditions on North American Monsoon Rainfall Variability. Journal of Climate, 18:16, 3104-3121.

Chapter 2:

Barry, R. G., R. Armstrong, T. Callaghan, J. Cherry, S. Gearhead, A. Nolin, D. Russell, and C. Zockler, 2007: Snow, in Global Outlook for Ice and Snow. pp. 39-62, UNEP (Ed.), Nairobi, Kenya.

Déry, S. J., J. Sheffield, and E. F. Wood, 2005: Connectivity between Eurasian snow cover extent and Canadian snow water equivalent and river discharge. J. Geophys. Res., 110, D23, D23106, doi: 10.1029/2005JD006173.

Deser, C., R. Tomas, M. Alexander, and D. Lawrence, 2010: The Seasonal Atmospheric Response to Projected Arctic Sea Ice Loss in the Late Twenty-First Century. J. Climate, 23, 333–351.

Frei, A., and G. Gong, 2005: Decadal to century scale trends in North American snow extent in coupled Atmosphere-Ocean General Circulation Models. Geophysical Research Letters, 32: L18502, doi:10.1029/2005GL023394.

IPCC, Third Assessment Report, Climate change, 2001.Cambridge University Press.

Raisanen, J., 2008: Warmer climates: less or more snow? Climate Dynamics, 30, 307-319, doi: 10.1007/s00382-007-0289-y.

Chapter 3:

Armstrong, R. L., and E. Brun, 2008: Snow and Climate: Physical Processes, Surface Energy Exchange and Modeling. Cambridge University Press, 256 pp.

Baker, D., R. Skaggs, and D. Ruschy, 1991: Snow Depth Required to Mask the Underlying Surface. J. Appl. Meteor., 30, 387–392.

Barnston, A.G., and R.E. Livezey, 1987: Classification, Seasonality and Persistence of Low-Frequency Atmospheric Circulation Patterns. Mon. Wea. Rev., 115, 1083–1126.

Blalock, H., 1961: Causal inferences in nonexperimental research. Chapel Hill, NC, UNC Press, 193pp.

Bretherton, C.S., C. Smith, and J.M. Wallace, 1992: An intercomparison of methods for finding coupled patterns in climate data. J. Climate, 5, 541–560.

Cayan, D.R., 1996: Interannual climate variability and snowpack in the western United States. J.Climate, 9, 928-948.

Cherry, S., 1997: Some Comments on Singular Value Decomposition Analysis. J. Climate, 10, 1759–1761.

Cohen, J., 1994: Snow cover and climate. Weather, 49, 150-156.

Coleman, J.S.M., and J.C. Rogers, 2003: Ohio River Valley Winter Moisture Conditions Associated with the Pacific–North American Teleconnection Pattern. J. Climate, 16,969–981.

Dyer, J. L., and T. L. Mote, 2006: Spatial variability and trends in snow depth over North America. Geophysical Research Letters, 33(L16503): doi:10.1029/2006GL027258.

Ellis, A.W., and D.J. Leathers, 1999: Analysis of Cold Airmass Temperature Modification across the U.S. Great Plains as a Consequence of Snow Depth and Albedo. J. Appl. Meteor., 38, 696–711.

Feldstein, S.B., 2000: The Timescale, Power Spectra, and Climate Noise Properties of Teleconnection Patterns. J. Climate, 13, 4430–4440.

Ge, Y., and G. Gong, 2008: Observed Inconsistencies between Snow Extent and Snow Depth Variability at Regional/Continental Scales. J. Climate, 21, 1066–1082.

Ge, Y., and G. Gong, 2009: North American Snow Depth and Climate Teleconnection Patterns. J. Climate, 22, 217–233.

Ge, Y., G. Gong, and A. Frei, 2009: Physical Mechanisms Linking the Winter Pacific–North American Teleconnection Pattern to Spring North American Snow Depth. J. Climate, 22, 5135–5148.

Grundstein, A., 2003: A synoptic-scale climate analysis of anomalous snow water equivalent over the northern Great Plains of the USA. Int. J. Climatol., 23, 871–886.

Hartley S., and M.J. Keables, 1998: Synoptic associations of winter climate and snowfall variability in New England. Int. J. Climatol., 18, 281–298.

Hurrell, J.W., 1995: Decadal trends in the North Atlantic Oscillation: Regional temperatures and precipitation. Science, 269, 676-679.

Hurrell, J. W., 1996: Influence of Variations in Extratropical Wintertime Teleconnections on Northern Hemisphere Temperature. Geophys. Res. Lett., 23(6), 665-668.

Jin, J., N. L. Miller, S. Sorooshian, and X. Gao, 2006: Relationship between atmospheric circulation and snowpack in the western USA. Hydrol. Process., 20, 753-767.

Kalnay, E., M. Kanamitsu, R. Kistler, W. Collins, D. Deaven, L. Gandin, M. Iredell, S. Saha, G. White, J. Woollen, Y. Zhu, A. Leetmaa, R. Reynolds, M. Chelliah, W. Ebisuzaki, W. Higgins, J. Janowiak, K. Mo, C. Ropelewski, J. Wang, R. Jenne, and D. Joseph, 1996: The NCEP/NCAR 40-Year Reanalysis Project. Bull. Amer. Meteor. Soc., 77, 437–471.

Kluver, D. B., 2007: Characteristics and trends in North American snowfall from a comprehensive gridded dataset. M.S. thesis, Department of Geography, University of Delaware,159pp.

Lanzante, J.R., 1984: A Rotated Eigenanalysis of the Correlation between 700 mb Heights and Sea Surface Temperatures in the Pacific and Atlantic. Mon. Wea. Rev., 112, 2270–2280.

Leathers, D.J., B. Yarnal, and M.A. Palecki, 1991: The Pacific/North American Teleconnection Pattern and United States Climate. Part I: Regional Temperature and Precipitation Associations. J. Climate, 4, 517–528.

McCabe, G.J., and M.D. Dettinger, 2002: Primary modes and predictability of year to year snowpack variations in the western United States from teleconnection with pacific ocean climate. J. Hydrometeorology, 3, 13-25.

McFadden, J.D., and R. A. Ragotzkie, 1967: Climatological significance of albedo in central Canada. J. Geophys. Res., 72(4), 1135–1143.

Morin, J., P. Block, B. Rajagopalan, M. Clark, 2007: Identification of large scale climate patterns affecting snow variability in the eastern United States. International Journal of Climatology, 28 (3), 315-328.

Mote, P.W., 2006: Climate-driven variability and trends in mountain snowpack in western North America. J. Climate, 19 (23), 6209-6220.

Namias, J., 1985: Some empirical evidence for the influence of snow cover on temperature and precipitation. Monthly Weather Review, 113, 1542–1553.

Prohaska, J.T., 1976: A Technique for Analyzing the Linear Relationships between Two Meteorological Fields. Mon. Wea. Rev., 104, 1345–1353.

Rajagopalan, B., E. Cook, U. Lall, and B.K. Ray, 2000: Spatiotemporal variability of ENSO and SST teleconnections to summer drought over the United States during the twentieth century. J. Climate, 13, 4244–4255.

Riviere, G., and I. Orlanksi, 2007: Characteristics of the Atlantic storm-track activity and its relation with the North Atlantic Oscillation. J. Atmos. Sci., 64, 241–266.

Shepard, D., 1968: A two-dimensional interpolation function for irregularly-spaced data. Proceedings of the 1968 23rd Association for Computing Machinery National conference, 517-524.

Sheridan, S.C., 2003: North American weather-type frequency and teleconnection indices. Int. J. Climatol., 23, 27-45.

Sobolowski, S., and A. Frei, 2007: Lagged relationships between North American snow mass and atmospheric teleconnection indices.International Journal of Climatology, 27, 221-231.

Walker, G. T., and E. W. Bliss, 1932: World Weather V. Mem. Roy. Meteor. Soc., 4, 53-84.

Wallace, J.M., and D. S. Gutzler, 1981: Teleconnections in the geopotential height field during the Northern Hemisphere Winter. Mon. Wea. Rev., 109, 784-812.

Wallace, J.M., C. Smith, and C.S. Bretherton, 1992: Singular Value Decomposition of Wintertime Sea Surface Temperature and 500-mb Height Anomalies. J. Climate, 5, 561–576.

Wettstein, J.J., and L.O. Mearns, 2002: The Influence of the North Atlantic–Arctic Oscillation on Mean, Variance, and Extremes of Temperature in the Northeastern United States and Canada. J. Climate, 15, 3586–3600.

Zhang, T., 2005: Influence of the seasonal snow cover on the ground thermal regime: An overview. Rev. Geophys., 43, RG4002, doi:10.1029/2004RG000157.

Chapter 4:

Alexander, M. A., U. S. Bhatt, J. E. Walsh, M. S. Timlin, J. S. Miller, and J. D. Scott, 2004: The atmospheric response to realistic Arctic sea ice anomalies in an AGCM during Winter. J. Climate, 17, 890-905.

Armstrong, R. L., and M. J. Brodzik, 2005: Northern Hemisphere EASE-Grid weekly snow cover and sea ice extent, Version 3, October 1966 to October 1978, http://nsidc.org/data/nsidc-0046.html. National Snow and Ice Data Center, Boulder, Colorado USA. Digital media.

Bretherton, C.S., C. Smith, and J.M. Wallace, 1992: An intercomparison of methods for finding coupled patterns in climate data. J. Climate, 5, 541–560.

Brown, R., and R. L. Armstrong, 2008: Snow-cover data: measurement, products, sources. in Snow and Climate: Physical Processes, Surface Energy Exchange and Modeling. edited by R. L. Armstrong and E. Brun, pp. 181-216 , Cambridge University Press.

Bulygina, O. N., V. N. Razuvaev, and N. N. Korshunova, 2009: Changes in snow cover over Northern Eurasia in the last few decades. Environ. Res. Lett., 4**,** 045026, 6 pp, doi: 10.1088/1748-9326/4/4/045026.

Cavalieri, D. J., P. Gloersen, C. L. Parkinson, J. C. Comiso, and H. J. Zwally, 1997: Observed Hemispheric Asymmetry in Global Sea Ice Changes. Science, 278 (5340), 1104, doi: 10.1126/science.278.5340.1104.

Cherry, S., 1997: Some Comments on Singular Value Decomposition Analysis. J. Climate, 10, 1759–1761.

Comiso, J., 1999: Bootstrap sea ice concentrations from NIMBUS-7 SMMR and DMSP SSM/I, updated 2008, october 1978 to December 2007, http://nsidc.org/data/docs/daac/nsidc0079_bootstrap_seaice.gd.html. National Snow and Ice Data Center, Boulder, Colorado USA. Digital media.

Comiso, J. C., C.L. Parkinson, R. Gersten, and L. Stock, 2008: Accelerated decline in the Arctic sea ice cover. Geophys. Res. Lett., 35, doi:10.1029/2007GL031972.

Deser, C., J.E. Walsh, and M.S. Timlin, 2000: Arctic sea ice variability in the context of recent atmospheric circulation trends. J. Climate, 13, 617-633.

Deser, C., R. Tomas, M. Alexander, and D. Lawrence, 2010: The Seasonal Atmospheric Response to Projected Arctic Sea Ice Loss in the Late Twenty-First Century. J. Climate, 23, 333–351.

Finnis, J., M. M. Holland, M. C. Serreze, and J. J. Cassano, 2007: Response of Northern Hemisphere extratropical cyclone activity and associated precipitation to climate change, as represented by the Community Climate System Model. J. Geophys. Res., 112, G04S42, doi:10.1029/2006JG000286.

Francis, J.A., W. Chan, D.J. Leathers, J.R. Miller, and D.E. Veron, 2009: Winter northern hemisphere weather patterns remember summer Arctic sea ice extent. Geophys.Res. Lett., 36, L07503, doi:10.1029/2009GL037274.

Gerdes, R., 2006: Atmospheric response to changes in Arctic sea ice thickness. Geophys.Res. Lett., 33(18), L18709.

Hassol, S. J., 2004: Impacts of a Warming Arctic: Arctic Climate Impact Assessment. 139 pp., Cambridge Univ. Press, Cambridge, U.K.

Holland, M. M., C. M. Bitz, and B. Tremblay, 2006: Future abrupt reductions in the summer Arctic sea ice. Geophys. Res. Lett., 33, L23503, doi:10.1029/2006GL028024.

Honda, M., K. Yamazaki, H. Nakamura, and K. Takeuchi, 1999: Dynamic and thermodynamic characteristics of atmospheric response to anomalous sea–ice extent in the Sea of Okhotsk. J. Climate, 12, 3347–33.

Honda, M., J. Inoue, and S. Yamane, 2009: Influence of low Arctic sea ice minima on anomalously cold Eurasian winters. Geophys. Res. Lett., 36, L08707, doi:10.1029/2008GL037079.

Kvamstø, N. G., P. Skeie, and D. B. Stephenson, 2004: Impact of Labrador sea-ice extent on the North Atlantic Oscillation. Int. J. Climatol., 24, 603–612.

Lanzante, J.R., 1984: A Rotated Eigenanalysis of the Correlation between 700 mb Heights and Sea Surface Temperatures in the Pacific and Atlantic. Mon. Wea. Rev., 112, 2270–2280.

Lawrence, D.M., A.G. Slater, R.A. Tomas, M.M. Holland, and C. Deser, 2008: Accelerated Arctic land warming and permafrost degradation during rapid sea ice loss. Geophys. Res. Lett., 35, L11506, doi:10.1029/2008GL033985.

Magnusdottir, G., C. Deser, and R. Saravanan, 2004: The effects of North Atlantic SST and sea-ice anomalies on the winter circulation in CCM3. Part I: Main features and storm-track characteristics of the response. J. Climate, 17, 857-876.

Parkinson, C. L., D. J. Cavalieri, P. Gloersen, H. J. Zwally, and J. C. Comiso, 1999: Arctic sea ice extents, areas, and trends, 1978–1996. J. Geophys. Res., 104(C9), 20, 837–20,856.

Prohaska, J.T., 1976: A Technique for Analyzing the Linear Relationships between Two Meteorological Fields. Mon. Wea. Rev., 104, 1345–1353.

Raisanen, J., 2008: Warmer climates: less or more snow? Climate Dynamics, 30, 307-319, doi: 10.1007/s00382-007-0289-y.

Rajagopalan, B., E. Cook, U. Lall, and B.K. Ray, 2000: Spatiotemporal variability of ENSO and SST teleconnections to summer drought over the United States during the twentieth century. J. Climate, 13, 4244–4255.

Rothrock, D.A., Y. Yu, and G.A. Maykut, 1999: Thinning of the Arctic sea-ice cover. Geophysical Resesearch Letters, 26(23), pp. 3469-3472.

Serreze, M. C., and J. A. Francis, 2006: The arctic amplification debate. Climatic Change, 76(3-4), 241-264, doi:1007/s10584-005-9017-y.

Serreze, M. C., M. M. Holland, and J. Stroeve, 2007: Perspectives on the Arctic's shrinking sea-ice cover. Science, 315, 1533-1536.

Serreze, M. C., A. P. Barrett, J. C. Stroeve, D. N. Kindig, and M. M. Holland, 2009: The emergence of surface-based Arctic amplification. The Cryosphere, 3, 11–19.

Simmonds, I., and K. Keay, 2009: Extraordinary September Arctic sea ice reductions and their relationships with storm behavior over 1979–2008. Geophys. Res. Lett., 36, L19715, doi:10.1029/2009GL039810.

Singarayer, J.S., J.L. Bamber, and P.J. Valdes, 2006: Twenty-first-Century climate impacts from a declining Arctic sea ice cover. J. Climate, 19, 1109-1125.

Stroeve, J. C., M. C. Serreze, F. Fetterer, T. Arbetter, W. Meier, J. Maslanik, and K. Knowles, 2005: Tracking the Arctic's shrinking ice cover: Another extreme September minimum in 2004. Geophys. Res. Lett., 32, doi:10.1029/2004GL021810.

Stroeve, J., M. M. Holland, W. Meier, T. Scambos, and M. C. Serreze, 2007: Arctic sea ice decline: faster than forecast. Geophys. Res. Lett., 34, doi:10.1029/2007GL029703.

Stroeve, J., A. Frei, J. McCreight, and D. Ghatak, 2008: Arctic sea-ice variability revisited. Annals of Glaciology, 48(1): 71-81, doi:10.3189/172756408784700699.

Wallace, J.M., C. Smith, and C.S. Bretherton, 1992: Singular Value Decomposition of Wintertime Sea Surface Temperature and 500-mb Height Anomalies. J. Climate, 5, 561–576.

Yang, D., D. Kane, L. Hinzman, X. Zhang, T. Zhang, and H. Ye, 2002: Siberian Lena river hydrologic regime and recent change. Journal of Geophysical Research-Atmospheres, 107(D23), 4694, doi:10.1029/2002JD002542.

Ye, B., D. Yang, and D. L. Kane, 2003: Changes in Lena river stream- flow hydrology: Human impacts vs. natural variations. Water Resour. Res., 39, 1200, doi:10.1029/2003WR001991.

Ye, H., D. Yang, D. Robinson, 2008: Winter rain on snow and its association with air temperature in northern Eurasia. Hydrological Processes, 22 (15), 2728 – 2736.

Chapter 5:

Barry, R. G., R. Armstrong, T. Callaghan, J. Cherry, S. Gearhead, A. Nolin, D. Russell, and C. Zockler, 2007:. Snow, in Global Outlook for Ice and Snow. pp. 39-62, UNEP (Ed.), Nairobi, Kenya.

Brown, R.D., 2000: Northern hemisphere snow cover variability and change, 1915-1997. J. Climate, 13(13), 2339-2355.

Brown, R. D., and P. W. Mote, 2009: The response of Northern Hemisphere snow cover to a changing climate. Journal of Climate, 22, 2124–2145.

Bulygina, O. N., V. N. Razuvaev, and N. N. Korshunova, 2009: Changes in snow cover over Northern Eurasia in the last few decades**.** Environ. Res. Lett., 4, 045026, 6 pp, doi: 10.1088/1748-9326/4/4/045026.

Clark, M.P., M.C. Serreze, and D. A. Robinson, 1999: Atmospheric control on Eurasian snow extent. Int. J. Climatol, 19, 27–40.

Collins, W. D., and Coauthors, 2006: The Community Climate System Model Version 3 (CCSM3). J. Climate, 19, 2122–2143.

Deser, C., and A.S. Phillips, 2009: Atmospheric Circulation Trends, 1950-2000: The Relative Roles of Sea Surface Temperature Forcing and Direct Atmospheric Radiative Forcing. J. Climate, 22, 396-413, doi:10.1175/2008JCLI2453.1

Deser, C., R. Tomas, M. Alexander, and D. Lawrence, 2010: The Seasonal Atmospheric Response to Projected Arctic Sea Ice Loss in the Late Twenty-First Century. J. Climate, 23, 333–351.

Frei, A., and D.A. Robinson, 1999: Northern Hemisphere snow extent: Regional variability 1972–1994. Int. J. Climatol., vol. 19, pp. 1535–1560.

Ghatak, D., A. Frei, G. Gong, J. C. Stroeve, and D. Robinson, 2010: On the emergence of an Arctic amplification signal in terrestrial Arctic snow extent. J. Geophys. Res., 115, D24105, doi:10.1029/2010JD014007.

Hassol, S. J., 2004: Impacts of a Warming Arctic: Arctic Climate Impact Assessment. 139 pp., Cambridge Univ. Press, Cambridge, U.K.

Hurrell, J. W., J. J. Hack, A. S. Phillips, J. Caron, and J. Yin, 2006: The dynamical simulation of the Community Atmosphere Model Version 3 (CAM3). J. Climate, 19, 2162–2183.

Iijima, Y., K. Masuda, and T. Ohata, 2007: Snow disappearance in Eastern Siberia and its relationship to atmospheric influences. International Journal of Climatology, 27: 169–177. doi: 10.1002/joc.1382.

McCabe, G.J., and D. M. Wolock, 2010: Long-term variability in Northern Hemisphere snow cover and associations with warmer winters. Climatic Change, v. 99, no. 1, p. 141-153.

Raisanen, J., 2008: Warmer climates: less or more snow? Climate Dynamics, 30, 307-319, doi: 10.1007/s00382-007-0289-y.

Serreze, M. C., A. P. Barrett, J. C. Stroeve, D. N. Kindig, and M. M. Holland, 2009: The emergence of surface-based Arctic amplification. The Cryosphere, 3, 11–19.

Skific, N., J.A. Francis, and J.J. Cassano, 2009: Attribution of Seasonal and Regional Changes in Arctic Moisture Convergence. J. Climate, 22, 5115–5134, DOI: 10.1175/2009JCLI2829.1.

Ye, B., D. Yang, and D. L. Kane, 2003: Changes in Lena river stream- flow hydrology: Human impacts vs. natural variations. Water Resour. Res., 39, 1200, doi:10.1029/2003WR001991.

Ye, H., 2001: Increases in snow season length due to earlier first snow and later last snow dates over north central and northwest Asia during 1937–94. Geophys. Res. Lett., 28(3), 551–554, doi:10.1029/2000GL012036.

Ye H, H. Cho, P. Gustafson, 1998: The changes of Russian winter snow accumulation during 1936–1983 and its spatial patterns. Journal of Climate, 11: 856–863.

Ye, H., and M. Ellison, 2003: Changes in transitional snowfall season length in northern Eurasia. Geophys. Res. Lett., 30(5), 1252, doi:10.1029/2003GL016873.

Ye, H., D. Yang, D. Robinson, 2008: Winter rain on snow and its association with air temperature in northern Eurasia. Hydrological Processes, 22 (15), 2728 – 2736.

Chapter 6:

Ogi, M., Y. Tachibana, and K. Yamazaki, 2003: Impact of the wintertime North Atlantic Oscillation (NAO) on the summertime atmospheric circulation. Geophysical Research Letters, 30: 1704, doi:10.1029/2003GL017280.

Rigor, I.G., and J.M. Wallace, 2004: Variations in the age of Arctic sea-ice and summer sea-ice extent. Geophysical Research Letters, 31: L09401, doi:10.1029/2004GL019492.

Rigor, I. G., J. M. Wallace, and R. L. Colony, 2002: Response of sea ice to the Arctic Oscillation. J. Climate, 15, 2648–2663.